Protein Cross-linking Capillary and Microchip Electrophoresis for Protein-Protein Interaction Analysis

by

Claire M. Ouimet

A dissertation submitted in partial fulfillment
of the requirements for the degree of
Doctor of Philosophy
(Chemistry)
in the University of Michigan
2018

Doctoral Committee:

Professor Robert T. Kennedy, Chair
Professor Anna K. Mapp
Professor Nouri Neamati
Professor Brandon T. Ruotolo

Claire M. Ouimet

cmoui@umich.edu

ORCID iD: 0000-0002-1172-7542

Acknowledgements

I would like to thank my advisor, Professor Robert Kennedy for allowing me to join his lab and work on these interesting projects. I would also like to thank my committee members Professors Nouri Neamati, Anna Mapp and Brandon Ruotolo for their time and suggestions that have greatly helped this work. I am very grateful to our collaborators in the labs of Professors Jason Gestwicki, Chad Dickey, and Anna Mapp including Hao Shao, Jennifer Rauch, Bryce Nordhues, Victoria Assimon, Jean Lodge and Julie Garlick. Without their generous contributions of protein, none of this work would have been possible.

I would like to thank Dr. Mohamed Dawod for his openness to discussions, endless patience, and encouragement. I am grateful to Dr. Kennon Deal, Dr. Erik Guetschow, Dr. James Grinias, Dr. Mohamed Dawod, and Cara D'Amico for providing mentorship and contributing their expertise. Thank you to the many other members of the Kennedy lab who have provided help and laughter along the way.

Thank you to Professors Tim Strein and David Rovnyak for investing their time and resources into getting me started on this path. Thank you to Mitch Lancaster and Jen LaBarre for listening to me and for providing respite outside of the lab. Lastly, thank you to my family for encouraging and supporting me even when you all thought I would be a student forever.

Table of Contents

List of Tables

List of Figures

List of Abbreviations

ADP	adenosine diphosphate
APCE	affinity probe capillary electrophoresis
ATP	adenosine triphosphate
Bag3	bcl2 associated athanogene 3
Bcl-2	B-cell lyphoma 2
BGE	background electrolyte
Bid	BH3-interaction domain
CBP	CREB-Binding Protein
CE	capillary electrophoresis
CE-FA	capillary electrophoresis frontal analysis
CE-Frag	capillary electrophoresis frontal analysis
CGE	capillary gel electrophoresis
CHIP	c-terminus of Hsp70 interacting protein
CZE	capillary zone electrophoresis
DMSO	dimethylsiloxane
DTT	dithiothreitol
EMMA	electrophoretically mediated microanalysis
EOF	electroosmotic flow
FCPIA	flow cytometry protein interaction analysis
FITC	fluorescein isothiocyanate
FRET	fluorescence resonance energy transfer
GAPDH	glyceraldehyde 3-phosphate dehydrogenase
HOP	heat shock organizing protein
Hsp70	heat shock protein 70
Hsp90	heat shock protein 90
HTS	high throughput screening
*IC*50	half maximal inhibitory concentration
i.d.	inner diameter
IMERs	immobilized enzyme reactors
ITC	isothermal titration calorimetry
Kd	dissociation constant
*K*i	inhibitory constant
KIX	kinase induscible domain interacting domain
LIF	laser induced fluorescence

MCE	microchip electrophoresis
MS	mass spectrometry
MWP	multiwell plate
N.D.	not determined
NMR	nuclear magnetic resonance
o.d.	outer diameter
PDMS	polydimethyl siloxane
PFA	perfluoroalkoxy alkane
PF-ACE	partial filling affinity capillary electrophoresis
PPI	protein protein interaction
PPIs	protein protein interactions
PXCE	protein cross-linking capillary electrophoresis
SDS	sodium dodecyl sulfate
SEC	size exclusion chromatography
SH2	src homology 2
SIRT5	sirtuin 5
SPR	surface plasmon resonance
Tar	transactivation-responsive RNA
Tat	transactivator of transcription
TDLFP	transverse diffusion of laminar flow profiles

Abstract

Proteins perform their functions as part of multi-protein complexes. These protein complexes are vital for carrying out and regulating cellular processes. As such, there is a need for tools to measure protein-protein interaction (PPI) affinity, stoichiometry, and inhibition in order to map interaction sites and screen for PPI modulators. Such measurements can be challenging because PPIs can span a wide range of affinities and stoichiometries. While many techniques exist for PPI analysis they often require large amounts of protein, have relatively low throughput, or have utility among a narrow range of PPIs.

Capillary electrophoresis (CE) has demonstrated utility for determination of PPI affinity and for screening of PPI modulators. CE has a number of advantages in PPI analysis including low sample volume requirements, direct detection of complexes, and the potential for high-throughput. However, method development for analysis of PPIs by CE is often hampered by the need to maintain the native interaction during the separation and prevent protein adsorption to the capillary wall. Here protein cross-linking capillary electrophoresis (PXCE) is reported and described. Covalently cross-linking interacting proteins prior to electrophoresis eliminates the need to maintain the native interaction during the separation, facilitating method development. The PXCE method is demonstrated for an antibody-antigen interaction and heterodimer and homodimer heat

shock protein complexes. Separation of free protein from protein complex is achieved either by using capillary zone electrophoresis or by capillary gel electrophoresis. PXCE is demonstrated to give quantitative results for PPI affinity and inhibition.

Next, we expanded the utility of PXCE to access a wide range of PPIs including weak and multimeric oligomers. A short cross-linking reaction time of 10 s is found to have sufficient yields for a variety of complexes. Factors influencing non-specific cross-linking are also explored with concentrations of protein >20 μM yielding non-specific complexes. Apparent dissociation constants for seven different PPIs spanning from low nanomolar to low micromolar are presented. Good agreement was found to non-cross-linking methods. Assays of point mutations in the protein interaction site and nucleotide state dependence of association are also presented. Protein complexes less than about 250 kDa are accessible using the presented method. Separation time is also reduced to about 1 min/sample.

Finally, a method for increasing the throughput of sample analysis is presented. Here, a microchip gel electrophoresis separation allowed for protein separation in 2.5 s. Further, a novel device for removing oil from segmented droplet flow based on density is demonstrated for coupling nanoliter-scale sample droplets to microchip separation for rapid and automated sample analysis. Throughputs of 10 s per sample are achieved with multiple injections made per sample. Utility of this device for application to PPI analysis and enzymatic reactions is presented. Specifically, Hsp70-Bag3 interaction and SIRT5 enzymatic reaction samples were assayed. The results suggest future utility of the device and PXCE method for screening of enzyme and PPI modulators.

CHAPTER 1: Introduction

Adapted with permission from Ouimet, C. et al. *Expert Opin. Drug Discov.* 2017, *12*, 213-224.

Capillary and Microchip Electrophoresis in Drug Discovery

Capillary electrophoresis (CE), and its microfluidic counterpart microchip electrophoresis (MCE), have emerged as promising techniques with use in the pharmaceutical industry for characterizing biopharmaceuticals[1] and drug discovery[2,3].

CE separates molecules based on their differential migration in an electric field. In free solution, capillary zone electrophoresis (CZE), the migration of a molecule in an applied field is dependent upon its charge and size, enabling separation by either property (Figure 1-1A). Modification of the separation media can alter the separation selectivity, e.g. capillary gel electrophoresis (CGE) enables separation on size only (**Figure 1-1B**).

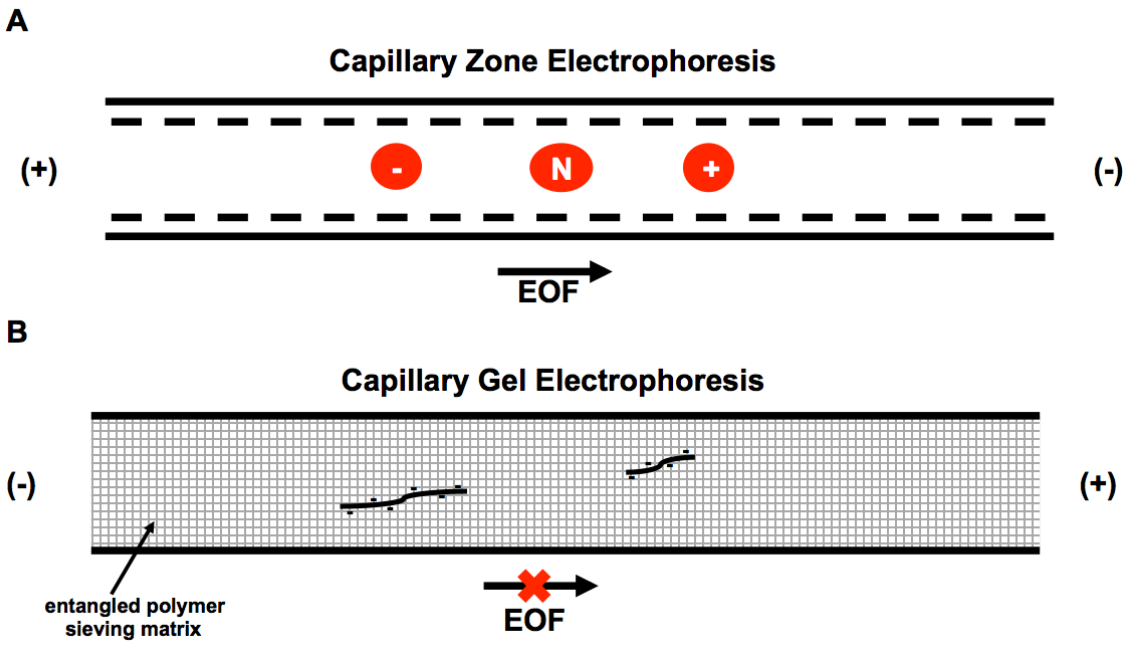

Figure 1-1. Schematic of capillary zone electrophoresis (A) and capillary gel electrophoresis (B). In capillary zone electrophoresis analytes migrate based on their charge and size. In capillary gel electrophoresis of proteins analytes are sieved an entagled polymer matrix based on their size.

Separated molecules are detected by a variety of methods including UV absorbance, capacitively coupled contactless conductivity, mass spectrometry (MS), and laser-induced fluorescence (LIF). The combination of separation and direct, on-line detection enable CE and MCE to be used for many kinds of assays useful for screening. Of relevance to drug screening, optical detection is well-suited for detecting enzyme activity and affinity interactions. Compared to other drug screening platforms, such as fluorescent plate readers, CE offers a number of potential advantages including low sample volume requirements (nanoliter or less), rapid separations, and sensitive detection of analytes. CE also allows for resolution of confounding components in the assay such as interference from optically active test compounds[2,4,5], non-specific protein aggregation[5], and compound precipitation[5].

A comparison of methods for a kinase screen against fluorescent test compounds determined electrophoresis to be preferred over fluorescence polarization, amplified luminescent proximity homogenous assay, and enzyme fragment complementation for quantifying fluorescent inhibitors.[4] The preference for CE was due to the tolerance of the CE assay to fluorescent compounds, the assay's sensitivity, and comparatively low substrate and enzyme requirements. In the CE assay the fluorescent compound was tolerated because test compound was resolved from the substrate and product. An example of similar benefits for a protein-protein interaction assay is illustrated in Figure 1-2.[6]

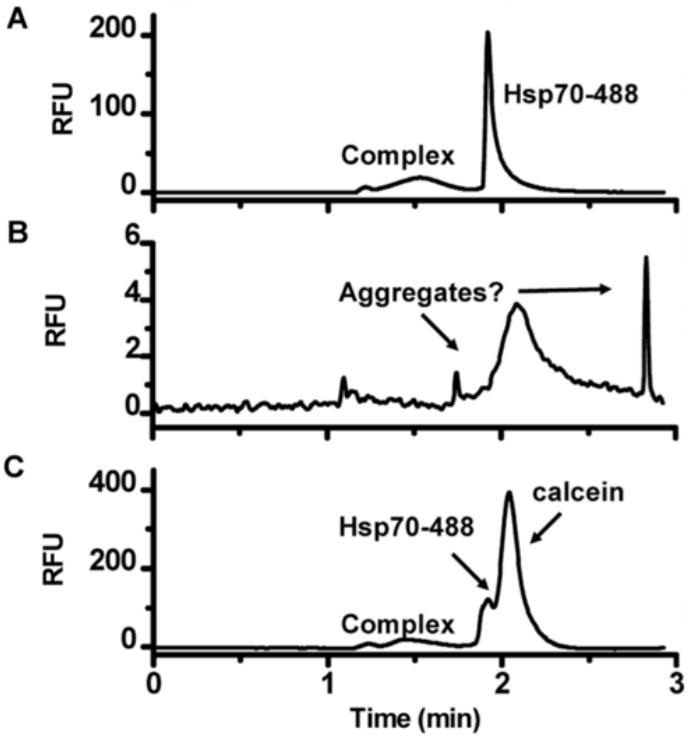

Figure 1-2. Identification of assay interference in CE based on electropherograms. Electropherograms of Hsp70-488 and Bag3 interaction in the presence of (A) complex inhibitor epigallocatechin gallate, (B) hematoxylin which caused aggregation identified by loss of signal and sharp, unexpected peaks, (C) fluorescent test compound calcein causing optical interference.[6] Reprinted with permission from reference [6]. Copyright 2013 American Chemical Society.

MCE systems have been commercialized for screening. Perhaps the most popular system is the LabChip instrument (PerkinElmer), which uses vacuum to pull sample from a multiwell plate (MWP) into the microfluidic separation channel with fluorescence detection. This system has been used to screen 10 x 384 well plates in 10 h.[7] The platform has been applied to diverse targets including kinases, phosphatases, proteases, phosphodiesterases, epigenetic targets, and nucleic acid binding proteins.[2,7–12]

Despite the apparent utility of CE in screening, the technique is not yet widely used. One reason for this may be due to the relative complexity of performing CE assays where injection, separation and detection are required in comparison to the simpler, more common, optical detection methods. Despite these challenges, a variety of strategies for improving throughput and sample requirements have emerged. New instruments and methods, have the potential to improve throughput and reduce sample consumption of CE or MCE for screening.

Rapid Electrophoretic Separations

High-throughput screening (HTS) using multiwell plates with optical readouts can perform $>10^4$ assays per day. The throughput of CE and MCE assays is usually limited by the separation time required to resolve the molecules of interest. As commonly practiced, CE separation times are a few minutes per sample, however it is possible to achieve separations on the second timescale. Throughput may also be improved by running separations in parallel or by multiplexing the assay.

Strategies for increasing the speed of a separation can be appreciated with a brief review of electrophoresis principles. The migration time of an analyte (t_{mig}) in an

electrophoresis separation channel with length (L) is dependent upon its electrophoretic mobility (μ_{ep}) under an applied voltage (V):[13]

$$t_{mig} = L^2/(V \times \mu_{ep}) \quad \text{(Eq. 1-1)}$$

Therefore, to decrease the separation time the applied voltage can be increased or the separation length can be decreased. For example, in an enzyme inhibition assay of metalloproteinase performed on a commercial CE instrument the separation time was decreased from about 250 s to 70 s by simply reversing the polarity of the applied electric field and injecting from the 'outlet' side of the capillary, near the detection window, resulting in a shorter separation length.[14] In general however, commercial CE instruments have limited accessible separation lengths so that it is difficult to reduce separations to shorter than this. Some custom-built CE systems have allowed sub-second separations;[15,16] however, with one exception[17,18], they have not been investigated for screening.

MCE allows for use of shorter separation channel lengths and smaller internal diameters than commercial CE systems. Increasing the applied voltage over a given separation length can increase the separation speed; however, this approach is limited because eventually Joule heating becomes significant enough to create mixing effects that destroy the separation. Effective heat dissipation can be achieved by using liquid cooling or by lowering separation channel diameters. These strategies enable higher voltages and faster separations. MCE with micrometer dimension channels enable separations in microseconds to seconds.[19] Decreasing the separation channel internal diameter places greater demands on the detector to achieve adequate sensitivity. LIF detection is often used when low internal diameters are employed because of the inherent sensitivity of

fluorescence detection. Despite inherent challenges in coupling electrophoresis to mass spectrometry (MS) recent advances in CE-MS interfaces[20] may eventually allow detection by this label-free, highly selective detector.

Another approach to improving throughput is to perform multiple injections rapidly so that multiple separations are overlapping in the separation channel at one time. This technique, which requires proper spacing of the injections relative to the separation times of peaks of interest, increases throughput by eliminating time between runs and taking advantage of the time between resolved peaks in a single separation. In one study, the total analysis time per sample was reduced by about half with sequential injection.[21] This approach is most common with CE where the separation time tends to be longer than MCE.

Parallelization and Multiplexing Strategies

Operating CE or MCE in parallel can also improve the throughput. Challenges in developing platforms for running parallel separations include achieving multichannel detection, connections to peripheral power supplies, and attaining reliable simultaneous separations across parallel separation channels.[22] Many of these challenges were met when CE was being developed for DNA analysis. The necessity of high throughput sequencing led to using arrays of capillaries to run many parallel assays.[23] This concept has been adapted to drug discovery. A commercial instrumentation with a 96-capillary array was successfully applied to enzyme screening with UV absorption detection and throughputs of about 30 min per 96 samples without overlapping injections, high fields, or short capillaries.[24]

With MCE, parallel separation channel arrays can be made with small footprints at no additional fabrication cost. Up to 384 parallel separations have been reported for genotyping on a single microfluidic device.[25] Such highly parallel chips for screening have not yet been reported; however, the LabChip system can be used with 12 channels. Higher parallelization may be possible. A 36 channel microfluidic device with gated injection has been demonstrated for a model enzyme inhibitor screen with 36 parallel assays completed in 30 s.[26] Parallelization on chip with fast optically-gated injection has been used to perform a high throughput enzyme assay with 4 parallel separations and 30 s separation time.[27]

Another way to improve throughput is by test compound sample pooling. With sample pooling, versus assaying each test compound individually to find hits, a mixture of test compounds is assayed. If a hit is identified then each compound in the original test compound mixture is assayed individually. The low hit rates typical with screening allow far fewer assays to be done if sample pooling is used. Sample pooling for CE screening has been demonstrated with 10 test compounds assayed at a time.[28]

Multiplexing takes advantage of the separation power of CE to assay multiple targets simultaneously.[29,30] A four-plexed assay of protein kinases demonstrated simultaneous resolution of distinct substrates and products.[29] A study of protein-peptide interaction targets with src homology 2 (SH2) domains simultaneously assayed three proteins (**Figure 1-3**).[30] Such multiplexed assays also provide additional information about hit specificity by readily identifying selective and non-selective inhibitors.[29,30]

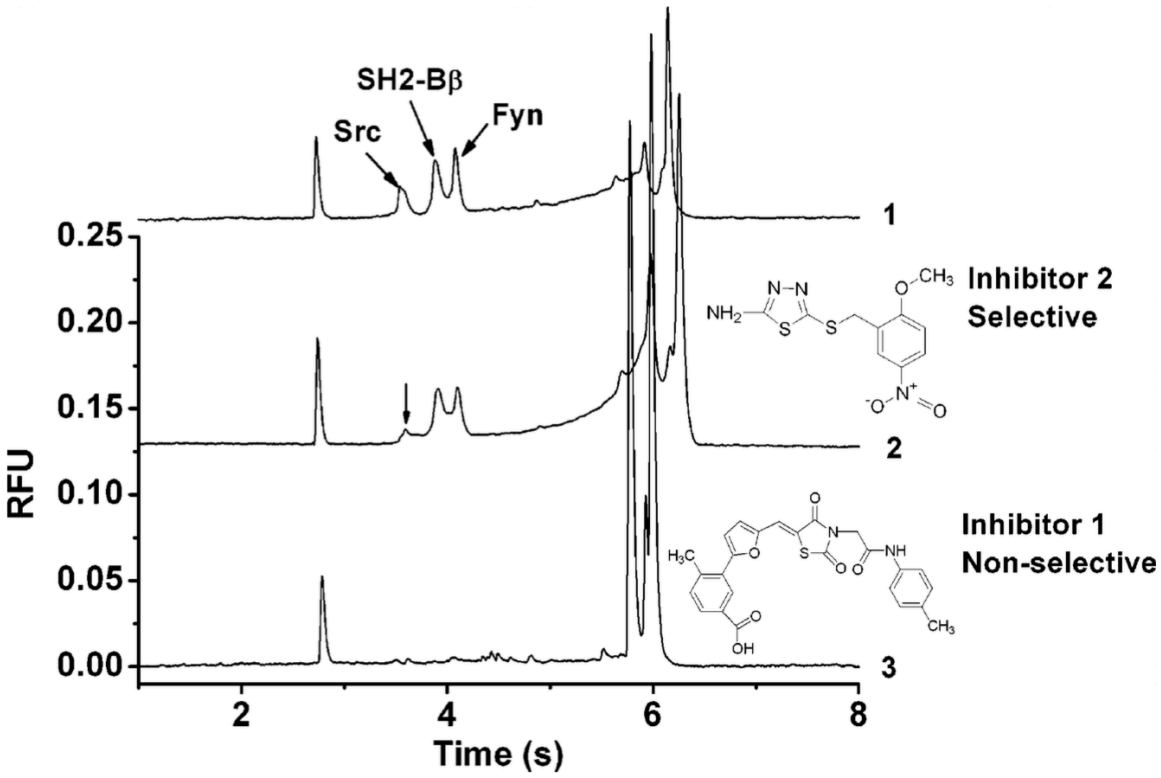

Figure 1-3. Multiplexed assay of affinity interaction between SH2 domain proteins and phosphopeptides. Electropherograms identifying selective (middle) and non-selective inhibitors (bottom) of these interactions. Reprinted with permission from reference [30] copyright 2007, American Chemical Society.

Data Processing

A challenge of using CE for screening is that large numbers of electropherograms are generated which must be analyzed to determine peak areas used for quantification.[2] It has been shown that batch analysis of electropherograms allows for rapid data processing. For example, data processing software (available for download at http://kennedygroup.lsa.umich.edu/downloads/) allows for simultaneous analysis of hundreds of electropherograms to allow for data analysis on the time-scale of the rapid separations. In this strategy hundreds of electropherograms can be aligned based on a common peak, corrected for baseline drift, and peaks of interest can be defined.[31]

Sample Introduction

Although very fast separations are possible by CE and MCE, sample introduction and injection are critical parameters to achieving high throughput. Rapid separations in short, low volume separation channels require special considerations for sample injection to avoid overloading the separation channel with sample. Typical injection volumes are less than 1% of separation channel volume, corresponding to 120 pL volume on a 2 cm long x 20 μm tall x 30 μm wide channel. Rapid, small volume injection techniques include gated injection[32], optically gated injection[27,33], flow-gating interfaces[34], and spontaneous injection[35,36]. These methods allow injection of small volumes onto the channel and therefore achieve high quality separations in < 10 s; however, commonly used designs require that much larger samples (microliters) be loaded into a sample reservoir mounted on the chip. This approach therefore requires more sample than necessary for the actual electrophoresis separation and is not compatible with rapidly changing from one sample to the next. Recent advances in sample introduction methods are showing potential for improved throughput of screening.

Direct Injection from Multi-well Plate

Most screens are performed from MWP. Transferring samples rapidly and in series from the MWP to MCE requires specific fluidic handling components. The LabChip system uses "sippers" (capillaries attached to the chip) to dip into the MWP and pull as little as 10 nL of sample into the chip through a vacuum system. Interestingly, this system does not use the high efficiency injection methods described above. Instead, vacuum is used to pull samples into the separation channel. Therefore, a limitation of this commercial system is that the vacuum-induced flow within the separation channel causes band

broadening, limiting the separation efficiencies that can be achieved. Nevertheless, this is the only commercial system that allows robust sampling for thousands of assays with MCE separations. The screen's data quality, has been demonstrated by determination of Z'-score, where σ_p and σ_n are the standard deviations of positive and negative controls and μ_p and μ_n are the averages of the positive and negative controls (eq. 1-2).

$$Z' = 1 - \frac{3(\sigma_p+\sigma_n)}{|\mu_p-\mu_n|} \quad \text{(Eq. 1-2)}$$

High Z'-scores (>0.8), have been reported using the LabChip platform.[2,10]

When assay reactions are performed in a MWP, the system does not reduce sample requirements even though only small volumes are removed from the MWP. The use of microfluidics, however, does allow enzymatic reactions to be performed on-chip. In on-chip mode, compounds are sipped from MWP and enzyme reagents are added in channels so that reactions occur on-chip. In one kinase screen, on-chip reactions reduced enzyme consumption 7-fold.[7] Due to short on-chip incubation times, however, the on-chip format requires high concentrations of enzymes and is limited to enzymes with rapid turnover (> 30% in 1 min).[9]

Injection from Small Sample Volumes

To reduce sample volumes required for injection, new designs for picoliter injections from low sample volumes have been developed.[37,38] One platform utilizes a "Slipchip."[39] This design consists of two plates; one contains sample well and a discontinuous separation channel and the other contains a small volume sample well aligned with the bottom of the sample well on the other plate. The plates are aligned such that by moving one plate relative to the other discrete sub-nanoliter volume samples can be formed in the small volume sample well and alignment of this well with the separation channel allows

for subsequent injection. The design is also parallelized for analysis from 10 discrete samples with 30 parallel separations.[38] Changing samples beyond the parallelized number, however, currently requires manual manipulations. In another platform, an array of nanoliter sample droplets was covered with immiscible oil and picoliter injections were achieved spontaneously by surface tension when the capillary tip was removed from the sample droplet. An array of 25 samples were injected with RSDs for peak height and migration time < 5%.[37] Potential exists to scale both of these systems to higher sample numbers to achieve higher throughput.

Injection from Segmented Flow

Another strategy for rapidly introducing new samples and miniaturizing sample requirements is use of droplet microfluidics. In droplet microfluidics, discrete aqueous samples are compartmentalized by an immiscible, often fluorinated, carrier fluid. Flow focusing and t-junctions can be used to make many droplets from one sample. [40–43] However, to make a few droplets from many samples, as is necessary in screening, different methods are required. In one approach, samples in MWPs are reformatted into segmented droplets of nanoliter volume inside tubing by using aspiration to sequentially draw up plugs of sample and carrier fluid.[17,18,44–47] Microfluidic droplets can then undergo further manipulations such as mixing,[48–52] merging,[53–57] splitting,[58–61] addition,[46,48,49,62,63] incubation and extraction,[17,64–69] which can enable entire assays to be performed at small scale. Indeed, this approach has been used with fluorescence detection to screen 704 compounds against protein tyrosine phosphatase and high-resolution dose response curves were obtained. Sample consumption per data point was reduced 25,000-fold.[70] Droplet microfluidics therefore is emerging as an exciting way to perform screens at

much reduced volume and instrument overhead relative to MWP. Use of droplet microfluidics offers the potential to take better advantage of the throughput and miniaturization possible with MCE.

One hurdle associated with using droplet microfluidics in CE screening is automated injection of droplet samples into the CE separation channel. Injection of immiscible, non-conductive, segmenting liquid is not compatible with CE separation and has been observed to cause electroosmotic flow instability and plug formation in the separation channel leading to shorting and dielectric breakdown of the channel and device.[64,65,71] Therefore, extraction of aqueous sample from the segmented flow is necessary. Passive, active, whole, and partial droplet extraction and injection strategies have been reported.[17,64–69]

Active extraction uses an electric field to destabilize the fluorinated liquid-aqueous interface and merge the aqueous sample with a parallel aqueous stream providing robust and selective extraction.[66] Active extraction coupled to electrophoretic separation has yet to be reported.

Passive extraction is somewhat simpler to integrate, as it does not require external input. As seen in Figure 1-4, several passive droplet extraction strategies have been coupled to downstream CE separations. Pillar arrays have been applied for complete extraction of carrier phase[67] and injection of the whole droplet into an electrophoresis channel (**Figure 1-4A**).[68] Passive droplet extraction strategies often rely on surface modifications to extract the hydrophilic aqueous sample droplet from the hydrophobic carrier phase. In one strategy, whole droplets are injected into an electrophoresis channel by a multilayer device where a portion of the separation channel is open to the segmented

flow channel. The droplet is simultaneously extracted and injected when the aqueous sample passes the junction and coalesces with the separation buffer (**Figure 1-4B**).[72] Interestingly, passive whole droplet extraction and injection assisted by a hydrophobic and oleophilic foam was also effectively coupled to capillary gel electrophoretic and free solution separations.[73] The limitation of whole droplet injection strategies is that large injection volumes limit the separation quality.

In another strategy, a microchip device with a 'virtual wall' between hydrophobic and hydrophilic channels was fabricated by derivatizing a channel surface to make it hydrophobic, allowing for aqueous sample to be discreetly injected (**Figure 1-4C**).[64,65] A hybrid polydimethylsiloxane (PDMS)-glass device passively extracted droplets from a segmented stream within the hydrophobic PDMS device into a hydrophilic capillary connected to a glass microchip for gated injection could be used to introduce small volume injections for electrophoretic separation (**Figure 1-4D**). For screening, droplets were catalogued by the presence of a positively charged, rapidly migrating analyte in every other droplet which was also used to visualize rinsing between droplets. High efficiency, rapid separations were reported with this platform (**Figure 1-5**).[17]

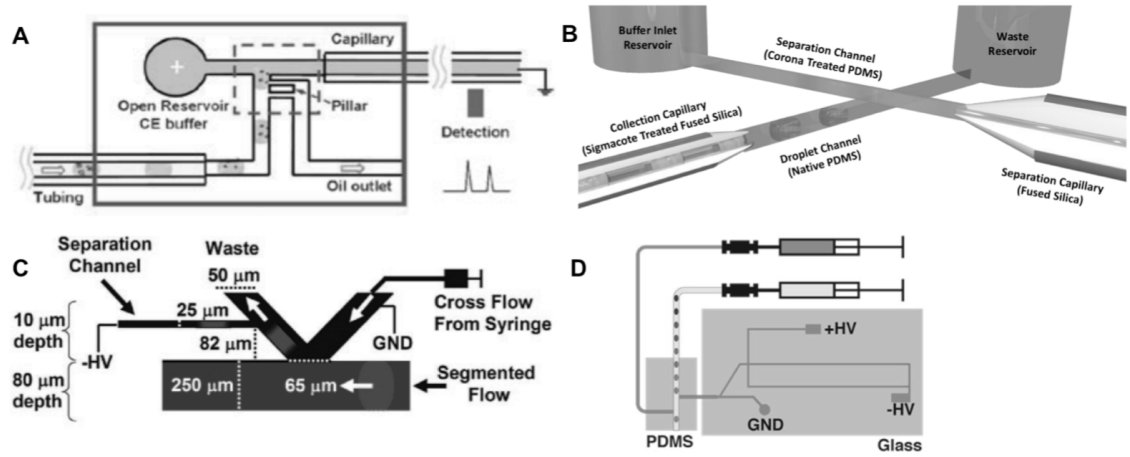

Figure 1-4. Passive extraction and injection strategies for coupling segmented flow sample droplets to electrophoresis separations. (A) Pillar array extraction of oil.[68] (B) Intersecting segmented flow and separation channel geometry for simultaneous extraction and injection.[72] (C) Virtual wall used for extraction.[64] (D) Hybrid PDMS-glass device used for decoupling extraction and injection processes (http://pubs.acs.org/doi/full/10.1021/ac502758h).[17] Reprinted with permission from references listed in sub captions. Copyright Royal Society of Chemistry and American Chemical Society.

Several screens have been reported using this technology. Z'-scores of 0.8 were reported for protein kinase A and Sirtuin 5 screens using the hybrid PDMS-glass extraction approach. Throughputs of 0.2 to 0.5 samples/s have been reported with this platform.[17,18] To date, these approaches have only been used for up to 1,408 compounds. If these rates could be scaled to a large number of samples, then throughput could be 14,400 samples/8 h day on a single channel system.

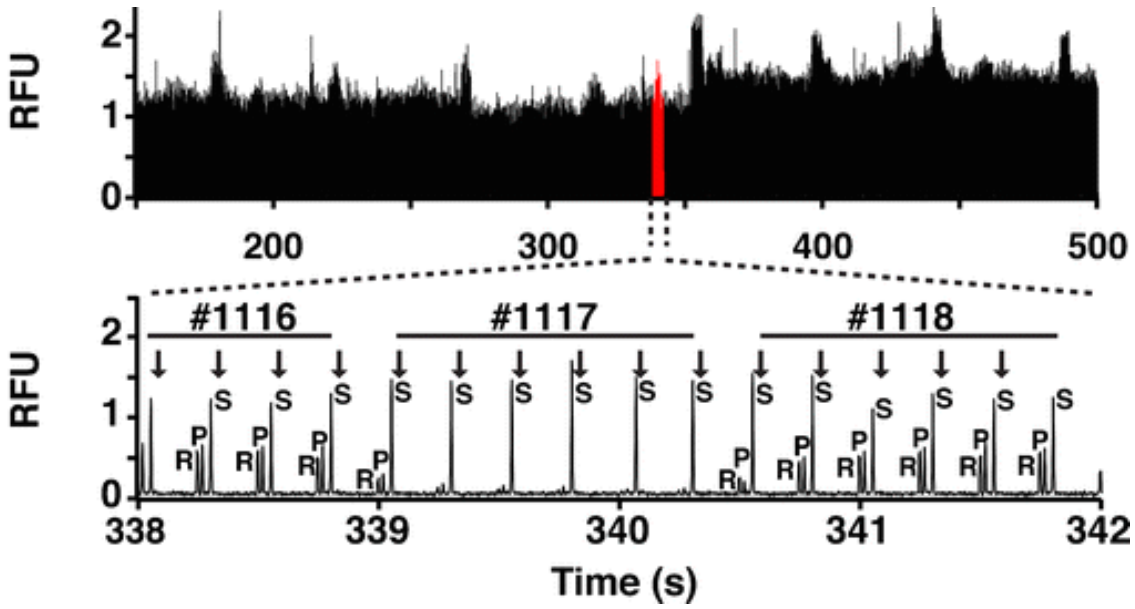

Figure 1-5. Example of rapid enzyme assay separations achievable by MCE for screen of SIRT5 1,280 compounds. Separations of internal standard (R), product (P), and substrate (S) were achieved in 250 ms, #1117 is an enzyme inhibitor. Reprinted from reference [18], copyright 2016, with permission from Springer.

The throughput of a droplet extraction 'virtual walls' device was improved by parallelization with three extraction channels on one device and was demonstrated for an enzyme assay achieving throughputs of 120 samples in 10 min.[69] It seems likely that higher throughput could be achieved by parallelizing newer droplet extraction techniques.[17,18]

Targets

Enzymes

As previously mentioned, CE and MCE are amenable to performing enzymatic assays. Large screens of over 10,000 compounds have only been achieved using commercial microchip systems based on sipping from MWP.[3] The advent of droplet microfluidics interfaced to MCE may prove to have enough throughput, miniaturization, and robustness to provide a step forward for electrophoresis-based screening[17,18,64,65,69,71–73]; however,

this has yet to be proven. The standard approach to enzyme assay by CE is to incubate enzyme with substrate and then separate substrate and product. The incubation may be performed in a MWP. Reduction in volume may be achieved by mixing on chip or in droplet samples as mentioned above. Other strategies, unique to CE, have also been demonstrated for analysis of enzyme modulation. These alternate methods include electrophoretically mediated microanalysis (EMMA), transverse diffusion of laminar flow profiles (TDLFP), and immobilized enzyme reactors (IMERs). Of the techniques, only "mix and separate" has been used for large scale screening with other techniques being demonstrated on small numbers of compounds (Table 1-1). Examples of screening using these techniques are described below.

Performing enzymatic reactions within the capillary can minimize enzyme requirements. In EMMA, reactants are sequentially injected onto the capillary and mixed based on their differential electrophoretic mobilities allowing for the enzymatic reaction to occur on-line (**Figure 1-6A**).[14,74–79] For enzyme screens, lower IC_{50} values have been determined using EMMA, in comparison to traditional assays. Lower observed inhibition has been attributed to the decreased incubation time typical in EMMA.[77] EMMA was also demonstrated for a two substrate enzyme, glycerol kinase, with four reactant plugs: incubation buffer, enzyme and two distinct substrate plugs, mixed in-capillary.[79] Small-scale screening of Chinese herbs and other crude products against enzymatic targets by EMMA demonstrated the utility of CE in screening of complex test compound mixtures, where potential optical interference is reduced compared to other optical platforms.[74–78] While EMMA requires very little enzyme per assay optimal conditions for the enzymatic reaction may be easier to achieve in well plate format. Off-line reactions can be

completed in parallel, often with automated liquid handling, by carrying out the enzymatic reaction within the capillary, however, on-line incubation limits the throughputs achievable.

Table 1-1. Representative CE enzyme assay screens and demonstrations

Target	Assay type	Compounds assayed	Z-score	Reference
Tyrosine phosphatase	Commercial microchip platform	12,648	0.61	[7]
Sirt5	Segmented flow coupled to MCE	1,280	0.8	[18]
Glycerol kinase	EMMA	1	N.D.	[79]
Aminopeptidase N	EMMA	30[a]	N.D.	[77]
Neuraminidase	EMMA	24[a]	N.D.	[74]
β-N-acetylhexosaminidase	TDLFP	1	N.D.	[80]
Four human kinases: GSK3β, DYRK1A, CDK5/p25, CDK1/cyclin B	TDLFP	13	N.D.	[81]
Adenosine deaminase and xanthine oxidase	CE-based IMERs	20[a]	0.82, 0.74	[82]
L-glutamic dehydrogenase	CE-based IMERs	26[a]	0.95	[83]
Glucose-6-phosphate dehydrogenase	CE-based IMERs	6	N.D.	[84]
Alkaline phosphatases	CE-based IMERs	3	N.D.	[85]
Acetylcholinesterase	CE-based IMERs	46[a]	0.9	[86]
Angiotensin-converting enzyme	CE-based IMERs	34[a]	N.D.	[87]

Not determined (N.D.); electrophoretically mediated microanalysis (EMMA); transverse diffusion of laminar flow profiles (TDLFP); Capillary electrophoresis based immobilized enzyme reactors (CE-based IMERs). [a] Includes crude product, natural extract, or Chinese traditional herb

In-line assays can also be performed with mixing of small volume pressure-injected plugs occurring by TDLFP.[88] Compared to EMMA, this method does not require prior knowledge of differential enzyme and substrate mobilities. The utility of this

strategy has been demonstrated first with an assay of a farnesyltransferase target[89] and was later demonstrated for measuring inhibition with other enzymatic targets.[80,81,90]

CE-based IMERs have also been demonstrated as useful for inhibition screening. Immobilized enzyme reactors can be fabricated within capillaries for on-line enzyme assays, saving enzyme in comparison to bulk assays (**Figure 1-6B**). CE-based IMERs for a wide variety of enzymes have been reported for characterizing enzyme inhibitors.[83–87,91,92] One study demonstrated the possibilities for multiplexing this CE-based IMER approach by fabricating an IMER of both immobilized adenosine deaminase and xanthine oxidase and was applied to screening of 20 natural extracts with a Z'-scores of 0.82 and 0.74, respectively. The separation was less than 3 min and the on-line incubation was 2.5 min. [82]

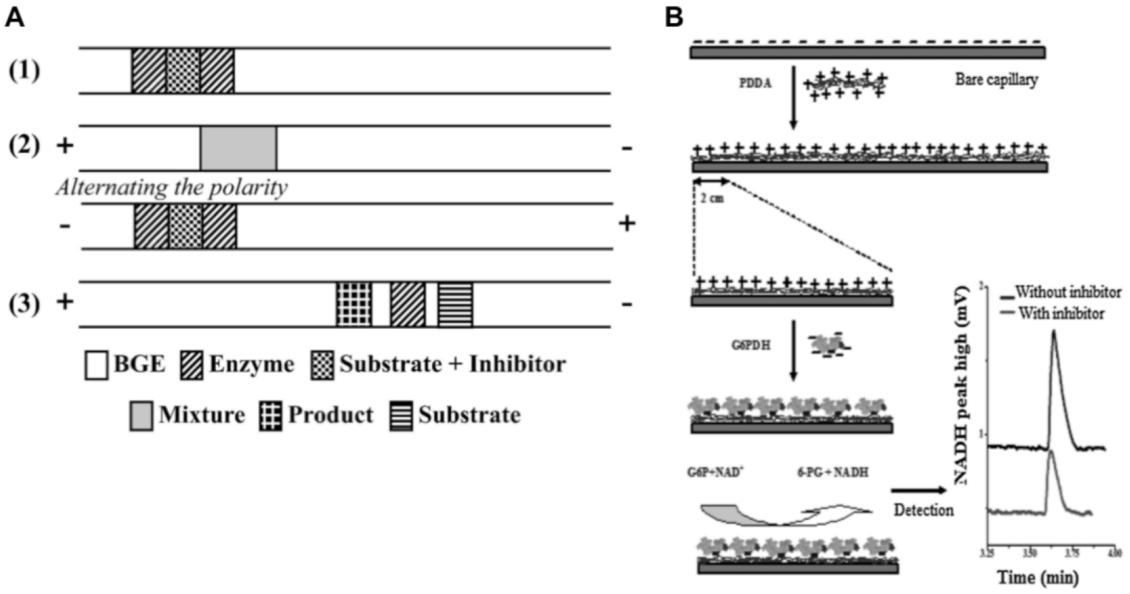

Figure 1-6. Schematic of an EMMA strategy for enzyme inhibitor screening where (1) is depiction of sequential injection of plugs (2) polarity switching for mixing between plugs (3) separation of enzyme, substrate and product (A).[14] Schematic of CE-IMER for GAPDH.[84] Reprinted with permission from reference [14] and [84]. Copyright 2011 American Chemical Society and Elsevier.

Affinity Interactions

Noncovalent binding between two molecules can induce a mobility shift allowing electrophoretic separation. Many different assay schemes have been demonstrated for detecting and quantifying affinity interactions by MCE.[1,93,94] Noncovalent interactions assayed by CE include protein-nucleic acid[1,12,93], protein-peptide[28,30,95], protein-protein [6,96–99], nucleic acid-small molecule[100,101], and protein-small molecule interactions[102–107]. Of these, a "mix and separate" approach, sometimes called affinity probe CE [106], is perhaps the most amenable for high throughput screening. If the kinetics of dissociation are slow in comparison to the separation time, distinct free protein and protein complex peaks are observed enabling quantification of the bound to free ratio. Rapid separations are therefore preferable for both throughput and maintaining the complex of interest. A limited number of affinity interaction-based screens have been reported (Table 1-2).

Table 1-2. Representative CE affinity interaction screens.

Target	Assay type	Compounds assayed	Separation Time [a]	Z-score	Reference
Tat-TAR	Commercial microchip platform	1	~3 min	N.D.	[12]
Hsp70-Bag3	APCE	3443	3 min	0.78	[6]
Bcl-X_L-Bid	CE-FA	105[b]	10 min	0.86	[28]
Hsp90α	CEfrag	609	10 min	0.6	[108]
Thrombin	PF-ACE	21	10 min	N.D.	[107]

Not determined (N.D.); affinity probe capillary electrophoresis (APCE); capillary electrophoresis-frontal analysis (CE-FA); fragment screening using capillary electrophoresis (CE-frag), partial filling affinity capillary electrophoresis (PF-ACE)

a. Does not include capillary regeneration time between samples.
b. Includes crude product, natural extract or Chinese traditional herb.

Affinity probe CE (APCE) on a microchip has been used to study protein-nucleic acid interactions.[12,94,95] In one example, the protein-nucleic acid interaction between human immunodeficiency virus 1 transactivator of transcription (Tat) and transactivation-

responsive RNA (TAR) was studied using a commercial microchip platform. Inhibition of the Tat-TAR complex was demonstrated using a known inhibitor and dose dependent inhibition of the Tat-TAR complex peak was observed, suggesting the potential application of this platform to screening of affinity complexes.[12]

Protein-protein interactions (PPIs) represent a large class of targets that were, until recently, considered intractable. It can be difficult to predict small molecule modulators of these interactions as they often occur with high affinities over large, flat surfaces. Recent success in targeting these interactions has led to an increased interest in screening against them.[109,110] CE has potential as a useful screening technique because of the capability of high efficiency separation of large molecules.

CE has been used in studies of amyloid aggregation[111–113], protein-peptide interactions[28,30,96], and full length PPIs [6,97–99,113]. Most of these studies have been proof of concept assays; however, one assay did investigate a screen of 3,443 compound library against a target PPI. In this study, a fluorescently labeled heat shock protein 70 (Hsp70) in complex with its co-chaperone Bcl2-associated athanogene 3 (Bag3) was separated by CE. The resulting screen yielded a 1.4% hit rate. A 3.4% hit rate was achieved for the same screen using flow cytometry protein interaction assay (FCPIA). The lower hit rate in the CE assay was attributed to the identification of detection interfering compounds that may be false positives in other assays, such as fluorescent test compounds in the screening library and unexpected aggregation of proteins which could be readily identified by visual inspection of the electropherograms (**Figure 1-2**). Comparable Z'-scores of 0.78 for CE and 0.86 for FCPIA were found for these parallel screening platforms. The CE assay was not optimized for throughput however, as it used a

commercial, single-channel CE system, and could only perform 220 assays/day. At this throughput CE is potentially more useful as a secondary screening platform.[6] In principle, such assays could be converted to parallel CE or MCE formats for higher throughput.

Although the APCE approach is most amenable to screening, CE-frontal analysis (CE-FA) has been used to measure affinity interactions. In CE-FA, relatively large volumes of equilibrated binding partner mixtures are injected. The large injection volume allows for maintenance of interaction during the separation because the free and complex zones are largely overlapping during the separation. The interaction between apoptosis regulatory, B-cell lymphoma 2 (Bcl-2) family proteins Bcl-X_L and BH3-interaction domain (Bid) was studied using a fluorophore-labeled peptide form of Bid. Quantification was achieved based on the plateau height of the free ligand. A high Z'-factor of 0.86 was determined for this method and a screen using sample pooling of 60 compounds with 10 compounds per sample was demonstrated with 10 min/sample separation times.[28]

Assays for small molecule ligand interactions with proteins, peptides, and nucleic acids have been demonstrated by monitoring the mobility shift of the large molecule in the presence of small molecule.[102–104] Small molecule mobility shift assays can be challenging, with some binding events only inducing small changes in large molecule mobility.[103] Still, fragment-based screening has been demonstrated by affinity CE (CEfrag).[105] Successful fragment library screening relies on the ability to detect small amounts of inhibition as well as assay compatibility with high concentrations of test compound. A screen of heat shock protein 90α (Hsp90α) by a mobility shift assay with competitive inhibition was successful applied to a fragment library screen. In this

method a small molecule affinity probe that is known to bind to the target molecule is used as an indicator of binding. When the affinity probe small molecule is unbound, it has a different migration time then when it is bound to its target. When another molecule competes with the affinity probe for target binding a mobility shift is observed and a hit is identified. For Hsp90α, using radicicol, a molecule known to interact with Hsp90α as the affinity probe, weaker affinity hits (>500 μM IC_{50} values) were identified using CE with UV detection versus with a fluorescence polarization assay in a screen of 609 compounds. The throughput of this screen was 100 samples/instrument/day using a 4-capillary instrument and a Z factor of 0.6 was determined.[108] Similarly, affinity CE was demonstrated for fragment based drug discovery targeting thrombin. In this method, the capillary was partially filled with a plug of target molecule, a plug of fragment was injected and a hit was identified based on a shift in migration time of the fragment in the presence of target.[107]

A number of obstacles still exist for developing CE methods for screening affinity interactions; the protein complex may dissociate during the separation, many interactions induce only a small shift in mobility, and proteins tend to adsorb to the wall of the fused silica capillary which, depending on severity can cause shifts in migration time as well as loss of signal. Capillary coatings are useful for reducing protein adsorption. A number of recent studies have successfully characterized capillary coatings several of which are compatible with physiological pH and avoid adsorption that was observed on bare-fused silica capillary.[114–117] Recently, a permanent coating for protein separation was observed to have an electroosmotic flow RSD of only 0.5% over one month.[118] Unfortunately, a coating that prevents adsorption of one protein may not be as effective at preventing

adsorption of a different protein[116,118] and replacing dynamic coatings between separations decreases throughput. The small mobility shift and protein adsorption issues must be overcome using conditions that maintain the non-covalent target interactions.

Target Protein-Protein Interactions

The CE methods should have wide use for different proteins. In this work, we have targeted chaperone proteins and transcription regulation machinery to test these methods.

Chaperone Proteins

Chaperone proteins are critical for maintaining proteostasis. Various heat shock proteins perform chaperone functions including binding, unfolding, disaggregation, and stabilization of target proteins.[119] Two such proteins, Hsp70 and Hsp90 perform chaperone functions regulated by a large number of co-chaperone binding partners. Hsp70 and Hsp90 have been implicated in cancer and neurodegenerative diseases making them potential therapeutic targets.[119–121]

Hsp70 function is regulated by interactions with Hsp40, nucleotide exchange factors[119] including Bcl-2 associated athanogene (Bag), and the ubiquitin ligase CHIP[122]. Interestingly, knockdown of Bag3 has been observed to decrease survival in cancer cell lines.[123] Benzothiazole rhodacyanine derivatives have been identified as small molecule inhibitors of Hsp70-Bag3 interaction.[124] These compounds bind to an allosteric site within the nucleotide-binding domain stabilizing the ADP state and preventing interaction of Hsp70 with Bag3.[125]

Hsp90 is notable among chaperone proteins for being a functional homodimer. Hsp90 undergoes dramatic nucleotide dependent structural rearrangements. For example, in the apo-nucleotide state the c-terminal domains of Hsp90 monomers interact, in the

ATP-bound state both the n-terminal and the c-terminal domains interact.[126] Hsp90 substrate binding is regulated by interactions with a large number of co-chaperones including p50 and FKBP52.[119,126] Heat shock organizing protein (HOP) serves as the link between Hsp70 and Hsp90 chaperone systems and is thought to be responsible for transferring client proteins from Hsp70 to Hsp90.[126] While these chaperone proteins are interesting biological targets with roles in cancer and neurodegeneration they also present an analytical challenge owing to the diversity of protein interaction affinities and binding interfaces.

KIX Domain of CREB-Binding Protein (CBP)

Transcription is regulated by protein-DNA and protein-protein interactions. One example is CREB-binding protein (CBP) which is a co-activator of transcription that interacts both with transcription factors and transcription machinery. The kinase inducible domain interacting domain (KIX) of CBP has been found to interact with a large number of transcription factors including c-myb, E2A, p53, and MLL.[127,128] CBP and transcription factors are thought to play a key role in tumors and neurological disorders.[129,130] Due to the role of the KIX domain in transcriptional activation targeting of its interactions is seen as of potential interest.[127,131]

Dissertation Overview

This work aims to simplify method development and increase throughput for analysis of protein-protein interactions by capillary and microchip electrophoresis. Difficulties in maintaining interactions during the separation are addressed by covalently cross-linking interacting proteins prior to electrophoresis. Improvements in capillary and microchip gel electrophoresis throughputs are also explored.

In Chapter 2, a covalent cross-linking approach is demonstrated to simplify method development for capillary electrophoresis of several protein-protein interactions with nanomolar dissociation constant (K_d) values. The strategy involves a 10 min formaldehyde cross-linking reaction and affords separation throughput of about 15 min/sample using capillary gel electrophoresis. The strategy was demonstrated for determination of dissociation constants and IC_{50} values for known interactions and inhibitors, respectively.

In Chapter 3, limitations of the method presented in Chapter 2 were addressed. The throughput of the above method was increased to about 1 min/sample, the cross-linking reaction time was decreased to 10 s, and the method was further applied to more diverse interactions with nanomolar to micromolar K_d values.

Chapter 4 presents the development of a microfluidic approach for further increasing the throughput of the protein cross-linking electrophoresis strategy by integrating segmented flow for sample introduction onto microchip gel electrophoresis device. Immiscible segmenting carrier phase was drained based on density using a novel device design. The device was then demonstrated for for enzyme and protein-protein interaction assays.

Chapter 5 discusses future directions for addressing the limitations of this work. Strategies for further improvements to separation and injection throughput are presented. Further, potential for label free and online protein cross-linking capillary electrophoresis assays are also discussed.

Chapter 2: Protein Cross-linking Capillary Electrophoresis for Protein-Protein Interaction Analysis

Introduction

Protein-protein interactions (PPIs) control many cellular functions. As a result, it is important to be able to quantify these interactions. It is also of interest to identify small molecule modulators of PPI for use as probes for chemical biology and as possible drugs. The diversity and transient nature of PPI can make them challenging to study. Several techniques have been developed for PPI analysis including flow cytometry protein interaction assays (FCPIA), isothermal titration calorimetry (ITC), fluorescence polarization, *in silico* methods, nuclear magnetic resonance (NMR), surface plasmon resonance (SPR), fluorescence resonance energy transfer (FRET) and AlphaLisa. Each of these techniques has strengths and weaknesses and can be chosen for different applications. For example, for screening chemical libraries to identify potential modulators of PPI, many of these techniques are impractical because of quantification, throughput, or sample consumption considerations. In this work we explore the use of protein cross-linking CE (PXCE) for detecting and quantifying PPIs.

PXCE is a variant of affinity probe capillary electrophoresis (APCE). In APCE, an equilibrated mixture of binding partners is electrophoresed to allow for detection of

non-covalent interactions.[93,106,132] APCE has been used to investigate many biomolecular interactions such as protein-protein[6,97,98,113], antibody-antigen[133–138], protein-DNA[114,135,139–141], protein-peptide[30,135] and protein-aptamer[115,142,143]. Typically, one binding partner is fluorescently labeled enabling sensitive detection by laser induced fluorescence (LIF). APCE offers advantages of low sample volume requirements, high throughput, and highly sensitive direct detection of free protein and protein complex. These advantages make APCE a potentially powerful approach for characterizing PPI and other non-covalent biomolecular interactions. The utility of this approach for screening for modulators of PPI was demonstrated in a study of the heat shock protein 70 (Hsp70) and Bcl-2 associated athanogene 3 (Bag3) interaction.[6] The CE assay was found to be more selective than an FCPIA screen based on the minimal perturbation of the proteins for the assay and the ability to discern fluorescent test compounds and protein aggregation in the CE data. These features eliminated many false positives.

Although possessing many advantages for detecting, quantifying, and screening PPIs, APCE is limited by the need to have separation conditions that both maintain protein interactions over the course of the separation and also prevent protein adsorption to the capillary. Strategies to minimize protein-wall interactions include capillary derivatization,[6,114,115,140] extreme pH,[144,145] surfactant additives[146] and high ionic strength buffers.[147,148] Techniques to minimize protein adsorption to the capillary are often not compatible with maintaining non-covalent protein interactions or require optimization for each protein binding partner of interest. As a result, it is often difficult and slow to develop CE methods for PPI, greatly limiting the use of this technique.

In this work, we examine protein cross-linking prior to CE separation for detecting and quantifying PPI. This process allows complexes to be formed under binding conditions and then separated under non-native or denaturing conditions, facilitating method development. Previously protein cross-linking prior to CE analysis has been used to check the success of cross-linking for different carbodiimide cross-linkers.[149] In another study, cross-linking prior to CE was used to screen for dimer formation in therapeutic antibody samples.[99] Good agreement was found for results by CE and size exclusion chromatography without cross-linking suggesting the potential for more in-depth, quantitative assays.

Here, the utility of PXCE was investigated for determining K_d of three protein-protein complexes: the antibody-antigen complex of lysozyme-anti-lysozyme, Hsp70-Bag3 heterodimer and heat shock protein 90 (Hsp90) homodimer. PXCE was also applied to quantify inhibition of PPIs with Hsp70-Bag3 binding site mutants and small molecule inhibitors. Formaldehyde was chosen as the cross-linking reagent because of its short reaction time and reactivity toward many amino acid residues.[150] The complexes chosen present different challenges and opportunities. Lysozyme and Bag3 have been identified as a difficult proteins to analyze using CE because they strongly adsorb to the inner wall of fused silica capillaries resulting in missing peaks[6] or poor peak shape[144]. Heat shock proteins including Hsp70 and Hsp90 and their co-chaperone interactions have been identified as potential drug targets.[121,151]

Experimental

Chemicals and Materials

Unless otherwise specified reagents were purchased from Sigma Aldrich (St. Louis, MO). Lysozyme, Alexa Fluor 488 5-SDP ester and Alexa Fluorophore 488 NHS ester were purchased from ThermoFisher Scientific (Waltham, MA). All separation and assay buffers were made using water deionized to 18 MΩ using a Series 1090 E-pure system (Barnstead Thermolyne Cooperation; Dubuque, IA).

Protein Purification and Labeling

Hsp70 and Bag3 were expressed and purified as previously reported.[6,152–154] Hsp90 was subcloned into pET28 vector to incorporate N-terminal 6x-His tag. Plasmid was transformed into BL21(DE3) One Shot start cells (Invitrogen; Carlsbad, CA) and purified on a Nickel-NTA column followed by size exclusion chromatography (SEC) on a HiLoad 16/600 Superdex 200 PG column (GE Healthcare; Piscataway, NJ). The concentrated SEC fraction was labeled with Alexa Fluor 488 NHS Ester according to manufacturer instructions and dialyzed into phosphate buffered saline, pH 7.4. Hsp70 and Hsp90 were labeled with Alexa Fluor 488 5-SDP ester. Lysozyme was incubated with a final concentration of 100 μg/mL fluorescein isothiocyanate (FITC) for 1 h at room temperature and dialyzed into phosphate buffer, pH 7.5.

Protein Cross-linking Capillary Electrophoresis

Protein samples were allowed to equilibrate in 25 mM HEPES, 10 mM KCl, 5 mM $MgCl_2$ and 0.3% (w/v) Tween-20, pH 7.5. Small molecules were dissolved in DMSO and spiked into protein samples to a final concentration of 1% DMSO for all dose response samples, including positive and negative controls. Samples were incubated for at least 15

min prior to cross-linking. Proteins were cross-linked at room temperature by addition of formaldehyde, prepared from paraformaldehyde, to a final concentration of 1% (w/v) formaldehyde for 10 min unless otherwise stated. Cross-linking reactions were quenched by adding Tris to a total concentration of 20 mM and, for gel electrophoretic analysis, 0.2% (w/v) SDS.

All CE experiments were carried out using a Beckman Coulter P/ACE MDQ (Fullerton, CA) equipped with a Sapphire laser (Coherent; Santa Clara, CA) with 488/520 nm $\lambda_{excitation}/\lambda_{emission}$ filters for LIF. Data were collected by 32 Karat software and analyzed using Cutter 7.0.[31] Binding data and IC_{50} curves were fit by non-linear regression using Prism 6.0 (GraphPad Software; San Diego, CA). All separations were carried out in 360 μm outer diameter fused silica capillary with 50 μm internal diameter for free solution electrophoresis and 40 μm internal diameter for gel electrophoresis separations (Polymicro Technologies; Phoenix, AZ). The total capillary length was 30 cm with 10 cm to detection window. Free solution electrophoresis of FITC labeled lysozyme (FITC-lysozyme) and anti-lysozyme was carried out in 10 mM sodium tetraborate, pH 10, electrophoresis buffer. Samples were injected by pressure at 0.5 psi for 5 s and electrophoresed with an applied field of 500 V/cm.

For gel electrophoresis separations of Hsp90 Alexa Fluor 488 (Hsp90-488), Hsp70 Alexa Fluor 488 (Hsp70-488) and Bag3 the capillary was pre-conditioned with 1 M NaOH, H_2O and UltraTrol LN (Target Discovery; Palo Alto, CA) for 3 min each followed by introduction of dextran sieving matrix (180 mM boric acid, 200 mM Tris, 1 mM EDTA, 13.8 mM SDS, 7% w/v 1.5-2.8 MDa dextran, 10% w/v glycerol) at 40 psi for 10 min. Samples were injected electrokinetically at 15 kV for 1 min and

electrophoresed with applied fields of 567 V/cm. Capillaries were regenerated by flushing with H_2O followed by preconditioning when a shift in migration time was observed, usually after 1 hour of use.

Isothermal Titration Calorimetry

Titrations were performed on a NanoITC 2G (TA Instruments; New Castle, DE). Data were collected using Nano ITCRun software and a dissociation constant value was calculated using NanoAnalyze software (TA instruments). The syringe contained 6 μM FITC-lysozyme for titration into 0.2 μM anti-lysozyme in the cell.

Results and Discussion

CE-LIF of Interacting Proteins

Hsp70, Hsp90 and lysozyme were fluorescently labeled to allow for sensitive LIF detection. We initially attempted separation of the free proteins and complexes with the binding partners by CE-LIF without cross-linking (**Figure 2-1 and 2-2**). For all three examples of interacting pairs, detection of complexes was difficult without cross-linking.

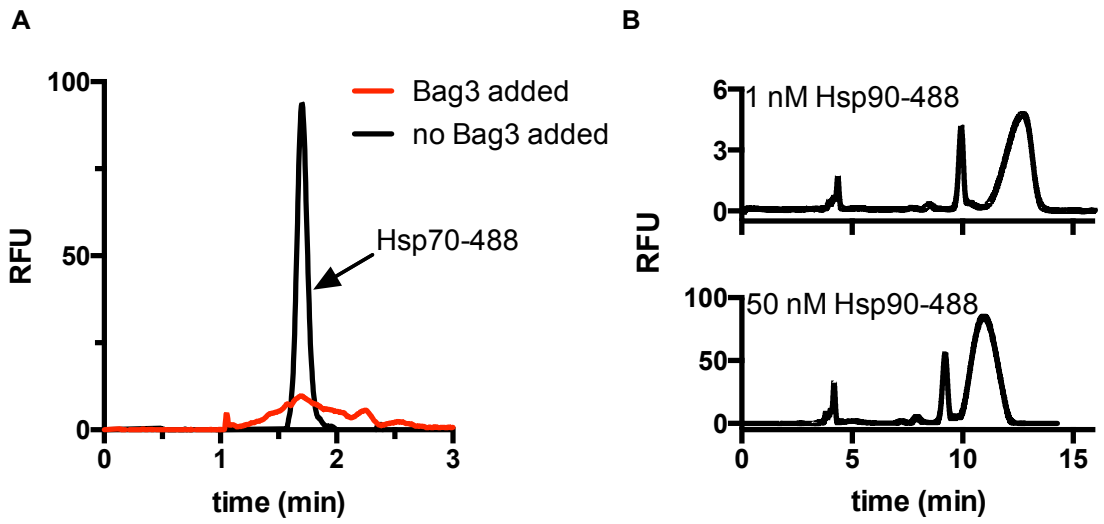

Figure 2-1. Free solution electrophoresis of chaperone complexes Hsp70-488-Bag3 (A) and Hsp90-488 homodimer (B). The electrophoresis buffer was 10 mM, pH 10 borate.

The Hsp70-Bag3 interaction has previously been identified as a difficult PPI for CE method development due to adsorption of Bag3 to fused silica capillary around pH 7.[6] We found adsorption of Bag3 to be a persistent problem, even at pH 10, so that no discernible complex peaks were observed in samples containing Hsp70-488 and Bag3 when using free solution CE (**Figure 2-1A**). Bag3 adsorption is likely a result of it being intrinsically disordered which is common with PPI targets.[155] (Previous study used capillaries covalently modified with a perfluorinated alkylating agent to prevent adsorption of Bag3.) With free solution electrophoresis of Hsp90-488 at pH 10, protein adsorption was not observed; however, monomeric Hsp90-488 was not readily resolved from the dimeric form suggesting very similar electrophoretic mobilities of dimer and monomer (**Figure 2-1B**). A free solution CE separation of FITC-lysozyme-anti-lysozyme at pH 10, in the absence of cross-linking, results in multiple unresolved peaks possibly

due to dissociation and association occurring on the time scale of the separation (**Figure 2-2C**).

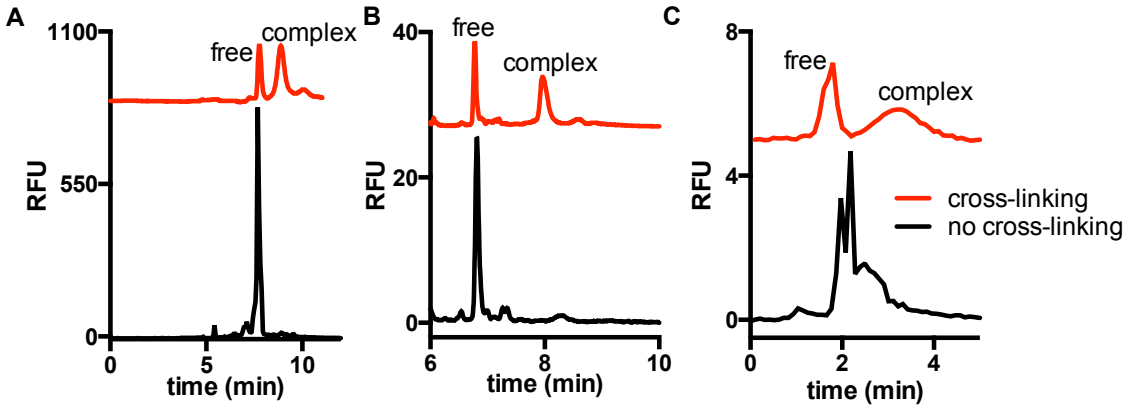

Figure 2-2. Electropherograms with (red trace) or without (black trace) cross-linking of protein complexes of (A) Hsp70-488-Bag3, (B) Hsp90-488 dimer, and (C) FITC-lysozyme-anti-lysozyme. Separation was performed with (A,B) dextran gel and (C) free solution with pH 10, 10 mM borate electrophoresis buffer. Cross-linking was with 1% formaldehyde for 10 min in HEPES buffer. Table 2-1 provides resolution between free and complex peaks for the cross-linked electropherograms.

A potentially better approach to separation of protein complexes is capillary gel electrophoresis (CGE) in presence of SDS, e.g. using an entangled polymer solution as a sieving media (SDS-CGE).[156] SDS-CGE facilitates predictable protein separation based on size; however, the denaturing conditions disrupt PPI so that Hsp70-Bag3 and Hsp90 dimer protein complexes could not be detected. Indeed, only free protein was detected for mixtures of these interacting proteins separated by SDS-CGE (**Figure 2-2**). A similar effect was observed for FITC-lysozyme-anti-lysozyme (**Figure 2-3**). The results with the non-cross-linked complexes illustrate the different challenges of developing APCE assays for PPI.

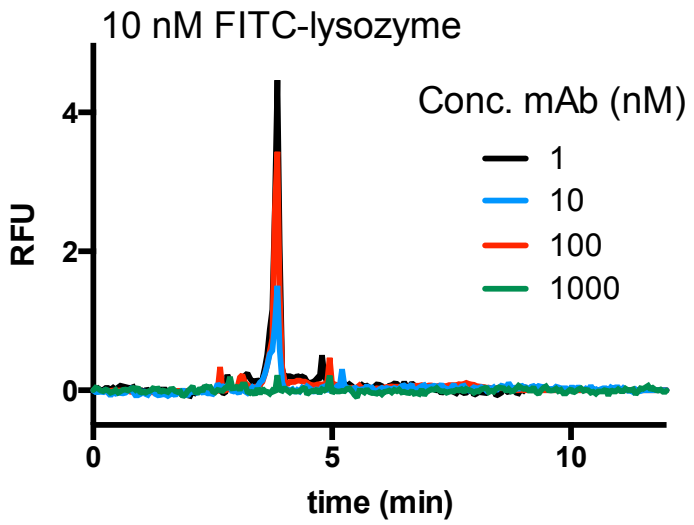

Figure 2-3. Capillary gel electrophoresis separation of FITC-lysozyme immunocomplex.

Cross-linking Conditions.

To overcome the challenges associated with detection of non-covalent interactions by CE, interacting proteins were cross-linked prior to electrophoresis. Covalent cross-linking of interacting proteins with formaldehyde allowed for the direct detection of free protein and protein complex using the denaturing gel separation for the chaperone complexes (**Figure 2-2A,B**) and a high pH electrophoresis buffer for FITC-lysozyme-anti-lysozyme (**Figure 2-2C**), with acceptable resolution (Table 2-1). This result shows that cross-linking facilitates detection of interacting proteins by free solution CE or SDS-CGE separations.

Table 2-1. Resolution of free proteins from protein complexes.

Complex	Resolution
Hsp70-Bag3	1.0
Hsp90 homodimer	2.0
Lysozyme-anti-lysozyme	1.1

The effect of cross-linking conditions, such as reaction time and formaldehyde concentration, on amount of complex detected was determined for the Hsp70-Bag3, lysozyme-anti-lysozyme and Hsp90 homodimer (**Figure 2-4**). In this study, the amount of complex formed was quantified as the complex peak area as a percentage of total peak area to account for any artifacts from instability of the laser source or injection variability. It has previously been reported that different PPIs require different cross-linking conditions;[157] however, most formaldehyde cross-linking assays, such as chromatin immunoprecipitation and mass spectrometry, utilize between 10 and 20 min of cross-linking with 0.05-1% formaldehyde.[158,159] A range of reaction conditions can be easily tested with CE separation to determine conditions that favor high yields for a particular PPI. Cross-linker concentration and reaction time are considered largely complimentary with a general increase in yield expected for an increase in either.[99,150,157]

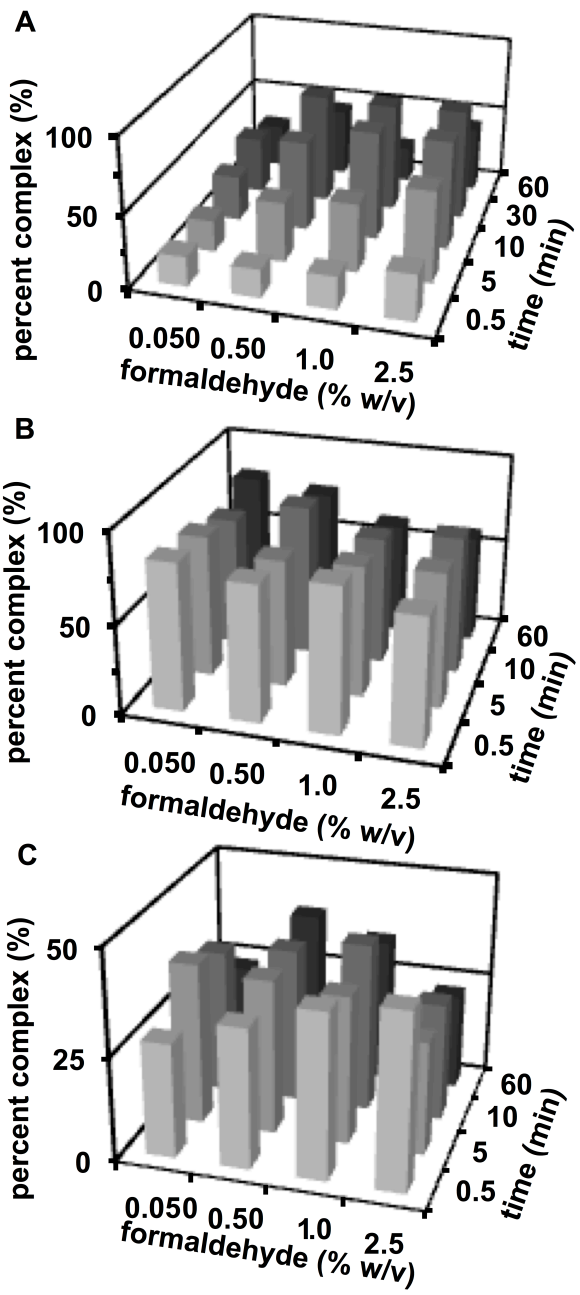

Figure 2-4. Dependence of (A) 25 nM Hsp70-488 and 100 nM Bag3 (B) 50 nM Hsp90-488 and (C) 10 nM FITC-lysozyme and 20 nM antibody on dimer complex detected on concentration of formaldehyde and cross-linking reaction time.

An increase in Hsp70-Bag3 complex peak area was detected with increasing formaldehyde concentration or time up to 2.5% formaldehyde or 30 min of cross-linking, respectively, while FITC-lysozyme-anti-lysozyme appeared relatively insensitive to the times assayed with 0.5 to 1% formaldehyde. The amount of Hsp90 dimer complex observed was fairly stable for all reaction times and concentrations assayed. Interestingly, the amount of complex detected decreased if the cross-linking reaction was allowed to proceed for 60 min. A trend toward decreasing apparent yields of complex at high cross-linking times has been previously reported by mass spectrometry.[157] This effect may be due to the formation of higher molecular weight aggregates, which are not injected onto the gel columns. For all complexes, the amount of complex observed was within a range of 13% for 10 min of cross-linking reaction with 0.5-2.5% formaldehyde. These results show that, at least for these proteins, finding conditions for maximal complex formation is straightforward and the results will be stable over a wide range of conditions.

To favor high yields of cross-linking and short reaction times, an intermediate cross-linking reaction condition of 10 min and 1% formaldehyde was chosen for further assay testing. To minimize artifacts when cross-linking high concentrations of protein[99,150], interacting proteins were investigated in the nanomolar to low micromolar concentration range. This concentration range is also more useful for determining quantitative binding data for many proteins.

PXCE fundamentally requires cross-linkable residues in the protein-protein interaction site. Although formaldehyde is efficient and reacts with many residues, other PPIs may benefit from different cross-linkers with longer spacer arms or more controlled reactivity.[160] Information about the PPI site may facilitate the choice of cross-linker.

Determination of Binding Affinities

To determine if PXCE allows for quantitative affinity information to be obtained, saturation binding assays were performed and the data fit by non-linear regression to determine K_d (**Figure 2-5**).

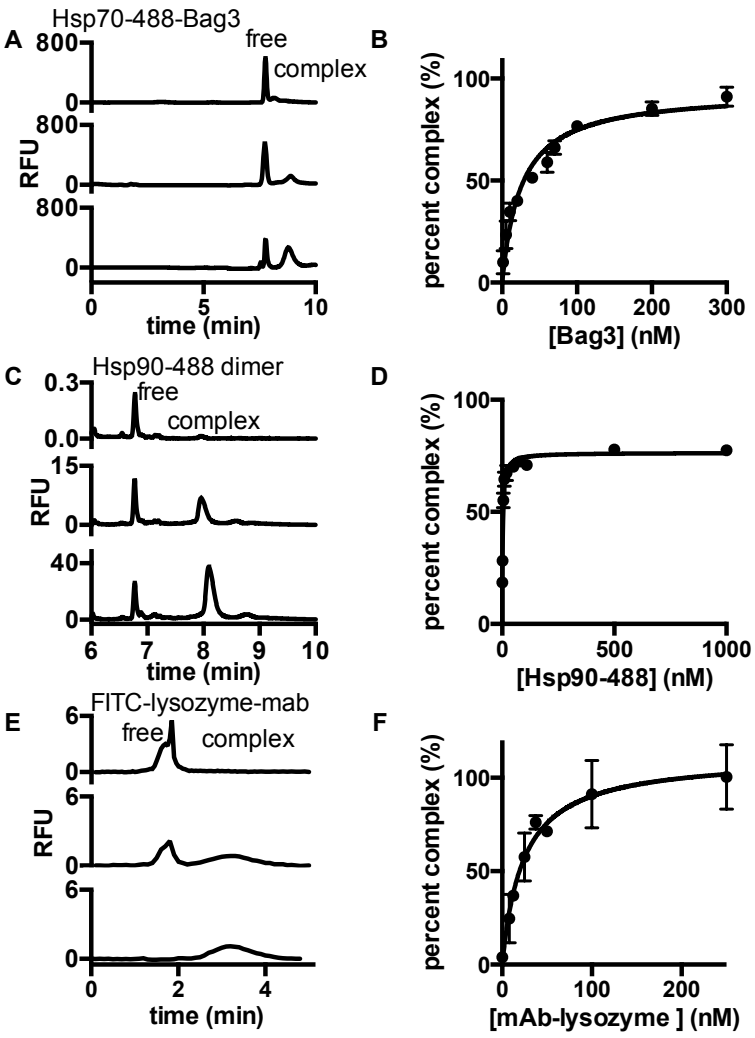

Figure 2-5. Determination of dissociation constant (K_d) for (A,B) Hsp70-488-Bag3 (C,D) Hsp90-488 dimer and (E,F) FITC-lysozyme-antibody. Electropherograms for (A) 25 nM Hsp70-488 at increasing concentrations of Bag3, (C) 1, 20 and 100 nM Hsp90-488 and (E) 10 nM FITC-lysozyme with increasing concentrations of monoclonal antibody (mAb). Non-linear regression determined a K_d of (B) 25 ± 5 nM for Hsp70-488-Bag3, (D) 2.6 ± 0.3 nM for Hsp90-488 and (F) 24 ± 3 nM FITC-lysozyme-antibody. Error bars are standard deviation (n = 3).

Hsp70-488 and Bag3 were found to interact with a K_d = 25 ± 5 nM by PXCE. Previously the K_d for this pair has been reported as 23 ± 8 nM with Hsp70-488 by APCE and 15 ± 2 nM with unlabeled Hsp70 by ITC, both without cross-linking.[6] Similar K_d values were found using 5, 10 and 20 min cross-linking reactions (**Figure 2-6, Table 2-2**).

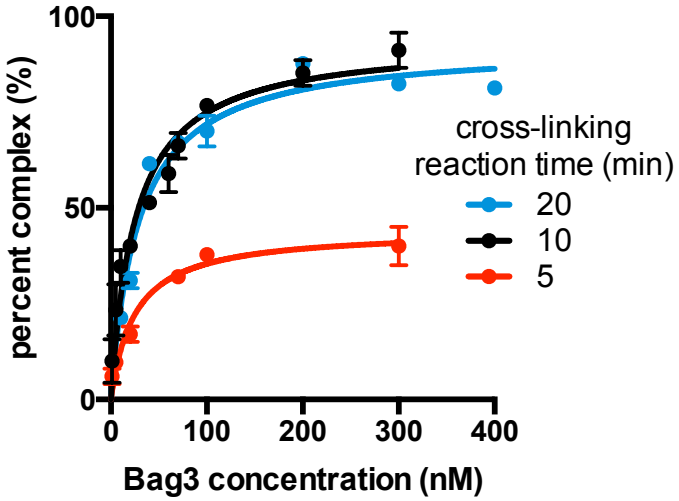

Figure 2-6. Saturation binding assays for Hsp70-488-Bag3 at different 1% formaldehyde reaction times. All samples contain 25 nM Hsp70-488, error bars are standard deviation (n = 3).

Table 2-2 Dependence of measured K_d of Hsp70-488-Bag3 interaction on cross-linking reaction time using 1% formaldehyde.

Cross-linking reaction time (min)	$K_{d,\ Hsp70\text{-}Bag3}$ (nM)
5	25 ± 8
10	25 ± 5
20	29 ±6

Hsp90-488 was found to form a homodimer with K_d = 2.6 ± 0.3 nM by PXCE. The K_d of Hsp90 homodimerization was previously reported to be 60 ± 12 nM by size exclusion chromatography. In this technique, association and dissociation occur over the timescale of the separation, and the elution time is used as an indicator of the degree of

dimerization.[161] A dissociation constant for the Hsp90 homodimer could not be obtained by ITC possibly due to the limitations with quantifying homodimers with nanomolar K_d values by ITC. More recently, a K_d value of 1.29 nM was reported for Hsp90 dimerization.[162] The K_d value determined for FITC-lysozyme-anti-lysozyme by PXCE was determined to be 24 ± 3 nM by PXCE and 17 ± 2 nM by ITC with 1:2 antibody to FITC-lysozyme stoichiometry (**Figure 2-7**). Thus, for Hsp70-Bag3 and FITC-lysozyme-anti-lysozyme PXCE gave K_d values similar to ITC, which used non-cross-linked proteins. The largest discrepancy was for Hsp90 dimerization and may be due to differences in the conditions used for the interacting proteins.

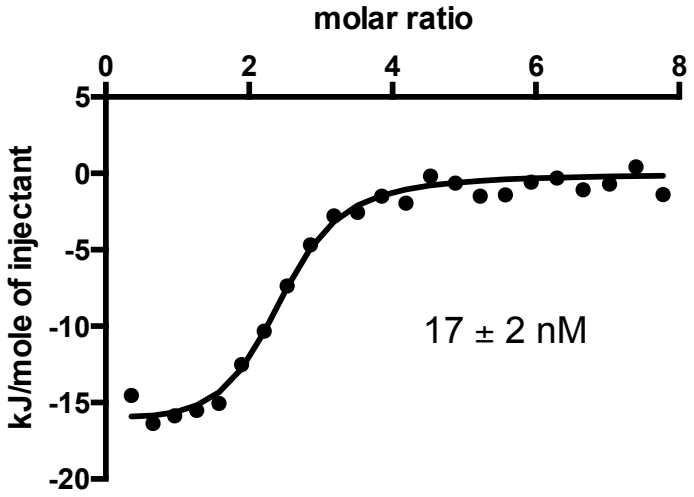

Figure 2-7. Calorimetric isothermal-titration measurement of FITC-lysozyme interaction with anti-lysozyme.

To determine if PXCE is useful for ranking PPI affinities, a competitive binding experiment was carried out with Hsp70 proteins containing mutations in key residues within the Bag3 interaction site that have previously been reported to inhibit Hsp70-Bag1 interactions (**Figure 2-8A**).[163] Unlabeled wild type and mutant Hsp70 were titrated into a fixed concentration of Bag3 and Hsp70-488 to determine the affinity of unlabeled Hsp70

for Bag3. In these experiments, adding unlabeled Hsp70 variants decreased the complex peak area for Hsp70-488 allowing quantification. A higher concentration of mutant Hsp70 than wild type Hsp70 was required to compete with the Hsp70-488 for Bag3 binding (**Figure 2-8A**). The data were normalized to positive (no Bag3 added) and negative controls (no unlabeled Hsp70) to quantify the percent inhibition. The inhibitory constant (K_i) was determined to be 9 ± 2 nM for unlabeled wild type Hsp70, 160 ± 60 nM for Hsp70 E,D 283, 292 A,A and 400 ± 200 nM for Hsp70 R,R 258,262 A,A by PXCE. The inhibitory constant for the unlabeled wild type Hsp70 is lower than the K_d found for the Hsp70-488, in agreement with the K_d = 15 ± 2 nM previously reported by ITC for the unlabeled Hsp70-Bag3.[6] For comparison, inhibitory constants were determined by FCPIA with similar K_i = 15 ± 8 nM determined for the wild type and 190 ± 30 for the E,D 283, 292 A,A mutant and 900 ± 300 for the R,R 258, 262 A,A mutant. In FCPIA one binding partner is immobilized on a bead while the other is fluorescently labeled, the binding partners are incubated and a flow cytometer is used to determine bead associated fluorescence. There are multiple differences in the PXCE and FCPIA assay formats including different fluorescent labels and the requirement of FCPIA to immobilize one of the binding partners on a bead, which could interfere with the PPI affinity. Despite these assay differences, the rank order of FCPIA and PXCE for the wild type and mutant interactions is the same (**Figure 2-8B**). K_is were also in good agreement with the largest discrepancy being a factor of two higher K_i for the Hsp70 R,R 258 262 A,A mutant by FCPIA.

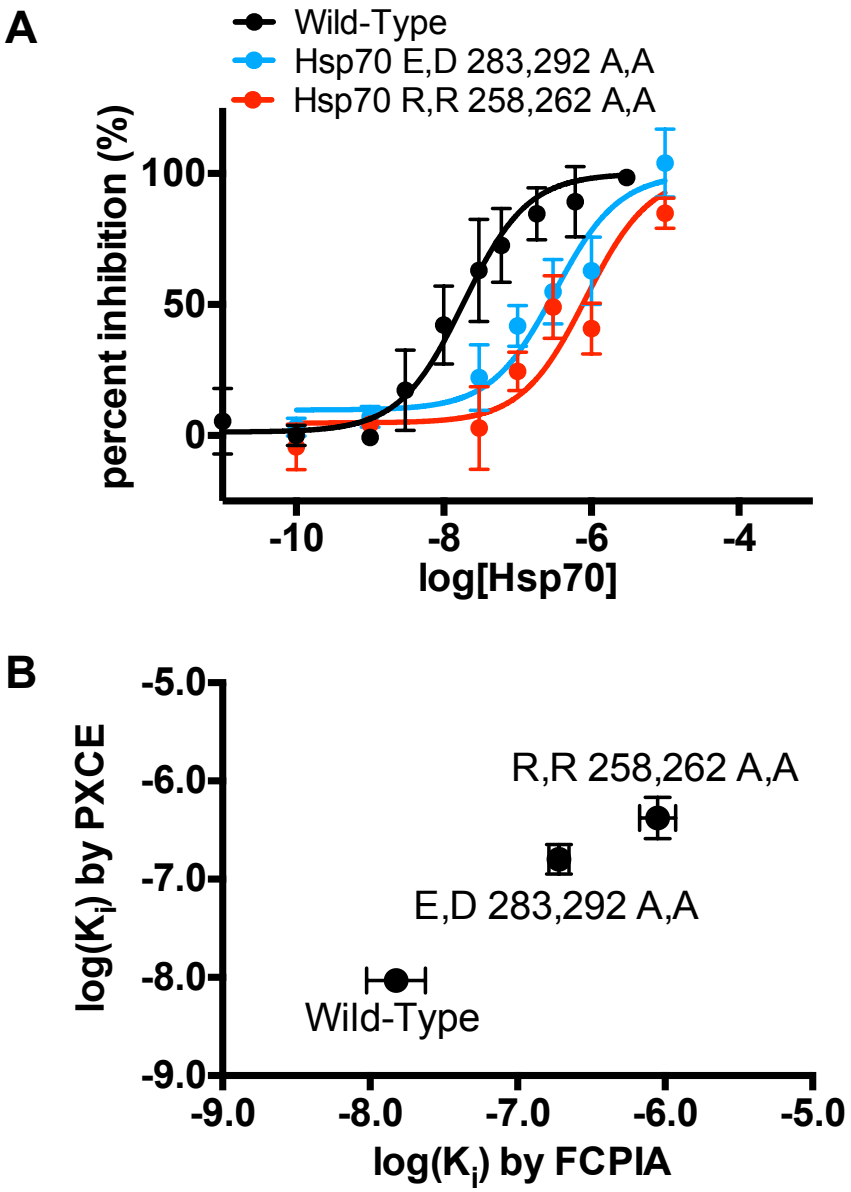

Figure 2-8. Determination of inhibition constant (K_i) of Hsp70 proteins by (A) PXCE. Increasing concentration of unlabeled Hsp70 (Wild-Type), Hsp70 E,D 283, 292 A,A or Hsp70 R,R 258, 262, A,A with 25 nM Hsp70-488 and 50 nM Bag3. Error bars are standard deviation (n = 3). (B) Comparison of K_i values obtained by PXCE and FCPIA.

Quantification of PPI Small Molecule Inhibitors

We next examined the possibility of using PXCE to determine the inhibition of PPI by small molecules. We tested 3 compounds that are known to inhibit the Hsp70-Bag3 interaction: JG-311, JG-98, and JG-231.[164–166] As shown in Figure 2-9, PXCE allowed detection of protein complex inhibition for these compounds. IC_{50} values were determined to be 1.3 ± 0.1 µM, 800 ± 200 nM and 400 ± 200 nM for JG-231, JG-98 and JG-311, respectively. The small molecules were all found to have similar IC_{50} values with similar associated errors by dose response using both PXCE and FCPIA assays (**Figure 2-10**).

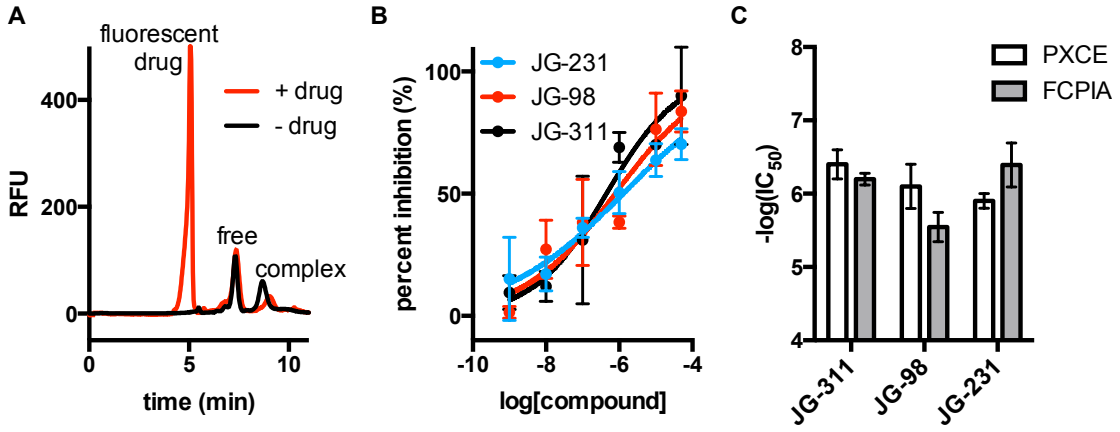

Figure 2-9. Quantification of small molecule inhibitors by PXCE. Electropherograms of (A) Hsp70-Bag3 negative control and Hsp70-488-Bag3 in the presence of fluorescent inhibitor. (B) Dose response curves for JG-231, JG-98 and JG-311. Log(IC_{50}) values were determined to be -5.9 ± 0.1 for JG-231, -6.1 ± 0.3 for JG-98 and -6.3 ± 0.2 for JG-311. JG-258 was used as negative control and 1 µM unlabeled Hsp70 was used as a positive control. Error bars are range of two trials. (C) Comparison of IC_{50} values obtained by PXCE and FCPIA.

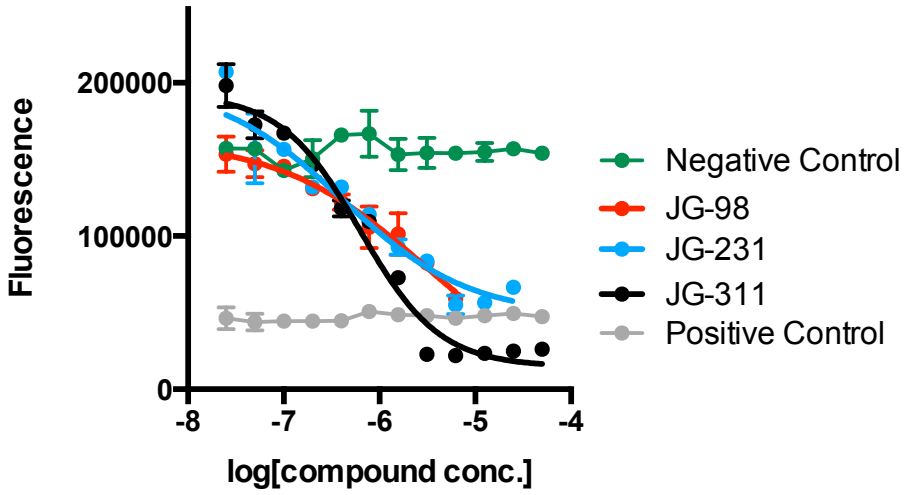

Figure 2-10. FCPIA data of small molecule Hsp70-Bag3 inhibitors JG-98, JG-231 and JG-311. Error bars are range of two trials.

These experiments also illustrate a potential advantage of PXCE for screening of new modulators of PPI. All of the tested molecules are fluorescent. Fluorescent drug molecules can interfere with detection of PPI modulators in many fluorescence assays. PXCE has the advantage of identifying potentially interfering fluorescent small molecules on the basis of extra peaks and allows for separation of the fluorescent small molecules from free protein and protein complex. Using a gel electrophoresis separation, small molecule compounds migrated much more rapidly than the high molecular weight proteins (**Figure 2-9A**) allowing for quantification of inhibitor potency despite fluorescence of small molecule. The denaturing gel conditions likely also promoted dissociation of the small molecule from the protein allowing for separation without quantitative interference. The limiting factor is that strongly fluorescent molecules can dominate the electropherograms at high concentrations. In this case, the assay allowed for quantification of free and bound protein peaks for up to 50 μM JG-311, JG-98 and JG-231.

Implications and Limitations

This work demonstrates the utility of formaldehyde cross-linking for nanomolar interaction affinities. It has been reported that equilibrium shifts are minimized and quantitative information is attainable with cross-linking for high affinity complexes when free proteins that react with the cross-linker do not then bind and cross-link to other proteins and when high efficiency cross-linkers are used in large excess.[167] Cross-linking of rapidly dissociating PPIs may be challenging as it has been reported that such PPIs are not readily captured with formaldehyde cross-linking.[168] Faster reacting reagents may be preferable for such cases to eliminate the chance of complex dissociation or additional complex formation. Despite these caveats, the data presented suggest that formaldehyde with PXCE will be broadly useful for different types of proteins and for different applications such as affinity determinations and detection of small molecule modulators.

This work demonstrated the application of PXCE to dimers and immunocomplexes; however, it may be possible to investigate more complex interactions using PXCE. In many cases multimeric complexes are of interest and alter protein function. As long as the proteins remain within the size range of gel used, it should be possible to detect and quantify the various complexes. PXCE may also be useful for studies of amyloid aggregates which have previously been investigated by CE.[111,113]

Conclusion

PXCE allows for quantifying protein-protein interaction affinities of target complexes including the lysozyme-anti-lysozyme immunocomplex, Hsp70-Bag3 heterodimer and Hsp90 homodimers. CE of protein complexes that are not cross-linked, as in traditional APCE, can be limited by the difficulty of developing methods that

maintain complexes but also allow separations. Use of cross-linking allows for simplified method development compared to APCE by making PPIs amenable to harsh separation conditions and separation times longer than the typical time-scale of the PPI. This development should make PXCE, with the associated advantages of speed, low sample consumption, resolution, and quantification, applicable to a wider range of proteins and accessible to more labs. CE-LIF allows for sensitive detection of PPIs with the requirement of having binding partners be fluorescently labeled for LIF detection. Quantitative information can be obtained for small molecule modulators including fluorescent molecules suggesting that PXCE may be a valuable strategy for characterizing such molecules. CE, especially in microchip format, has the advantage of providing rapid separations, suggesting the possibility of use of PXCE for high-throughput screening.[99,169]

Chapter 3: Protein Cross-linking Capillary Electrophoresis at Increased Throughput for a Range of Protein-Protein Interactions

Reproduced from Ref. [170] (Ouimet, C. et al. *Analyst* **2018**, *143*, 1805)
with permission from the Royal Society of Chemistry.

Introduction

Many proteins participate in protein-protein interactions (PPIs) of varying affinities and complexities. Although a variety of methods for PPI analysis exist, most have limitations such as requiring large amounts of protein sample, utility only in a narrow affinity range, or suitability for analysis of only one interaction at a time. Affinity Probe Capillary Electrophoresis (APCE) has the potential to overcome these limitations and become a useful tool for measurement and screening of PPIs. In APCE, one of the binding partners is labeled with a fluorophore, pre-equilibrated with binding partner, and then analyzed by capillary electrophoresis with laser induced fluorescence detection (CE-LIF) so that free and bound proteins can be detected.[106] APCE is an attractive platform for addressing challenges in PPI analysis as sample requirements are low, complexes of varying affinity are tractable, and the separation component provides resolution between different complexes.

APCE method development for PPIs can be difficult if electrophoretic mobility changes upon protein binding are small, proteins adsorb to the capillary wall, or complexes dissociate during the separation. Protein adsorption causes irreproducibility

and distorts peak shapes and areas preventing accurate quantification. Conditions that mitigate adsorption, such as extreme pH or SDS-denaturation with sieving separation, are not generally compatible with native protein interactions. Complex dissociation during separation is problematic for transient interactions where complex dissociation occurs on the timescale of the separation. Identification of conditions that are suitable for separation and maintenance of multiple interactions is even more challenging. Quantification of multiple peptides binding to the same protein has been reported by CE;[30] however, APCE of multimeric protein-protein complexes has not been reported. As a result of these challenges, APCE is not yet a widely used method for analysis of PPIs.

Previously we reported a modified APCE method, termed protein cross-linking capillary electrophoresis (PXCE), which simplified method development and may be more generally applicable for PPI analysis. In this method, interacting proteins are covalently cross-linked prior to electrophoresis. By decoupling the binding reaction and separation step, it is possible to use harsh separation conditions, such as denaturing capillary gel electrophoresis (CGE), which can reliably resolve protein complexes based on size using standard conditions. The original report of PXCE used cross-linking with formaldehyde for 10 min and was demonstrated for analysis of dimeric PPIs with low nanomolar K_d values.[171] As reported here, these conditions are limited to high affinity PPIs. An ideal method would allow for the quantification of low to high affinity PPIs as well as complexes that consist of higher order oligomers. Also, the method required at least 10 min for gel separation, limiting its throughput.

Here we report a PXCE method capable of quantitative analysis of PPIs with low nM to low μM K_d values by using glutaraldehyde as the cross-linker, a reagent previously

demonstrated to have rapid reaction kinetics and high yields.[172,173] We also demonstrate higher throughput CGE through use of a lower viscosity separation media and overlapping injections so that individual assays can be completed in 1 min. Finally we demonstrate the potential for analyzing multimeric complexes. The method is demonstrated on an array of chaperone and transcription factor proteins including heat shock protein 70 (Hsp70) homodimer, Hsp70-heat shock organizing protein (HOP), Hsp70-bcl2 association athanogene 3 (Bag3), heat shock protein 90 (Hsp90) homodimer, Hsp70-c-terminus of Hsp70 interacting protein (CHIP), KIX domain of CREB-binding protein (KIX)-E2A17, and KIX-c-Myb.

Experimental

Materials and Reagents

All reagents were purchased from Millipore Sigma (St Louis, MO), unless otherwise specified. All buffers were made using 18 MΩ water deionized by a Series 1090 E-pure system (Barnstead Thermolyne, Dubuque, IA).

Protein Purification and Labeling

Hsp70 and Hsp90 were purified and labeled with AlexaFluor488 as previously described.[171,6] Recombinant human CHIP, HOP, and HOP mutants were purified as described previously.[174] The peptides c-Myb and E2A17 were synthesized using 9-fluorenylmethoxycarbonyl (Fmoc) solid phase synthesis with CLEAR-Amide Resin (Peptides International, Inc.). c-Myb (FITC-βAla-KEKRIKELELLLMSTENELKGQQALW-NH_2) and E2A17 (FITC-βAla-GTDKELSDLLDFSAMFS-$CONH_2$) were FITC labeled, dried under nitrogen, precipitated, washed with cold ether, purified by reverse phase HPLC, lyophilized and

dissolved in DMSO. The KIX domain of mouse CREB-binding protein was expressed and purified as previously described,[128] for a resulting molecular weight of 12 kDa.

Protein Cross-linking

Proteins were allowed to equilibrate in assay buffer at room temperature for at least 30 min prior to cross-linking. For nucleotide state dependence experiments proteins were incubated with either 10 mM ATP or 10 mM ADP. For KIX-c-Myb and KIX-E2A17 interaction the assay buffer was 10 mM sodium phosphate, 100 mM NaCl, pH 6.8. For Hsp70-HOP the assay buffer was 50 mM HEPES, 75 mM NaCl, 0.001% Triton X pH 7.4. For all other PPIs an assay buffer of 25 mM HEPES, 10 mM KCl, and 5 mM $MgCl_2$, pH 7.5, was utilized. Cross-linking was carried out at room temperature by a 1:20 dilution of 40% w/v glutaraldehyde to a final concentration of 2% w/v glutaraldehyde, unless otherwise specified. The cross-linking reaction was quenched with 800 mM Tris after 10 s for a final concentration of 400 mM Tris unless otherwise stated. Lastly, SDS was added prior to injection to a final concentration of 0.2% w/v for sieving separations.

Capillary Electrophoresis

A Beckman Coulter P/ACE MDQ Capillary Electrophoresis instrument (Fullerton, CA) was used for all experiments. The excitation wavelength filter was 488 nm and the emission wavelength filter was 520 nm. Fused silica capillary (Polymicro Technologies; Phoenix, AZ) was 360 μm outer diameter 40 μm inner diameter unless otherwise stated. The total capillary length was 30 cm and the capillary length to detector was 10 cm. Electropherograms were acquired using 32 Karat software (Beckman Coulter), were analyzed using Cutter 7.0 software,[31] and data were fit using GraphPad Prism 7.

For PXCE separations the sieving media was 180 mM tris, 200 mM borate, 1 mM EDTA, 13.8 mM SDS, 7% dextran (1,500-2,800 kDa), and 10% glycerol unless otherwise specified. Samples were introduced by hydrodynamic injection at 5 psi for 15 s. A field of 567 V/cm was applied for separation. Capillaries were preconditioned by sequentially rinsing with water, hydrochloric acid, water, sodium hydroxide, water, UltraTrol LN (Target Discovery, Palo Alto, CA), and finally gel media. Capillaries were reconditioned after a noticeable shift in migration time was observed, typically after one hour of continuous operation.

For affinity probe capillary electrophoresis (APCE) without cross-linking the capillary was conditioned sequentially with sodium hydroxide, water, and run buffer. The running buffer was 25 mM HEPES, pH 7.5. Samples were introduced electrokinetically with an applied voltage of 5 kV for 5 s. The separation field was 1,000 V/cm. The capillary was reconditioned between injections with sodium hydroxide followed by running buffer.

For increased throughput PXCE, the sieving media was 90 mM Tris, 100 mM borate, 1 mM EDTA, 13.8 mM SDS, 3.5% dextran (1,500-2,800 kDa), 5% sorbitol and a 25 μm inner diameter 360 μm outer diameter capillary with 30 cm total length and 10 cm to detector was used. Samples were introduced sequentially by hydrodynamic injection for 15 s followed by separation at 1 kV/cm.

Size Exclusion Chromatography

Size exclusion chromatography (SEC) was carried out on an Agilent 1100 (Santa Clara, CA) using a TSKgel SuperSW3000 column (Millipore Sigma) with a flow rate of 0.3 mL/min and a sample injection volume of 1 μL. Detection was by UV absorbance at 280

nm. The mobile phase was 0.05% sodium azide, 0.1 M sodium sulfate, 0.1 M sodium phosphate, pH 6.7. Data were sampled at 20 Hz with a 14-bit data acquisition card (National Instruments, Austin, TX). Chromatograms were acquired using an in-house LabView (National Instruments, Austin, TX) program.

Results and Discussion

Cross-linking Conditions and Characterization of Non-specific Interactions

It has been reported that for highly dynamic interactions, formaldehyde cross-linking is not effective because of an insufficiently fast reaction under certain conditions.[168] If the cross-linking reaction kinetics are not much faster than the dissociation kinetics, then the fraction of complex cross-linked will be lower than that present under equilibrium conditions.[167] Glutaraldehyde reacts rapidly at high cross-linker concentration[175] which is expected to minimize under-cross-linking, even of transient complexes[173]. We hypothesized that such a reaction might be better able to capture complexes for a PXCE experiment. We tested the hypothesis that glutaraldehyde would be a sufficient cross-linker for the highly dynamic interaction between Hsp70 and HOP which has previously been observed to have fast dissociation and association kinetics.[176,177] We found 10 min of formaldehyde cross-linking was insufficient to covalently capture this interaction; however, a 10 s reaction with glutaraldehyde led to a large amount of complex being detected (**Figure 3-1**).

We then tested the effect of glutaraldehyde concentration and reaction time on yield of complex for three interactions with K_d values in the low μM range: Hsp70 homodimer, Hsp70-HOP and c-Myb-KIX. These results showed that the highest yields of covalent complex were achieved with less than 1 min of cross-linking with 2% w/v

glutaraldehyde. Interestingly, for both Hsp70-HOP and c-Myb-KIX, reactions as short as 10 s were sufficient for the highest yields of cross-linked product (**Figure 3-1**).

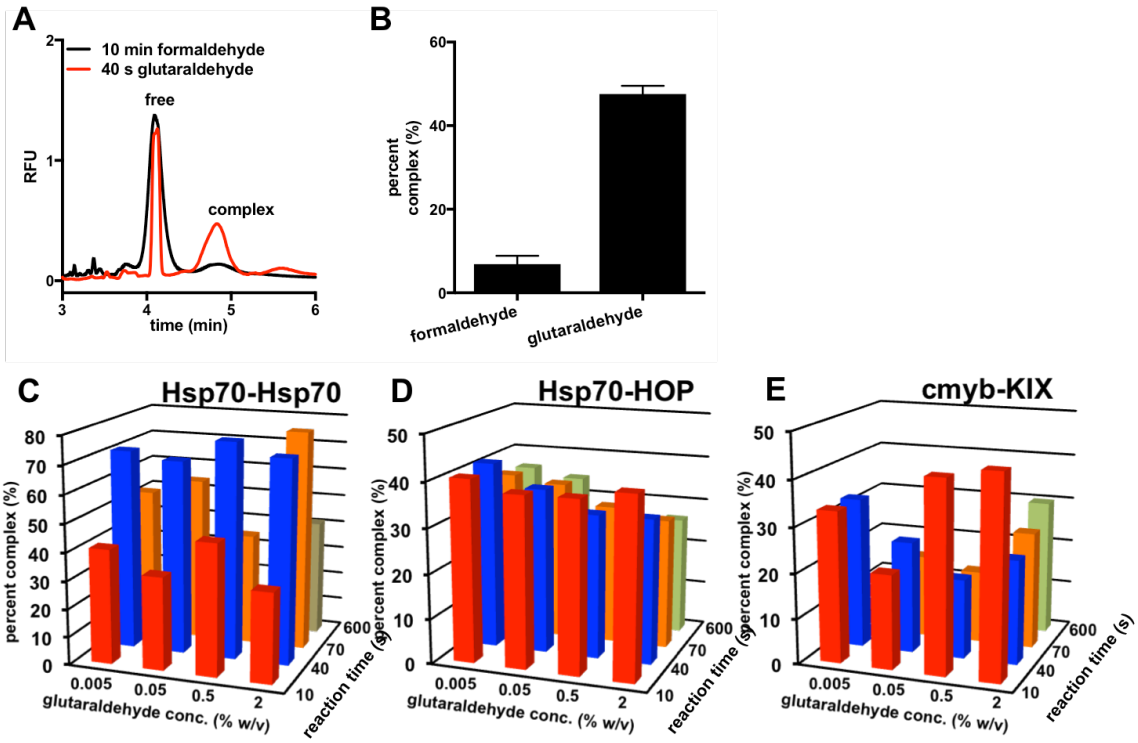

Figure 3-1. Evaluation of glutaraldehyde cross-linking yield for low affinity PPIs. Comparison of yield of Hsp70-HOP complex with glutaraldehyde or paraformaldehyde cross-linking reactions (A). Dependence of Hsp70 homodimer (B), Hsp70-HOP (C), and c-Myb-KIX (D) complex yields on glutaraldehyde cross-linking time and concentration.

To further investigate the effects of cross-linking and the conditions under which specific interactions are favored over nonspecific interactions, SEC was employed. SEC mobile phase is sometimes compatible with native PPI conditions and, as a result, complexes can be observed without cross-linking. The high mass range of SEC also allows for high molecular weight aggregates resulting from nonspecific cross-linking to be monitored. Bag3 and HOP were chosen as model proteins to determine the cross-linking reaction conditions that result in non-specific aggregation. Bag3 and HOP are not

expected to self-associate into high mass complexes[154,178] and minimal aggregation was observed by SEC without cross-linking even at high protein concentration. With a 10 s cross-linking reaction however, higher molecular weight species, presumably aggregates, were detectable at protein concentrations of 20 μM and above (**Figure 3-2A**). This result suggests an upper limit to protein concentrations that can be studied using this method. Non-specific interactions have been reported to dominate in this concentration range potentially due to the presence of non-specific interactions between proteins. For example, with NHS ester cross-linking, non-specific complexes were observed at protein concentrations at 40 μM[167] and at 33 μM[179].

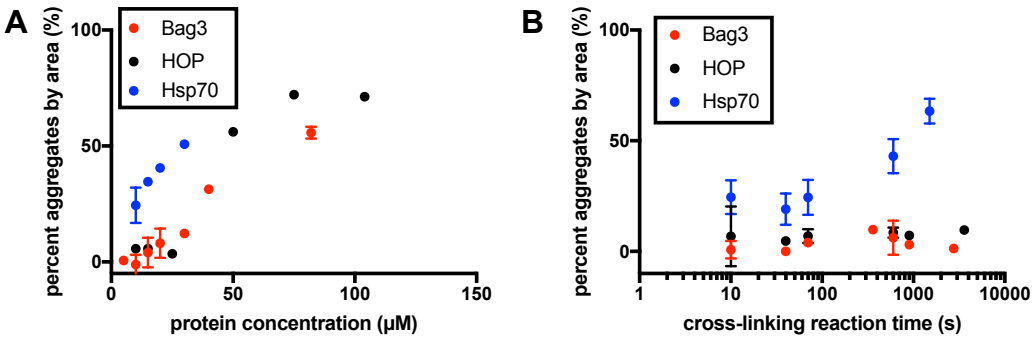

Figure 3-2. High molecular weight aggregates of Bag3, HOP, and Hsp70 observed by glutaraldehyde by size exclusion chromatography. Effect of protein concentration (A) on observation of high molecular weight aggregate after 10 s of glutaraldehyde cross-linking. Effect of increasing cross-linking reaction time on high molecular weight aggregates (B) protein concentration was 10 μM.

Besides high protein concentrations, we also considered the possibility that long cross-linking times could lead to additional aggregation. It has previously been reported that glutaraldehyde cross-linking is specific only at short reaction times[180]. At 10 μM, Bag3 and HOP were not found to aggregate even at long cross-linking reaction

times. Hsp70, however, was found to exhibit increasing aggregation by SEC at cross-linking times greater than about ~70 s (**Figure 3-2B)**. Slow, higher order aggregation of Hsp70 has been observed previously[181,182], potentially explaining the increase seen at long cross-linking times. This result explains previous observations of decreasing yields of complex at long cross-linking reaction times with formaldehyde cross-linking PXCE.[171] That is, higher molecular weight aggregates are preferentially excluded from the gel during injection this preventing detection and the result is observation of low complex formation. This effect likely explains the apparent drop in complex yield in the PXCE experiments at longer reaction times (600 s) in Figure3-1C,D. To minimize the effects of non-specific or additional high mass aggregation, we limited our assays to total protein concentrations of 20 μM or less with cross-linking reaction times of 10 s. These conditions circumscribe the assay to PPIs with low μM or lower K_ds where saturation binding experiments can be completed without using overly high concentrations of protein, circumventing the need to subtract nonspecific cross-linking to determine binding affinity.

Determination of PPI Affinity

We next determined if 10 s reactions with proteins below 20 μM would be sufficient for quantification of binding affinity for a variety of PPIs. For these experiments, saturation binding curves were carried out by PXCE on PPIs with low μM to low nM K_d values (**Figure 3-3**).

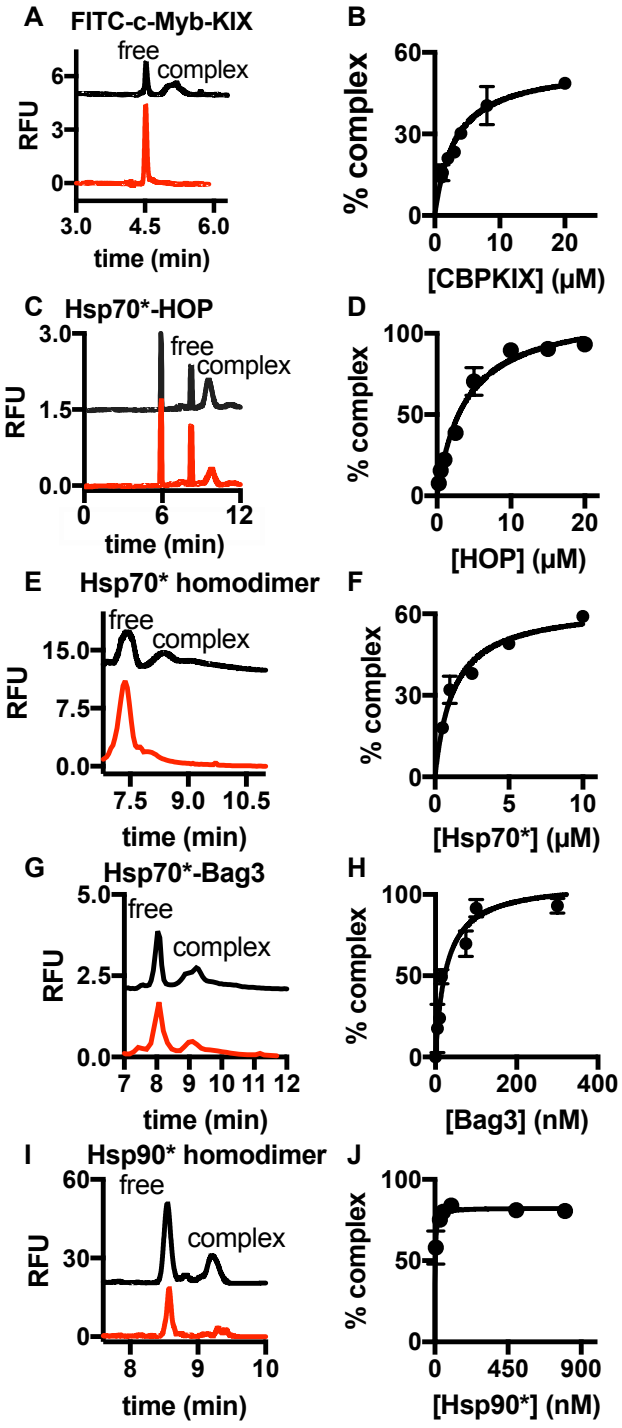

Figure 3-3. Electropherograms and saturation binding curves for μM to nM affinity complexes by 10 s glutaraldehyde cross-linking PXCE. Saturation binding curves were fit by nonlinear regression to find K_d = 3.1 ± 0.5 μM, 3.8 ± 0.7 μM, 1.2 ± 0.3 μM, 26 ± 6 nM, 2.1 ± 0.3 nM for FITC-c-Myb-KIX (A), Hsp70*-HOP (B), Hsp70* homodimer (C), Hsp70*-Bag3 (D), and Hsp90* homodimer (E), respectively. The first peak in the Hsp70* electropherograms corresponds to a low molecular weight impurity.

Good agreement was found between the K_d values determined by PXCE and values reported by non-cross-linking methods for Hsp70-Bag3, Hsp90 homodimer, Hsp70 homodimer, Hsp70-HOP, and KIX-c-Myb (**Figure 3-4, Table 3-1**). We conclude that PXCE with 10 s glutaraldehyde cross-linking time is sufficient for measuring the affinities of these complexes for K_d values spanning three orders of magnitude from low nM to low μM values.

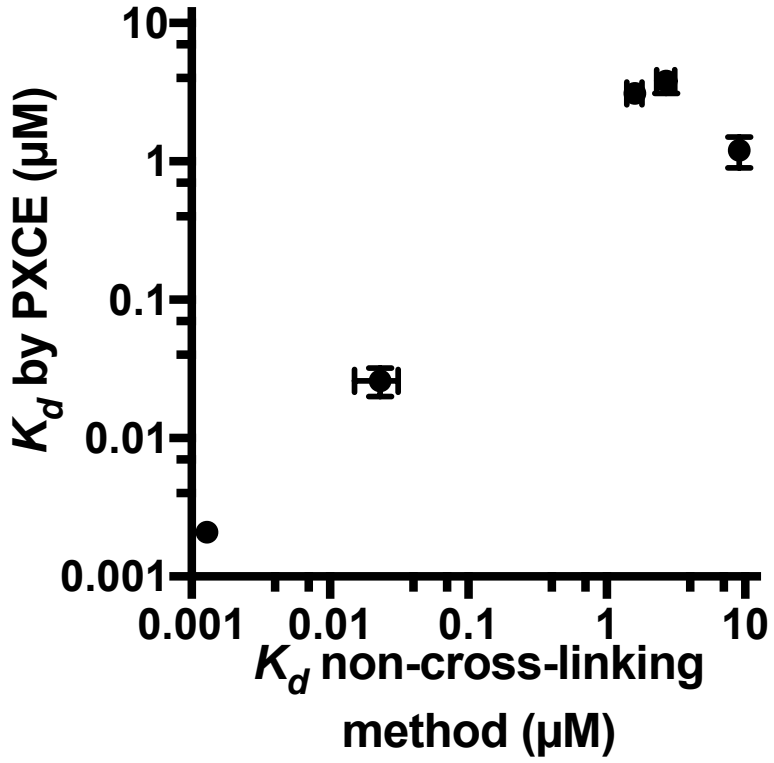

Figure 3-4. Comparison of PXCE K_d values from data in Figure 2 to K_d values from non-cross-linking methods for Hsp90 homodimer[162], Hsp70-Bag3[6], Hsp70 homodimer[181], Hsp70-HOP[174], and FITC-c-Myb-KIX.

Table 3-1. Comparison of PXCE and Literature K_d values for μM to nM PPIs.

Protein Interaction	K_d PXCE	K_d Literature
c-Myb-KIX	3.1 ± 0.5 μM	1.6 ± 0.2 μM
Hsp70-HOP	3.8 ± 0.7 μM	2.7 ± 0.4 μM[174]
Hsp70 homodimer	1.2 ± 0.3 μM	11 μM[181]
Hsp70-Bag3	26 ± 6 nM	23 ± 8 nM[6]
Hsp90 homodimer	2.1 ± 0.3 nM	1.29 nM[162] 60 ± 12 nM[161]

Sensitivity of Assay to Point Mutations and Nucleotide State

We next determined the sensitivity of the glutaraldehyde PXCE method to changes in protein structure by measuring the effect of binding site point mutants and the nucleotide state on interaction affinity. Hsp70 is an ATPase known to undergo nucleotide state dependent structural changes leading to changes in the degree of homo-oligomerization.[181,183] Here, clear differences in homodimerization affinity were seen for Hsp70 with the ATP state having the weakest affinity and the ADP state having the greatest affinity for homodimerizing (**Figure 3-5**). The sensitivity of the PXCE assay to such structural changes lends further evidence to the specificity of this method.

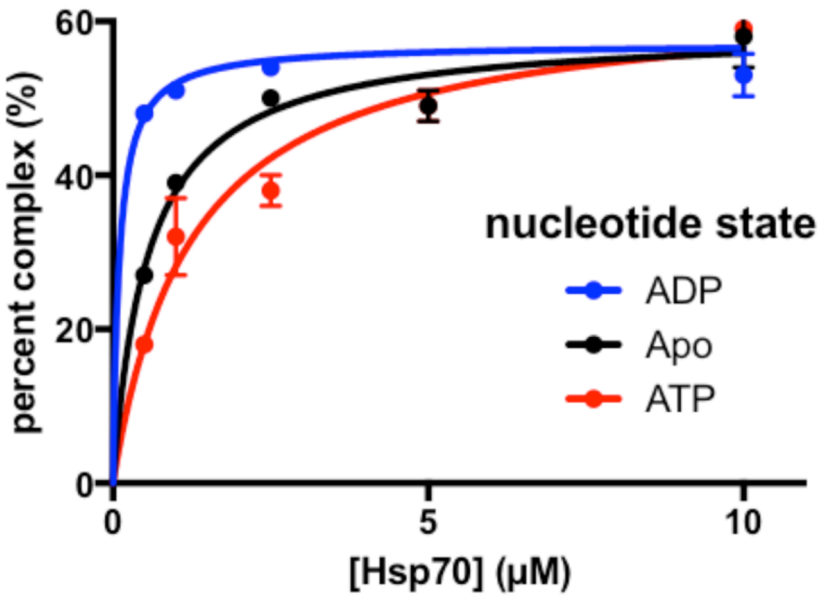

Figure 3-5. Sensitivity of 10 s glutaraldehyde cross-linking assay to nucleotide dependent homodimerization of Hsp70*.

HOP proteins with one-site substitution mutations in the Hsp70 binding site were also investigated. HOP with mutations R77A and N223A inhibit the interaction of HOP with Hsp70.[174] Using a 10 s glutaraldehyde cross-linking reaction the wild type protein had a lower K_d value than the mutants, as expected (**Figure 3-6**). In fact, the rank order for the K_d values of the two mutants was in agreement between PXCE and values obtained using fluorescence polarization[174]. The R77A mutant HOP however, was found to have a much higher K_d value by fluorescence polarization (>25 μM) than by PXCE (3 ± 1 μM), indicative of a much lower apparent affinity for Hsp70 by fluorescence polarization compared to PXCE. Notably, the PXCE assay was carried out on full length proteins while the fluorescence polarization assay was of the interaction between full length HOP and a peptide consisting of the EEVD domain of Hsp70.

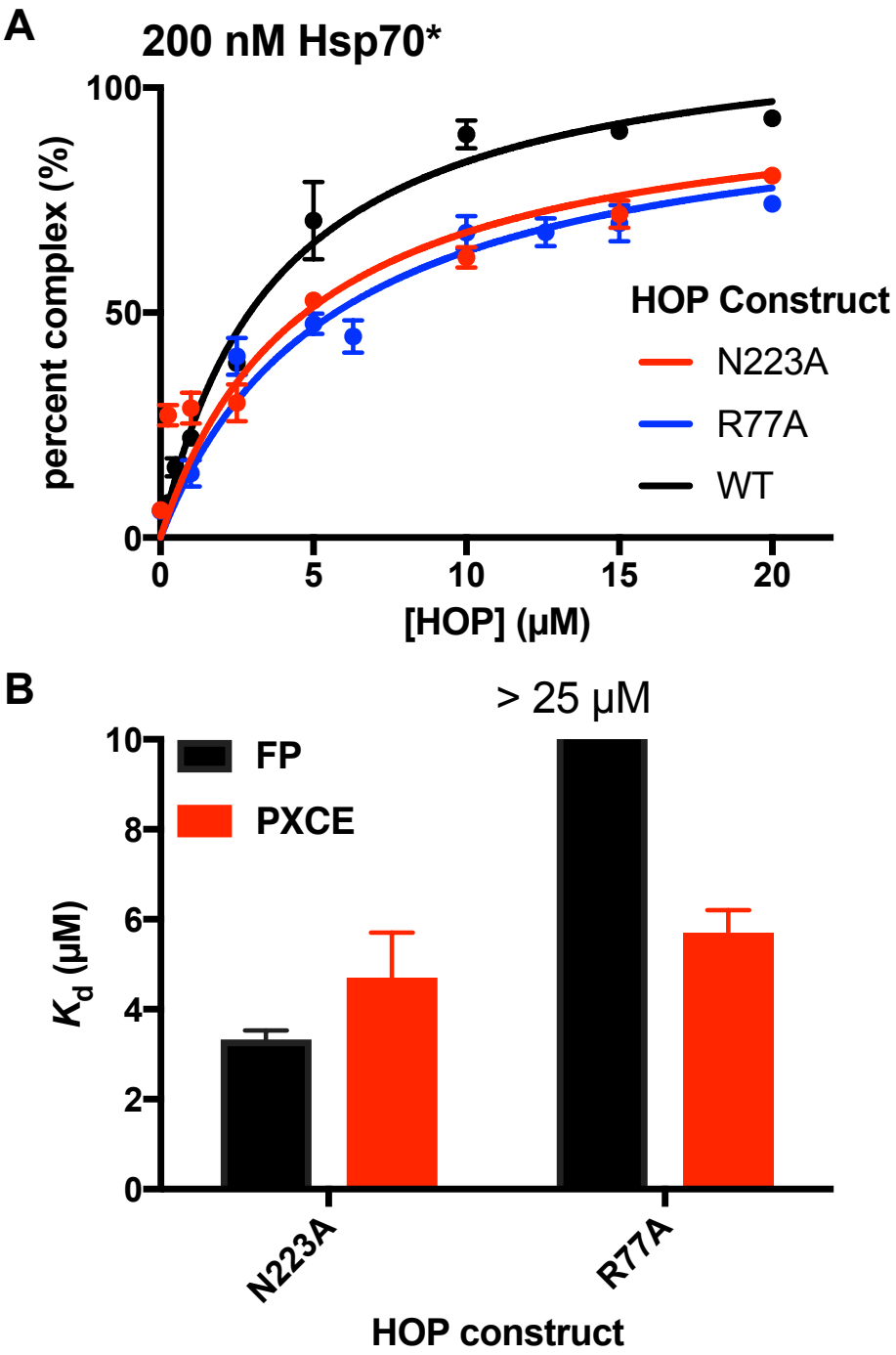

Figure 3-6. Sensitivity of 10 s glutaraldehyde cross-linking assay to point mutants of HOP. Saturation binding curves (A) and comparison to APCE and fluorescence polarization [174] data (B).

Two potential explanations for the discrepancy in K_d values between the fluorescence polarization and PXCE assays were explored: 1) The PXCE K_d is an artifact of cross-linking and 2) Full length Hsp70 has a higher affinity for HOPR77A than does the EEVD domain alone. The affinity of full length Hsp70 for HOPR77A was confirmed by APCE without cross-linking (K_d = 4 ± 2 μM, **Figure 3-7**) suggesting that the K_d measured by PXCE was not a cross-linking artifact.

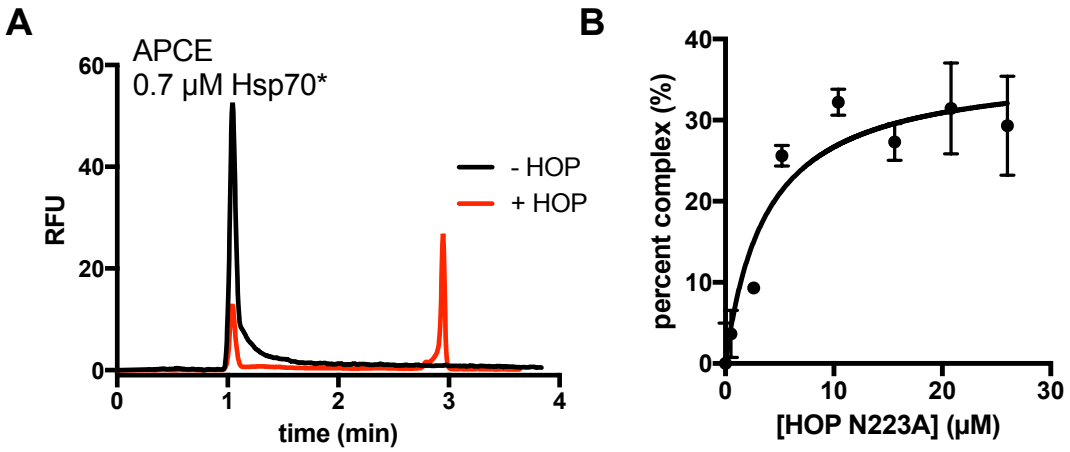

Figure 3-7. APCE electropherograms (A) and saturation binding curve for Hsp70-HOP interaction without cross-linking (B).

To compare the affinities of full length Hsp70 and the EEVD domain alone for HOPR77A a competitive binding experiment was carried out (**Figure 3-8**). Full length Hsp70 was found to have higher affinity for HOPR77A than either the EEVD domain or the full-length form of Hsp70 with a deletion in the EEVD domain. This result is in agreement with other reports which have found the EEVD domain to be important for the Hsp70-HOP interaction while not accounting for all of the affinity.[174,177] Compatibility with full length protein is an advantage of this CE assay as use of full length protein

eliminates the method development or artifacts associated with use of peptide necessary for fluorescence polarization.

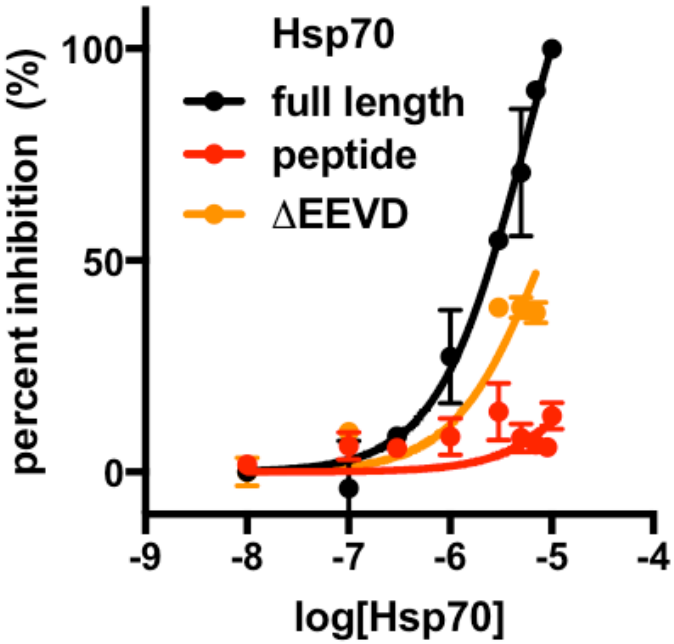

Figure 3-8. Comparison of increasing concentrations of unlabeled Hsp70 constructs binding to 1 µM HOPR77A in the presence of 100 nM Hsp70*.

Increased Throughput Electrophoretic Sieving Separation

In view of the apparent utility of the method for measuring affinities for a wide range of PPIs, we sought to improve the throughput of the method. Although microchip CE and other techniques can achieve separations in seconds, in this case we used a commercial CE instrument to maintain accessibility to a wider range of potential users. Decreasing the viscosity of the sieving media was seen as a key to improving throughput because it both allows faster migration at a given electric field and allows smaller bore capillaries to be used. Higher fields can be applied without detrimental heating effects by use of lower diameter capillary; however, with viscous sieving matrix it can be difficult to rinse the matrix through small bore capillaries. Use of ultralow viscosity sieving matrices have

been reported for DNA separations[184,185] and are compatible with rapid capillary regeneration. Here, an ultralow viscosity sieving matrix (7.45 ± 0.05 cP) was utilized for protein separation. This matrix is about 1/5th as viscous as the matrix used above however sufficient separation of 11-155 kDa proteins was maintained (**Figure 3-9**). The ultralow viscosity matrix can be rinsed through a 25 µm capillary in 5 min (at 50 psi > 3 capillary volumes are replaced) while the higher viscosity matrix would require 26 min to be rinsed through a 25 µm capillary. Using the ultralow viscosity matrix, a 1 kV/cm field can be applied in a 25 µm capillary without observing the heating effects that were observed in 40 µm capillary (**Figure 3-10**). This high field allows for 11-155 kDa proteins to be separated in 2 min (**Figure 3-9)**.

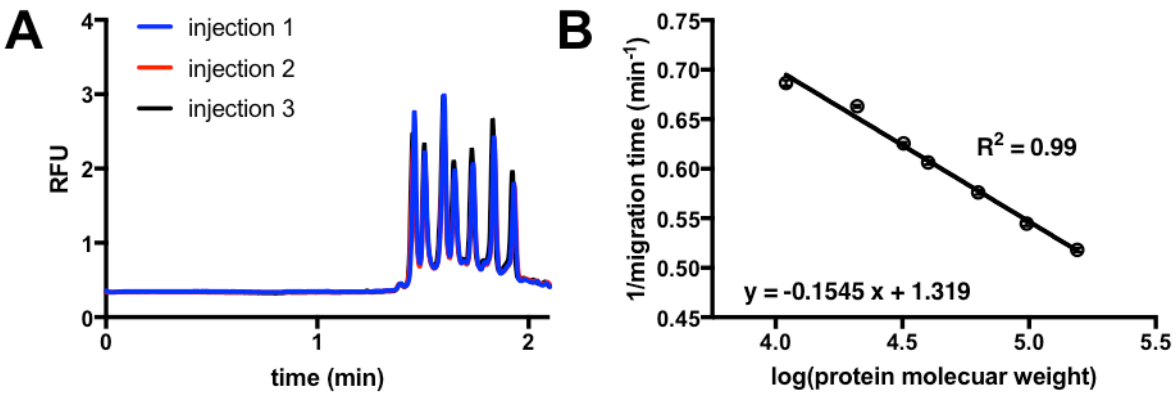

Figure 3-9. Separation of 11, 21, 32, 40, 63, 98, and 155 kDa protein ladder (BenchMark™ Fluorescent Protein Standard, Life Technologies, Carlsbad, CA) on low viscosity sieving matrix at 1 kV/cm at 10 cm effective separation length.

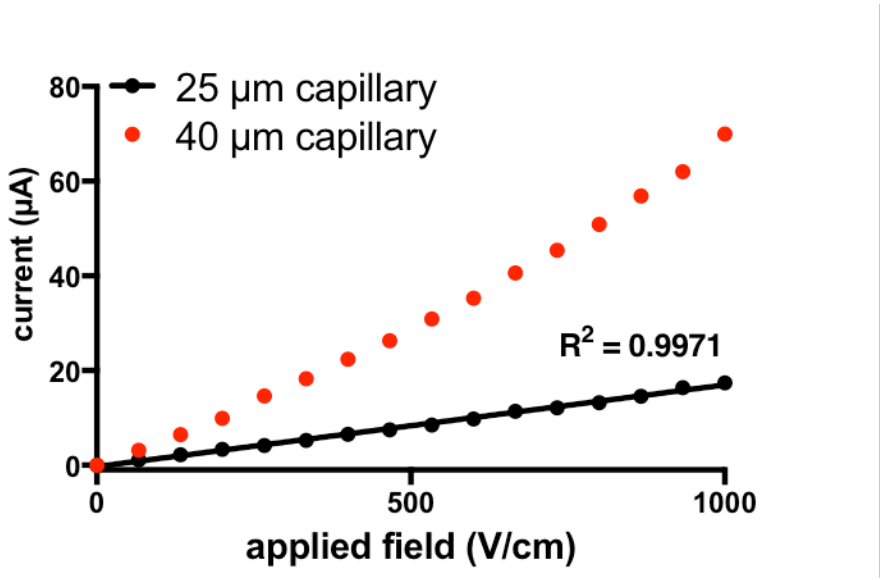

Figure 3--10. Ohm's plot of low viscosity sieving matrix in 40 µm or 25 µm capillary.

It is possible to further increase the throughput of sequential injections by overlapping the injections based on the separation window and the time that occurs prior to the first peak in the separation.[186] By using overlapping injections on a 25 µm capillary with the ultralow viscosity sieving matrix it was possible to make sequential injections and separations with a throughput of 1 sample/min (**Figure 3-11**). The samples could be repeatedly injected for up to about 70 min before the capillary needed rinsing. Saturation binding curve data was obtained from this electropherogram and a K_d for the binding interaction was determined to be 1.1 ± 0.2 µM (**Figure 3-11C**), in good agreement with the K_d value obtained by fluorescence polarization of 1.1 ± 0.2 µM. This strategy could also be used for determination of small molecule PPI inhibitor potency. A dose response curve for Hsp70-Bag3 inhibitor JG-98 was carried out using overlapping injection for 8 samples in 10 min for a single replicate. A log(IC_{50}) value of -6.4 ± 0.1 was determined (**Figure 3-11F**) which is in good agreement with the previously reported log(IC_{50}) value of -6.1 ± 0.3 showing good accuracy of the method.[171]

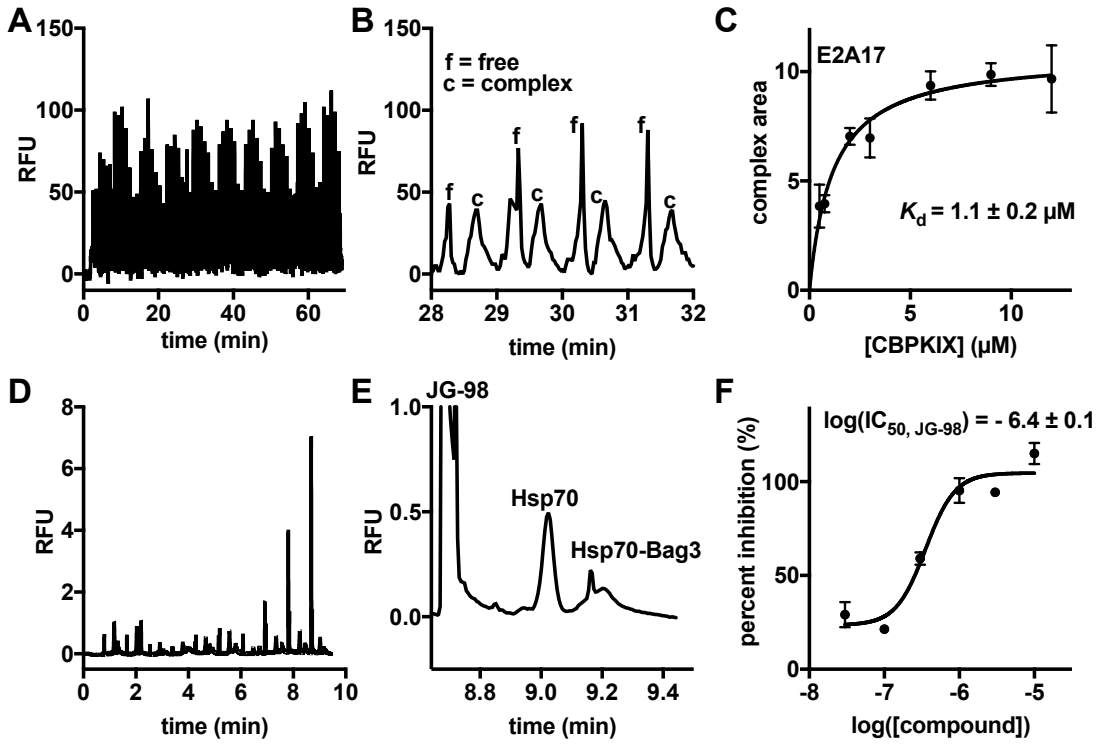

Figure 3-11. Overlapping injections for saturation binding curve and IC_{50} determination at increased throughput. Electropherogram of continuous overlapping injections of samples at various KIX concentrations (A). A section from 28 to 32 min of the electropherogram with analytes from injection of four different samples (B). Determination of the K_d value for the E2A17-KIX interaction from the electropherogram shown in A (C). Electropherogram of continuous overlapping injections of Hsp70-Bag3 and fluorescent small molecule inhibitor JG-98 (D). A section of the electropherograms corresponding to analytesfrom one injection. Determination of IC_{50} for Hsp70-Bag3 complex inhibition by JG-98 (F).

Application to Higher Order Oligomers

Many of the proteins discussed here form additional higher order or multi-protein complexes. To determine the utility of this method for application to higher order oligomers, the binding of Hsp70 to CHIP was investigated. At 0.5 µM Hsp70 in the apo nucleotide state both monomeric and dimeric Hsp70 are observed. Upon addition of 1 µM CHIP a 2:2 Hsp70:CHIP complex was evident (**Figure 3-12**). Previous reports of Hsp70-CHIP complex have found similar results with CHIP forming a homodimer and

binding to two Hsp70 to form a 210 kDa complex.[122,187] This result demonstrates the potential utility of this method for the investigation of multimeric complexes. Most methods for PPI analysis, such as isothermal calorimetry (ITC) and fluorescence polarization, are incompatible with resolving multiple interactions in a single assay.

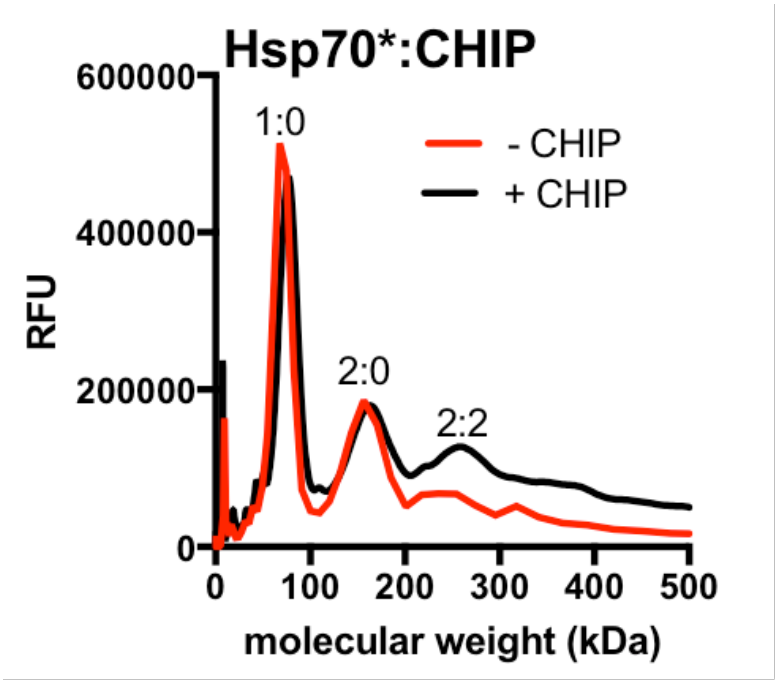

Figure 3-12. Electropherograms of multimeric complexes $Hsp70_{apo}$:CHIP. Hsp70* concentration is 1 μM (both traces) and CHIP concentration is 4 μM (black track). Molecular weight was calculated based on size standards.

Conclusions

With a fast (10 s) cross-linking reaction, protein complexes with K_d values spanning 3-orders of magnitude, from low nM to low μM, could be quantified by PXCE. The 10 s cross-linking reaction is 60-fold faster than the previous cross-linker used for PXCE. The presence of possible non-specific aggregation at high protein concentrations limits the practical applicability of this method to investigations of low μM or lower K_d values. The

molecular weight range of the gel matrix used also limits the method to complexes less than 250 kDa. There is potential to further tune the size limit of the gel as has been demonstrated for other entangled polymer gel matrices.[188]

This method has a number of advantages over other PPI analysis methods. PXCE is compatible with full-length proteins eliminating the need to prepare short peptide mimics of the protein, as is often necessary in fluorescence polarization assays. The ability to distinguish multiple complexes suggests that this method will be useful for evaluating the specificity of a PPI inhibitor as has previously been demonstrated for protein-peptide interactions[30]. By using overlapping injection methods the separation time can be decreased to about 1 min per sample suggesting potential utility of the method when higher throughput is necessary. Dissociation constants and IC_{50} values can each be determined in about 10 min compared to hours required by other methods such as ITC. There is potential for further increasing throughput by using 96- or 384-capillary arrays or microchip electrophoresis.

Chapter 4: Towards High Throughput Protein Cross-linking Microchip Electrophoresis

Introduction

Capillary electrophoresis (CE) has demonstrated utility in screening for modulators of enzymes and protein-protein interactions.[2,189] CE has demonstrated low false positive rates in screening[6] because it directly detects reactants and products and discriminates against potential sources of interference including optically active test compounds[2,4,6], non-specific protein aggregation[6] and test compound precipitation[6]. For electrophoresis to reach throughputs compatible with screening large chemical libraries, rapid separations are required. Microchip electrophoresis (MCE) can provide separations on the timescale of milliseconds for free-solution electrophoresis[19] and seconds for gel electrophoresis[190], however, one of the biggest limitations to throughput is achieving sample introduction at commensurate throughput. For microchip electrophoresis, samples are typically manually loaded into reservoirs on the device limiting the actual throughput achievable for multiple samples. One exception is the commercial LabChip instrument (Perkin Elmer). This instrument introduces samples to a microchip directly from a multiwell plate, affording a throughput of about 1 min per sample.

Beyond commercial instrumentation, automated sample introduction has been reported using droplet microfluidics approaches.[64,65,67–69,73] In these methods, samples are

contained within nanoliter volume aqueous droplets and separated from one another by an immiscible carrier phase. The low volume droplets are sequentially introduced into an aqueous separation channel for electrophoresis. While this strategy can provide rapid automated sample introduction, injection of immiscible, non-conductive segmenting liquid is incompatible with electrophoretic separations. Introduction of carrier phase may cause electroosmotic flow instability and plug formation leading to shorting and dielectric device breakdown.[64,65,71]

A number of devices have been reported for coupling droplets to electrophoresis without introducing the segmenting phase to the electrophoresis channel [17,64,65,68,69,72]. These devices rely on surface patterning[17,64,65,72], modified channel geometries [68] or use of an oleophilic membrane [73]. While most devices have been demonstrated with throughputs on the order of ~1 min/sample, one device has been used to perform high throughput screening of enzyme modulators at 2 s/sample, however, this device is limited to performing free solution electrophoresis.[18] In fact, most devices have been demonstrated for compatibility with free solution electrophoresis alone. There is only one report of coupling droplets to gel electrophoresis. In this design, an oleophilic membrane was used to extract the carrier phase from the droplet stream while the entire droplet was injected into the separation channel. This was demonstrated for gel electrophoresis using a hybrid PDMS fused silica device and using a PDMS device for free-solution electrophoresis with separation times of about 60 s and 30 s per sample, respectively.[73] In this device, resolution was sacrificed due to injection of relatively large sample volumes.

Here, we report a chip for coupling droplets to gel and free solution electrophoresis, which allows controlled injection size for rapid and high efficiency

separations. Separation time for gel electrophoresis of proteins achieved in 2.5 s, a significant improvement over our previously reported 1 min/sample separation time[170] with high resolving power compared to previous reports of sieving electrophoresis on the second timescale[191]. The utility of the device is demonstrated for both enzyme and protein-protein interaction (PPI) samples at a throughput of ~10 s per sample with multiple injections per sample.

Experimental

Chemicals and Materials

Proteins were expressed, purified, and labeled as previously described.[18,171] Benchmark™ fluorescent protein standard ladder was purchased from Life Technologies (Carlsbad, CA). Chemicals and reagents were purchased from Sigma-Aldrich, Saint Louis, MO, unless otherwise stated.

Device Fabrication

Glass (Telic Company, Valencia, CA) was fabricated by photolithography and etching with hydrofluoric acid as previously described[192–194]. For the capillary insertion channel both top and bottom slides are etched to 75 μm. For separation channels, the top slide is etched to 8.8 μm. Access holes were drilled in the top slide with 400 μm drill bits (Kyocera Precision Tools, Henderson, NC). Both slides were aligned under microscope such that insertion channels on each slide are flush. Chips were thermally annealed at 610 ˚C for 8 h. Subsequently, reservoirs and fused silica capillary 150 μm o.d. 75 μm i.d. (Polymicro Technologies; Phoenix, AZ) were secured to the device using Loctite Epoxy Marine (Loctite, Düsseldorf, Germany).

Microchip Operation

For imaging an Olympus IX71 (Tokyo, Japan) fluorescence microscope was used. For all other experiments a previously described in-house confocal laser-induced fluorescence (LIF) detector was used.[17] A 488 nm laser (CrystLaser, Reno, NV) was used for excitation with emission filtered through a 520 nm filter. Data were analyzed using Cutter 7.0 [31] and Graphpad Prism 7.

Free-solution Microchip Electrophoresis

For free-solution electrophoresis Rain-X (ITW Global Brands, Houston, TX) was pulled by vacuum through the fused silica capillary for 1 min to coat the inner surface of the capillary and facilitate droplet transfer. Reservoirs were then filled with 10 mM sodium tetraborate, 0.9 mM 2-hydroxypropyl-β-cylcodextrin, pH 10 and vacuum was applied at the waste reservoir for at least 5 min to fill all channels with this running buffer. For separation, 800 V/cm was applied with 100 ms gated injections[195] every 900 ms. The separation length to detector was 3 mm.

Microchip Gel Electrophoresis

For gel electrophoresis, microchips were conditioned sequentially with 1 M sodium hydroxide, water, ultratrol LN (Target Discovery, Palo Alto, CA) and water by pulling vacuum at the waste reservoir. Rain-X was then pulled through the fused silica capillary by applying vacuum at the sample reservoir for 1 min. Next, all channels were filled with air by applying vacuum until all channels were observed to be empty. Finally, gating and sample reservoirs were filled with gel and vacuum was applied at the waste reservoir to fill all channels with gel. Sieving matrix used was 90 mM Tris 100 mM borate, 1 mM EDTA, 13.8 mM SDS, 3.5% dextran (1,500-2,800 kDa). Gated injections were carried

out every 100 ms, separations were at 1,200 V/cm, and detection was at 3 mm, unless otherwise stated.

Droplet Generation and Introduction to Microchip

Droplets were generated from a multiwell plate into 360 o.d. 150 i.d. PFA Plus teflon tubing (Idex Health & Science, Oak Harbor, WA) as previously described [44] with the following exceptions: a flow rate of 0.3 μL/min was used and the carrier phase was silicone oil (10 cSt). The train of droplets was then connected to the microchip by threading the 150 μm o.d. fused silica capillary into the lumen of the teflon tubing. The junction was then secured using Crystal Wax (ULTRA TEC, Santa Ana, CA) to prevent leaking.

Droplet Analysis of Enzyme Samples

SIRT5 enzymatic reactions were carried out in 10 μL reaction volume with 45 nM SIRT5, 1 μM substrate peptide, 10 mM Tris, 1 mM DTT, 0.5 mM NAD+, 4.5 % (v/v) glycerol, 30 mM NaCl, and 2 mM sodium phosphate. Reactions were allowed to proceed for 15 min prior to quenching with 45 μL of free solution electrophoresis running buffer (described above).

Droplet Analysis of Protein-Protein Interaction Samples

Hsp70-Alexafluorophore 488 (Hsp70*) and Bag3 samples were prepared in 25 mM HEPES, 10 mM KCl, 5 mM $MgCl_2$, 10 mM ATP, pH = 7.5. Proteins were cross-linked as previously described.[170] Briefly, proteins were allowed to equilibrate at the desired concentration for at least 15 min prior to cross-linking with glutaraldehyde to a final concentration of 2% for 10 s prior to quenching with Tris to a final concentration of 400 mM.

Results and Discussion

Microchip Gel Electrophoresis

Microchip electrophoresis allows short separations lengths and high electric fields to be readily accessed enabling decreased separation times relative to conventional CE. Rapid MCE separations have potential to analyze large numbers of samples at high throughput. Figure 4-1 demonstrates the separation of standard protein ladder in less than 2.5 s by SDS-microchip gel electrophoresis. A similar separation by microchip gel electrophoresis was reported with a separation time of 2.7 s achieved resolution of 1.66 between 22 and 67 kDa proteins.[191] Resolution of 5.3 between 21 and 63 kDa proteins was achieved in this case. The higher resolution achieved is attributed to the longer separation length and higher electric field along with differing sieving media and device material.

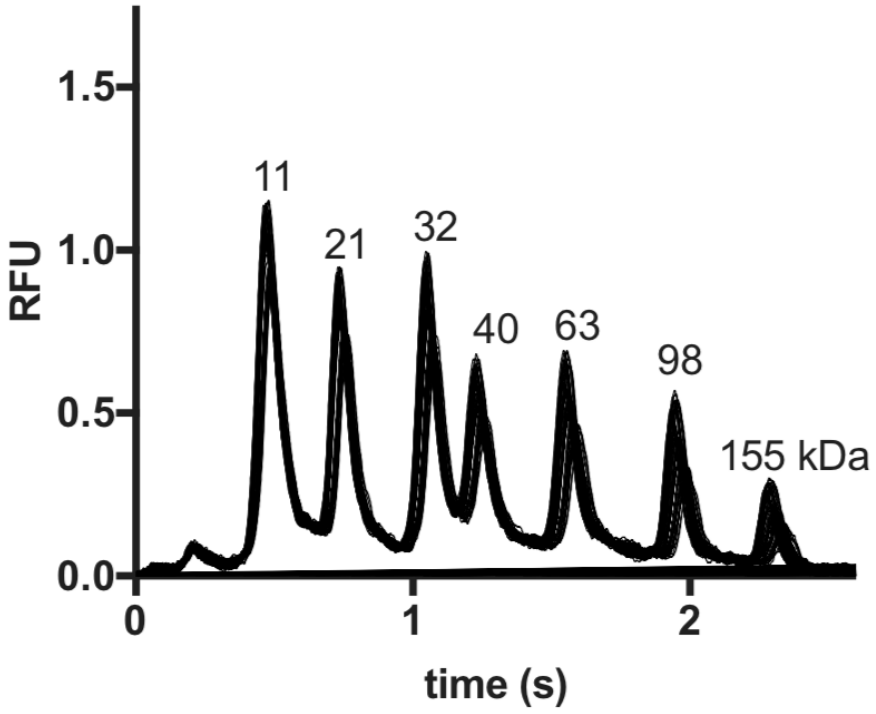

Figure 4-1. SDS-microchip gel electrophoresis separation of 11, 21, 32, 40, 63, 98 and 155 kDa standard protein ladder on microchip with 70 separations overlaid. Separation length was 3 mm and electric field was 800 V/cm.

Further, the separation tolerated repeated injections without reconditioning of the microchip. Up to 1,250 injections and separations were carried out on a single device without reconditioning. This result suggests utility of this separation for high throughput sample analysis if injection of sequential samples could be performed at equivalent throughput. While several reports of rapid gel electrophoresis separations exist[169,190,191] none have demonstrated sample introduction throughput needed to fully take advantage of such rapid separations.

Previously, throughputs of ~1 min/sample were achieved for separation of standard protein ladders using commercial CE[170] and microchip instrumentation[169]. These instruments are compatible with injection from multiwell plate; however, commercial

instrumentation is often limited to fixed separation distances limiting potential for faster separations. To take advantage of the rapid separation reported here automated sample introduction is required.

Operation of Density Based Oil Drain

To couple droplets to microchip electrophoresis, complete extraction of the oil from the droplet train is necessary. Removal of oil from droplet train was performed by taking advantage of the density difference between the segmenting phase (ρ_{oil}) and the background electrolyte (ρ_{BGE}) (**Figure 4-2**). Silicone oil was chosen as the segmenting phase for its relatively low density (0.93 g/mL). Other lower density oils, such as light mineral oil caused difficulties in droplet generation likely due to relatively higher viscosity (data not shown).

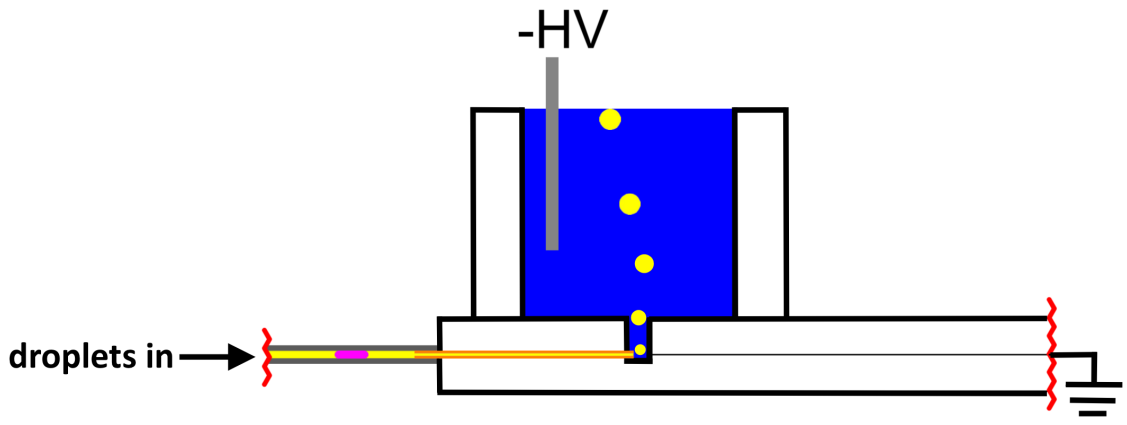

Figure 4-2. Schematic of cross-section of density based oil drain microchip. Nanoliter volume droplets are pumped into the device and the low density segmenting phase (yellow) drains to the top of the buffer filled reservoir (blue) where high voltage (HV) is applied. Aqueous droplets merge with the buffer and analytes are electrophoresed toward grounded reservoir (not shown).

The train of droplets is driven into the microchip via syringe pump. The train first enters the fused silica transfer capillary which directs the droplets into the area beneath a reservoir filled with background electrolyte. As the droplet train is flowed into the device the segmenting phase, which is immiscible with and less dense than the background electrolyte, pools at the outlet of the transfer capillary and floats to the top of the buffer-containing reservoir. This observation is consistent with the net buoyancy force (F_{net}) being able to overcome the force of gravity (g) once a certain volume of oil displaces the running buffer ($V_{displaced}$) at the outlet of the transfer capillary (equation 4-1).

$$F_{net} = V_{displaced}\, g(\rho_{BGE} - \rho_{oil}) \qquad \text{(Eq 4-1)}$$

High voltage was continuously applied at the oil removal reservoir such that upon exiting the transfer capillary the droplet coalesces with the background electrolyte and the contents are electrophoresed toward the grounded waste reservoir (**Figure 4-5A**). Importantly, the outlet of the droplet transfer capillary and the inlet of the separation channel are on the same plane such that the analytes migrate minimal distance to enter the separation channel. This geometry was designed to minimize the dead volume prior to electrophoresis. After analytes enter the channel they reach the injection cross where gated injection affords control of injection size. As sample reaches the injection cross, discrete injections can be made from each sample droplet (**Figure 4-3B**).

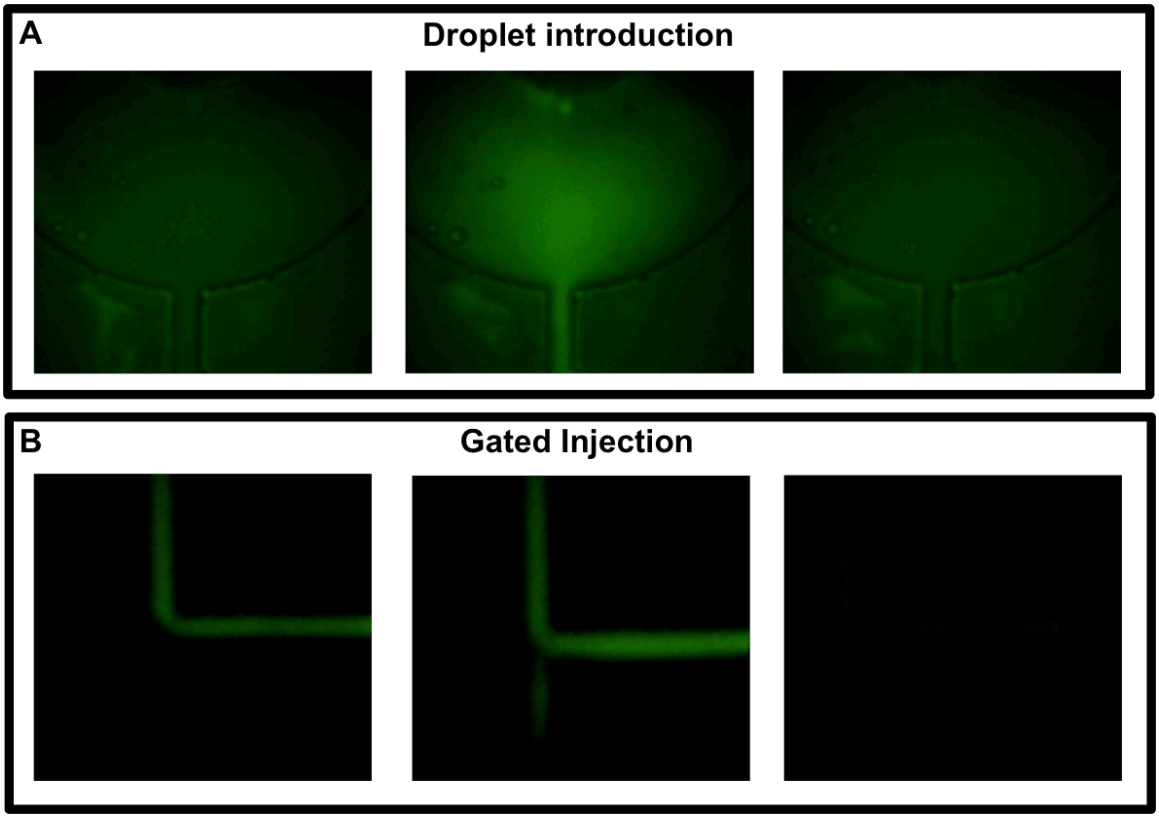

Figure 4-3. Fluorescence imaging of droplet introduction. Droplet exits fused silica capillary and is electrophoresed towards injection cross. Clearing of droplet sample is observed (A). Droplet content is then gated or injected to separation channel (B).

In this design, the number of injections made from each droplet was dependent on the volume of the droplet, the separation time, and the electric field applied. Injection volumes were ~40 pL, corresponding to 5% of separation channel volume. Once the droplet coalesces with the background electrolyte the analytes begin to migrate towards the injection cross where a controlled fraction of the droplet is injected. To obtain multiple picoliter injections from each droplet, each sample was converted into 3 nL sample droplets. During injection, the high voltage at the gating reservoir is floated to allow for a discrete low volume plug of sample to be injected. To maximize throughput and the number of injections per sample, the timing of the injections was determined by the minimum separation time required. A series of injections from the same droplet

showed varying intensity likely resulting from sampling from the droplet as it passes the injection cross is depicted in **Figure 4-4**.

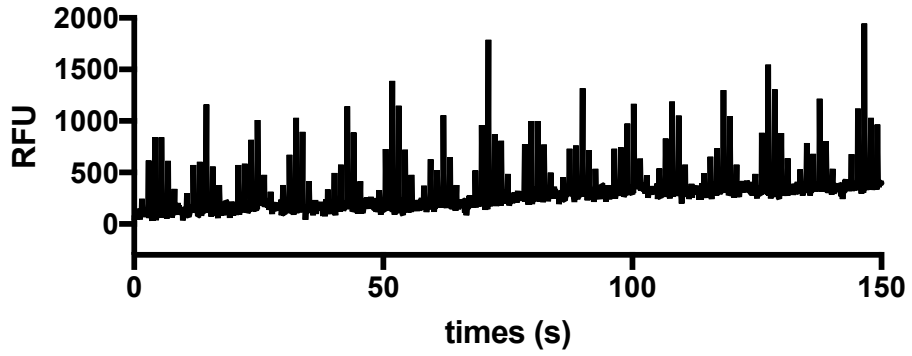

Figure 4-4. Signal from droplet introduction for microchip gel electrophoresis immediately downstream of injection cross. Injections of 2 μM FITC-insulin were carried out every 1.3 s with detection directly downstream of injection cross.

The electric field applied controls the time required for a sample droplet to clear the injection cross. To facilitate rapid clearing of samples and subsequently maximize throughput the highest accessible electric field is preferred. In this system, for microchip gel electrophoresis, the maximum electric field allowed without causing detrimental heating effects was determined by Ohm's plot to be approximately 1,200 V/cm (**Figure 4-5)**. This high electric field was used in order to maximize the rate of droplet clearing and separation throughput.

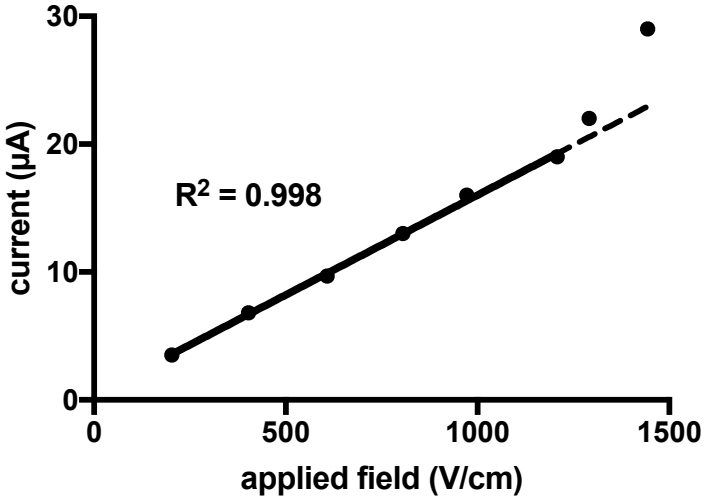

Figure 4-5. Ohm's plot for microchip gel electrophoresis. Linearity (R^2 = 0.998, $y=(1.56\pm0.03)x10^{-2}\ x+(0.4\pm0.3)$) was observed up to 1,200 V/cm.

Microchip Gel Electrophoresis of Droplets

To determine if the density oil drain was compatible with the fast microchip gel electrophoresis separation of protein-protein interaction samples, droplets containing Hsp70 and Bag3 were generated and analyzed. Separation of the protein complex (Hsp70*-Bag3) from free protein (Hsp70*) has been completed in 3 min using CZE[6] and 1.25 min by CGE separation with protein cross-linking[170]. This PPI could be separated in 2 s by microchip gel electrophoresis (**Figure 4-6B**). Overlapping injections were used to minimize separation time and allow for the greatest number of injections per droplet sample. In this approach, injections and separations are overlapped such that the peaks from the first injection migrate past the detector after the second injection has been made. While this approach is most common with capillary electrophoresis, where separation times tend to be longer, here we also applied overlapping injections to improve throughput of microchip gel electrophoresis.

To determine how the device would perform for multiple samples, droplets of alternating concentrations of Bag3 were introduced into the device. The complex peak area was quantified as a percentage of total peak area to account for the variations in intensity observed over time (**Figure 4-6A**). This change in intensity could be attributed to instability in the laser source, change in conductivity over time caused by introduction of sample matrix to chip, and injection occurring at various intensities along the introduced droplet plug (**Figure 4-4**). A total of 630 separations of 175 sets of sample droplets were analyzed without reconditioning of device for a throughput of approximately 10 s/sample. This is an improvement in separation throughput of 30-fold and a sample throughput improvement of 6-fold compared to a previous droplet-microchip gel electrophoresis device. Further this previous device was shown to have decreased performance over just three separations.[73]

Alternation in samples entering the chip was evident from quantifying the percent complex for each sample (**Figure 4-6C,D**). In the transition between high and low Bag3 concentration, some data points corresponding to intermediate complex were observed before the complex area stabilized (**Figure 4-6D**). This result may be attributed to the discontinuous nature of the droplet injection and mixing between droplets. One possible source of carry-over is the fused silica transfer capillary. In future device designs this could be eliminated allowing direct transfer of droplets from the Teflon tubing to the oil removal reservoir. Another possibility is that sample does not completely clear the injection cross before the next sample enters. This effect could potentially be mitigated with larger spacing between droplets, the incorporation of dedicated wash droplets, smaller volume droplets, or higher electric fields.

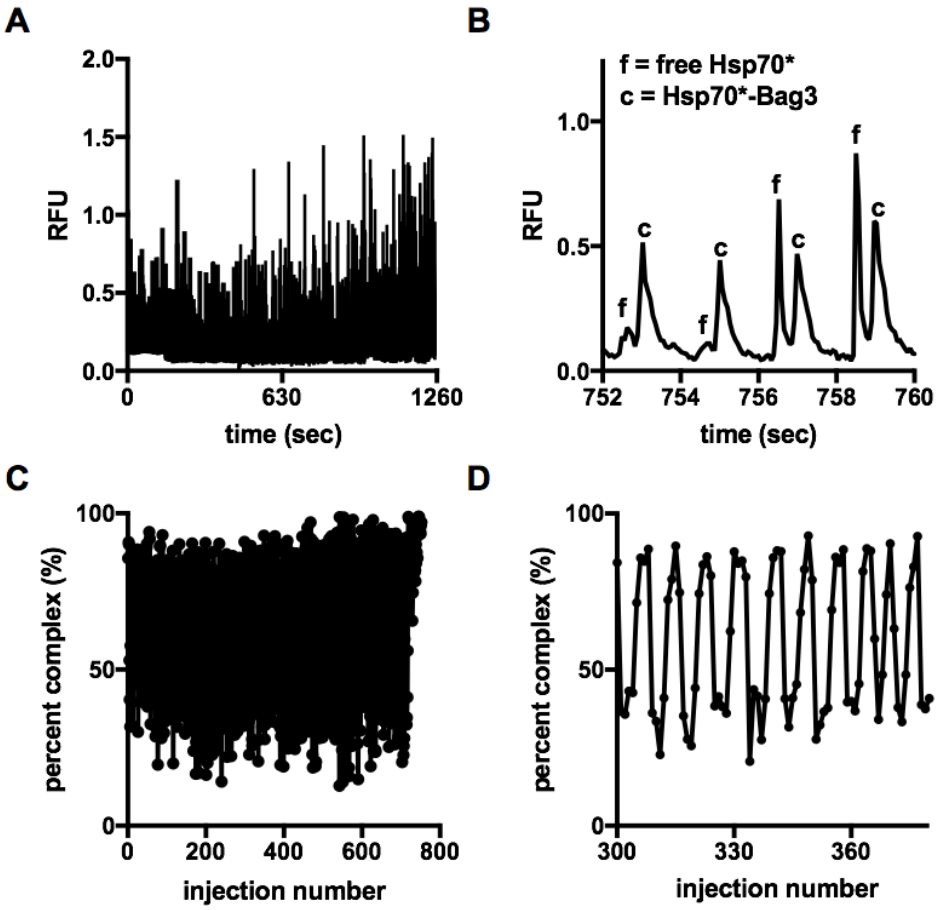

Figure 4-6. Electrophoresis and performance of density-based oil drain for analysis of Hsp70*-Bag3 samples by microchip gel electrophoresis. Concatenated electropherograms of 630 separations (A,B). Quantification of relative percent Hsp70*-Bag3 complex present in each electropherograms (C,D).

Nevertheless injections resulting from clearing between samples may be easily detected. Cataloguing of droplet samples was previously demonstrated for a device used in enzyme screening. In that work an internal standard was incorporated into alternating samples to deconvolute the data and select data from appropriate electropherograms.[17] A similar strategy was employed to investigate the utility of the device for analysis of known small molecule Hsp70-Bag3 inhibitors. In this case, separations were catalogued based on presence or absence of additional, rapidly migrating peak corresponding to

fluorescent small molecule (**Figure 4-7A)**. Data were normalized to positive (no target Bag3) and negative control (JG-258) and results for known inhibitor test compounds were analyzed (**Figure 4-7B**). Inhibition was detected for all compounds (JG-231, JG-311, rolitetracycline, YM-01, and JG-98) which were previously known to inhibit the Hsp70*-Bag3 interaction. The high degree of inhibition shown by JG-311 (>100%) suggests potential interference of Hsp70 homodimerization in the positive control sample. Interestingly, large differences in the degree of inhibition by these compounds was detected, with JG-311 and JG-98 exhibiting the greatest inhibition. JG-311 and JG-98 have been reported to have lower IC50 values than rolitetracycline, YM-01 and JG-231.[6,164,171] The differences in degree of inhibition may be attributed to the relatively high protein concentrations resulting in low degrees of inhibition for weaker inhibitors.

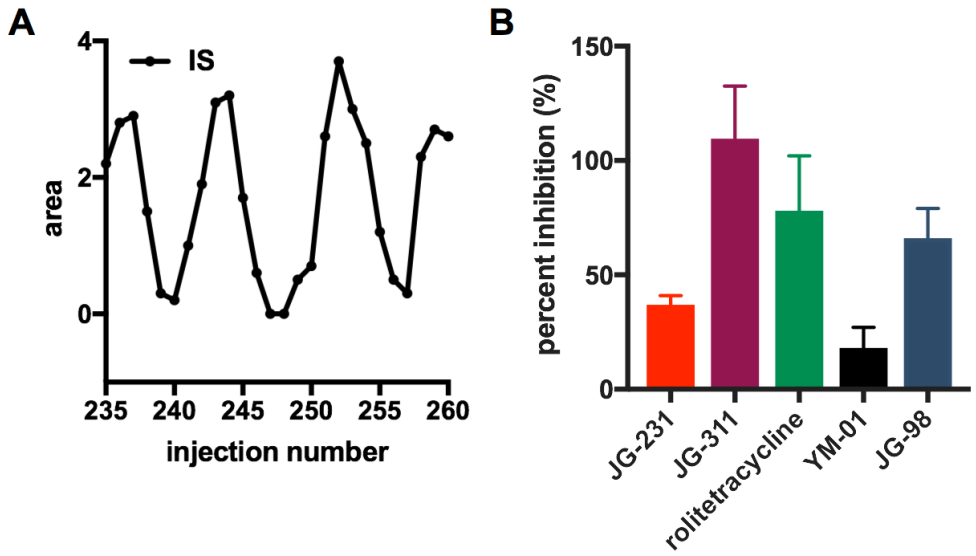

Figure 4-7. Demonstration of small molecule Hsp70-Bag3 screening using density drain microchip. Indexing of samples using fluorescent small molecule internal standard (IS) (A). Percent inhibition determined for droplet samples containing potential small molecule Hsp70*-Bag3 interaction inhibitors (B).

Free-Solution Microchip Electrophoresis of Droplets

To determine if the density based oil drain device was compatible with free-solution microchip electrophoresis, separation of Sirtuin 5 catalyzed desuccinylation of succinate dehydrogenase based substrate from desuccinylated product was performed based on previously described assay[18]. SIRT5 is, to date, the only known enzyme for lysine desuccinylation[196], regulating the mitochondrial lysine succinylome[197]. SIRT5 has been demonstrated as responsible for cancer cell growth in non-small cell lung cancer[198] and is therefore an interesting screening target. Droplets of alternating sample content (with and without enzyme) were generated and electrophoresed (**Figure 4-8**). A total of 1,250 separations were performed without reconditioning of microchip with 160 sets of sample droplets analyzed. The average reaction yield measured for the sample containing enzyme was 49 ± 5 % across all droplets analyzed.

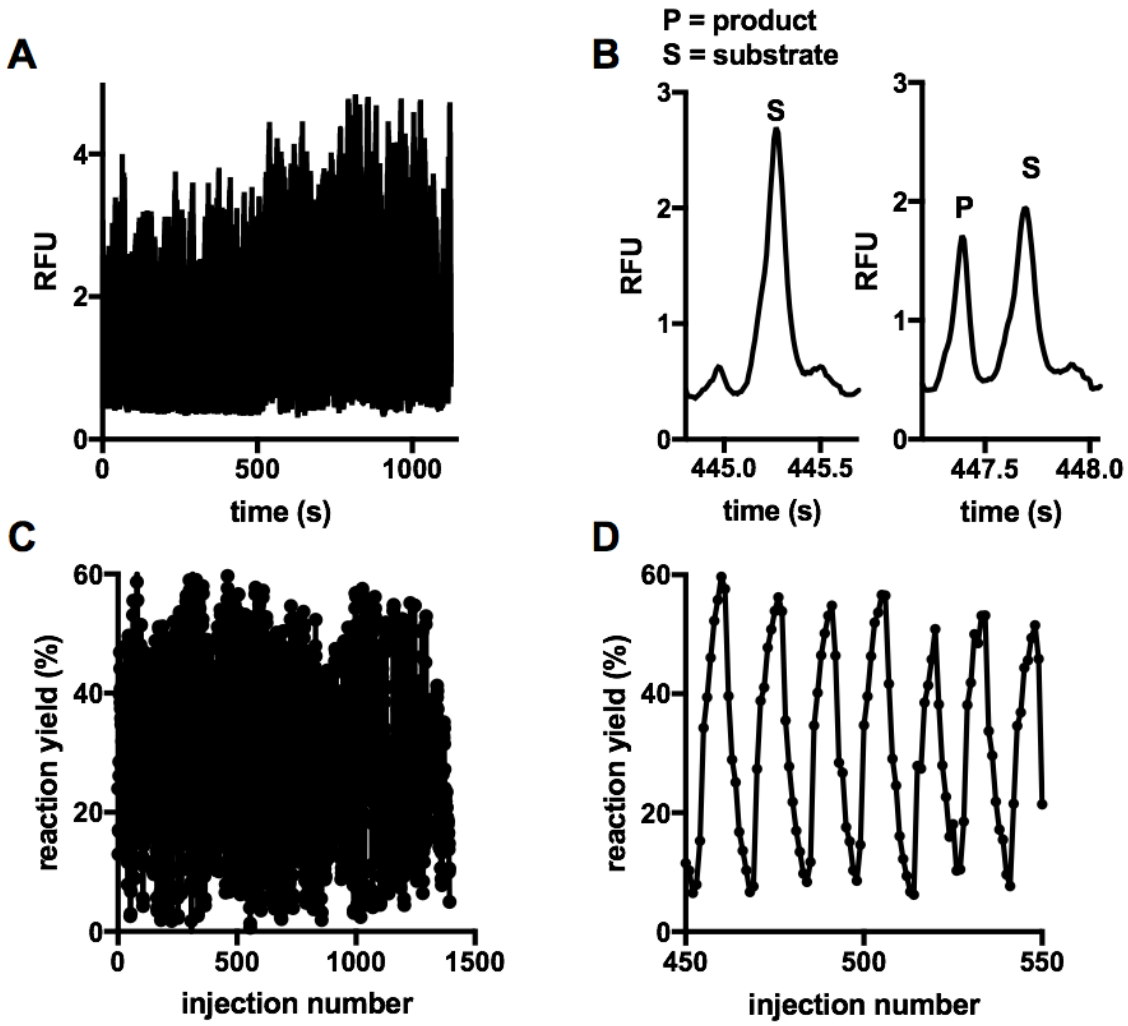

Figure 4-8. Electrophoresis and performance of density-based oil drain for analysis of SIRT5 reaction samples by free-solution microchip electrophoresis. Concatenated electropherograms of 1,250 separations (A,B). Quantification of reaction yield derived from each electropherogram (C,D).

This separation was previously reported for screening of SIRT5 modulators using a hybrid PDMS-glass device with droplets extracted from the aqueous stream at the interface to the PDMS.[18] A throughput of ~10 s/sample was obtained using the density based oil drain in comparison to the reported throughput of 2 s/sample reported with the hybrid PDMS-glass device.[18] Separation time of 900 ms was achieved compared to a 250 ms separation time reported previously when a shorter separation length and higher field were employed. Chips were etched to 8.8 μm whereas in previous report chips were

etched to 3 μm. This lower depth allowed for higher fields to be applied without detrimental heating effects, however, considerations of conditioning time and potential for clogging favor the current device design. Fabrication of the density based oil drain requires fewer steps and requires fewer connections compared to the hybrid device design.

Limitations and Considerations

Several limitations inherent to the density-based oil drain device exist including sensitivity to sample matrix, decreased signal compared to bulk injection methods, and limited compatible carrier phases. The performance of this device is highly dependent on the droplet sample matrix. Salty sample matrices will increase conductivity of the background electrolyte causing an increase in current over continuous operation of the chip. This is a limitation of all currently reported devices for coupling droplets to electrophoresis. This limits device application either to low numbers of salty droplet samples or to samples where the sample matrix matches the background electrolyte.

An approximately 10-fold lower signal was observed when introducing samples via nanoliter volume droplets compared to introducing samples by manually filling a reservoir with microliter volumes of the same sample (**Figure 4-9**). This result may be attributed to dilution of the droplet sample in background electrolyte upon introduction to the device as well as electrokinetic injection of bulk sample allowing for injection of a larger number of total analytes available in the much higher volume sample. The device was limited to analysis of low micromolar FITC-protein concentrations.

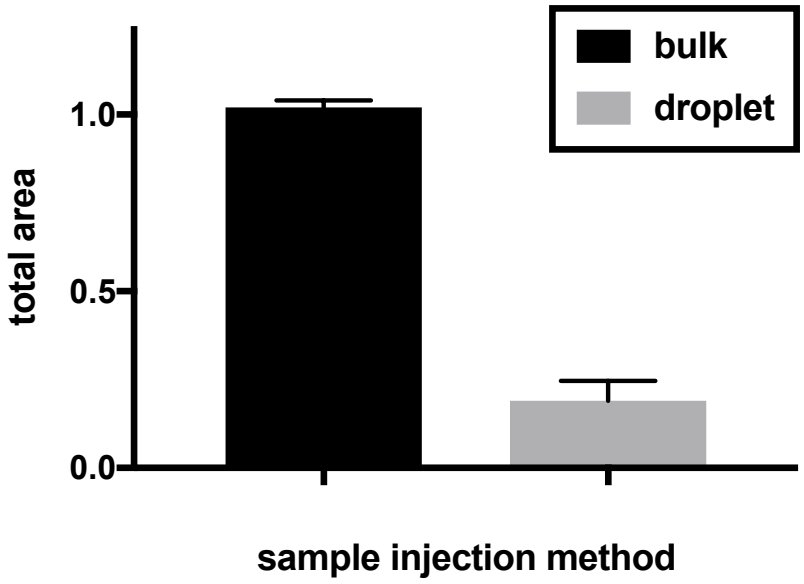

Figure 4-9. Comparison of signal obtained from injection of bulk sample to injection from droplet samples containing 500 nM Hsp70* diluted in water.

The current design is limited to use with carrier phases with lower density than the background electrolyte. Often fluorinated carrier phases are preferred for their inert properties and low partitioning of many analytes. Fluorinated carrier phases have relatively high densities which would allow them to be separated from a lower density background electrolyte by modification of the current device design. This is appealing for future applications of this device where molecules that are soluble in silicone oil may transfer between droplets.

Conclusions

This work demonstrated a novel method for coupling droplets to microchip separations by removing the carrier phase based on its density. The density-based oil drain was compatible with both sieving and free solution electrophoresis with throughput of about 10 s/sample. Interference of segmenting oil with electrophoresis was not observed for up

to 175 samples analyzed. Similar to other devices, the operation is sensitive to sample matrix effects, limiting the number of samples that can be analyzed without reconditioning. The utility of this device was demonstrated for protein-protein interaction and enzyme assay samples suggesting future utility in screening of diverse targets.

Chapter 5: Future Directions

This thesis has described a method for investigating protein-protein interactions by capillary electrophoresis with high throughput separations demonstrated using microchip electrophoresis. Using the PXCE method described here, many PPIs can be studied using CE with minimal method development. Separation times of 1 min, using commercial CE instrumentation, and 2.5 s, using microchip electrophoresis were demonstrated for separation of PPIs. Further, a method for fast, automated, sample introduction using droplet microfluidics allowed for throughputs of 10 s/sample for free solution and gel electrophoresis separations. While these results suggest this platform may have utility in screening, a large scale screen has yet to be performed using this platform. Further, the presented methods are still limited by sample introduction throughput, required labeling of one of the protein-binding partners, and necessitated microliter sample volumes. Opportunities for improved throughput, label-free and small volume assays are proposed.

Improving Throughput for Microchip Electrophoresis of PPIs

While Chapter 4 presented a method for automating sample introduction to improve assay throughput the separation times achievable by microchip electrophoresis remain faster than the sample introduction throughput achieved. Fast sample introduction could also be achieved by incorporation of multiple sample reservoirs per device or parallelization of separation channels.

Devices with multiple sample reservoirs from which injections could be made have been reported. This strategy allows for rapid switching between samples, a process that could be easily automated. To demonstrate the utility of this approach for protein-protein interaction samples a microchip with 5 sampling reservoirs and a single separation channel was fabricated (**Figure 5-1A)**. Injections from each sample reservoir could be made sequentially simply by switching which sample reservoir was held at high voltage (**Figure 5-1B)**. This strategy eliminates the need to reformat samples into droplets prior to electrophoresis. As demonstrated in figure 5-1, such a device is ideally suited for assays requiring <10 samples such as for K_d, K_i, or IC_{50} determination.

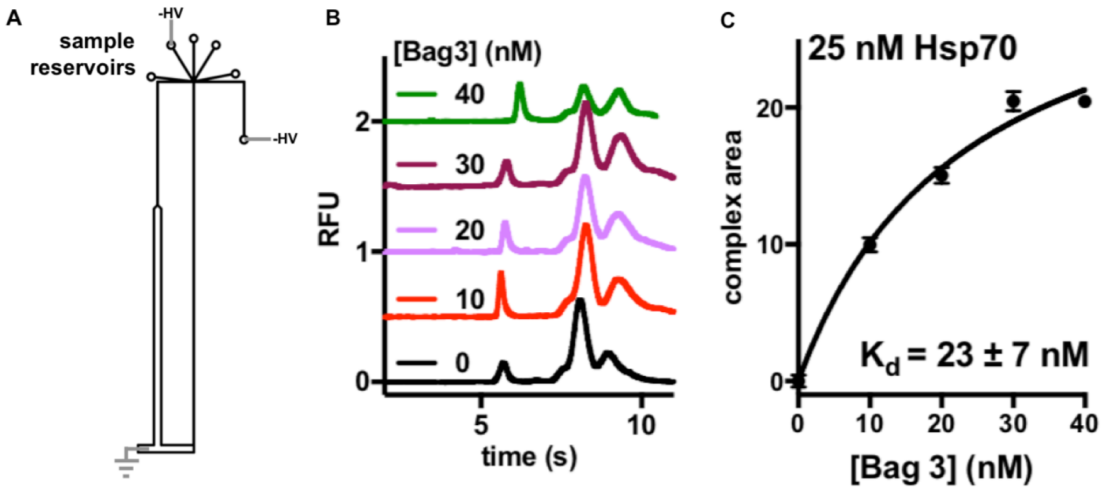

Figure 5-1. Schematic of electrophoresis device for introducing five samples in the same device (A). Use of device for K_d determination (B and C).

To further improve throughput a device with multiple separation channels could be fabricated. Parallelization affords increased throughput by allowing multiple separations to be performed simultaneously. A parallel density oil drain system may be possible for high throughput analysis of a large number of droplet samples (**Figure 5-2**). Detection on a parallelized device can be achieved by fluorescence imaging.[22] Incorporation of three separation channels on a single device triples the throughput in

comparison to a single channel device. Further, the number of droplets that can be produced in a single train is limited. This device would allow for a 3-fold increase in the number of droplets that could be analyzed in a single run.

Previously, parallel oil-removal and electrophoresis has been demonstrated using a device with surface patterning for oil removal.[69] This device contained three extraction channels and achieved throughput of 120 samples in 10 min (15 s/sample/channel). This sort of parallelization has yet to be applied to newer oil extraction techniques, including the density oil drain, which affords easier fabrication. A degree of higher parallelization (> 3 simultaneous extraction channels) may also be possible. Up to 384 parallel separations have been reported by MCE without oil extraction.[25]

A device consisting of just 3 parallel density oil drains and separation channels would allow for increased analysis throughput. Using conditions described in Chapter 4, a microchip device with three parallel density oil drains would afford a throughput of 21 min per 384 well plate. Further, a 10,000 compound library could be analyzed within a day with just 3 parallel extraction and separation channels.

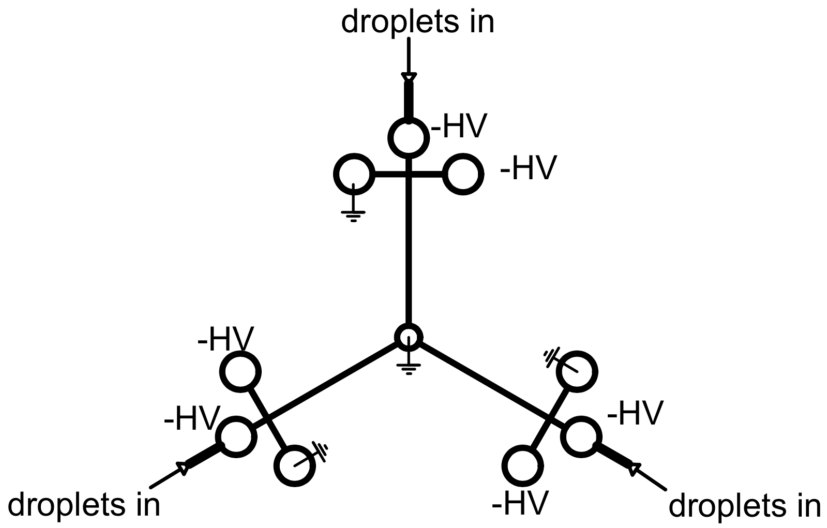

Figure 5-2. Schematic of multi-channel density oil drain device for high-throughput PPI modulator screening Three droplet trains can be introduced and electrophoresed simultaneously by introduction to three independent separation channels and detecting with fluorescence imaging.

Label-Free Protein Cross-linking Capillary Electrophoresis

An inherent limitation of affinity probe CE-LIF for PPI analysis is the requirement for one of the protein binding partners to be fluorescently labeled. Protein labeling is a potential source of assay interference as labeling can affect binding affinity.[171] Label free detection strategies compatible with CE include capacitively coupled contactless conductivity, MS, and UV. Use of MS is problematic due to the high concentration of SDS in the background electrolyte[199] of the SDS-gel electrophoretic separations used in this work to readily resolve free proteins from protein complexes. Similarly, the use of conductivity detection can be challenging due to electrode fouling.[200] Without changing separation conditions, UV detection of unlabeled samples is possible due to inherent absorbance of peptide bond at 200 nm and aromatic amino acids at 280 nm. To determine if PPI analysis of unlabeled protein is possible by CE-UV 3 μM Hsp70 was cross-linked injected and separated by capillary gel electrophoresis (**Figure 5-3)**. At this

concentration, in the apo nucleotide state, Hsp70 is expected to homodimerize. Both free and homodimeric Hsp70 were observed with UV detection, demonstrating the potential of label-free PXCE.

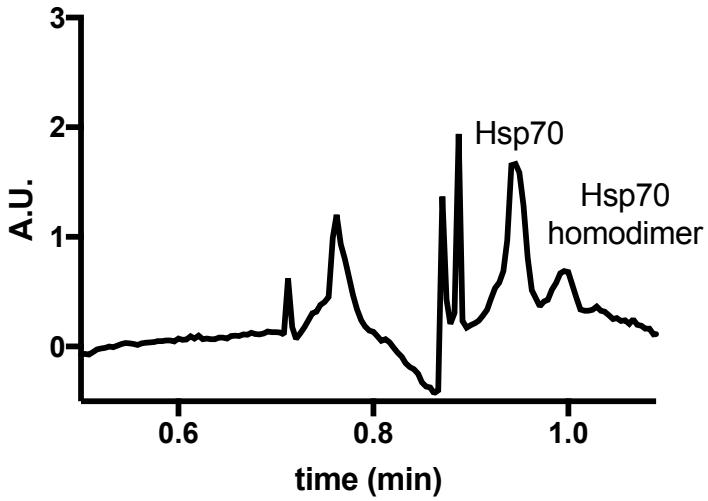

Figure 5-3. Detection of 3 μM unlabeled Hsp70 using CE-UV. Separation conditions were as in Figure 3-9 with the exceptions of the capillary temperature which was 60 ˚C and detection method which was UV absorbance at 200 nm.

CE-UV typically suffers from poor limits of detection. In this work, low micromolar concentrations of protein were observed to be required for detection. While analysis of PPIs with low micromolar K_d values (such as Hsp70 homodimer) is possible, the poor sensitivity limits the potential applications of this approach.

Several possibilities exist for improving CE-UV detection sensitivity. Increasing the inner diameter of the capillary increases the path length resulting in linear increase in signal. Here a 25 μm internal diameter capillary was employed. Simply increasing the internal diameter of the capillary to 50 μm is expected to double the signal. Additional sample preconcentration strategies, common in CE[201], such as field amplified sample

injection and isotachophoresis are compatible with this separation. To demonstrate this potential, a combination of field amplified sample injection followed by isotachophoresis, termed electrokinetic supercharging, was applied to separation of fluorescently labeled Hsp70 (**Figure 5-4**). A limit of detection of 72 pM was achieved using this method with fluorescence detection, suggesting potential to improve sensitivity of CE-UV as well.

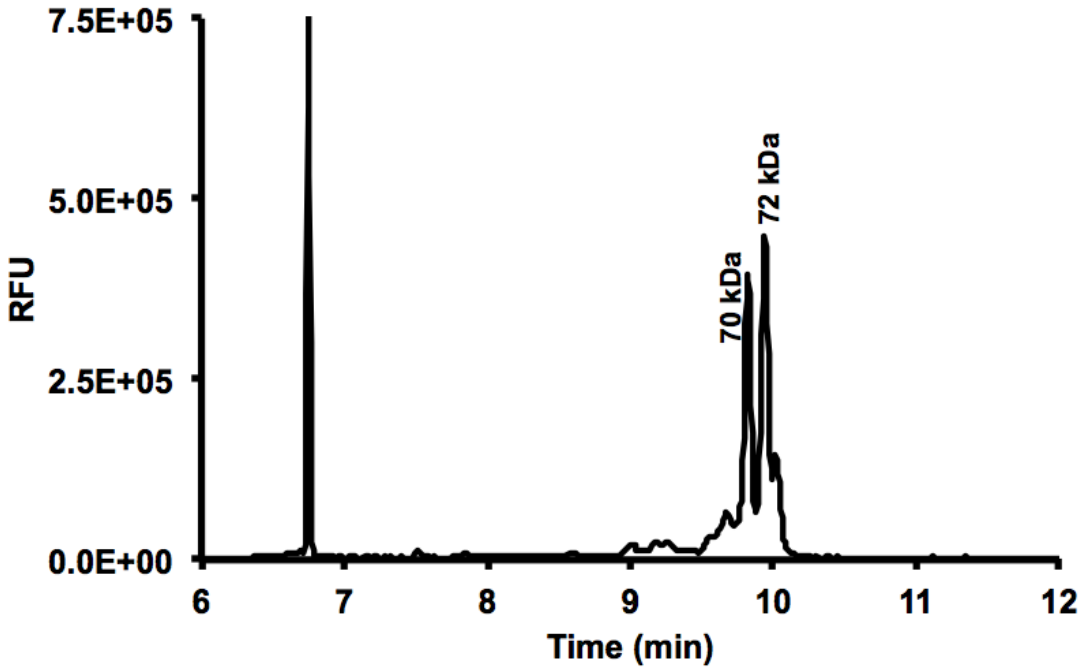

Figure 5-4. Separation of 33 nM Hsp70* using electrokinetic supercharging. Sample was injected electrokinetically at 9 kV for 30 s. Separation voltage was 400 V/cm. Separation distance was 10 cm. The sieving matrix was 7% w/v dextran (1.5-2.8 Mda), 220 mM Tris, 180 mM boric acid, 10% glycerol, 13.8 mM SDS, and 3 mM EDTA.

An alternative to label free detection is to cross-link unlabeled proteins and label them after the cross-linking is complete. Proteins could be labeled before separation and immediately analyzed by CGE as the unreacted, small molecule fluorophore would be readily resolved from the proteins. This puts greater burden on the separation to resolve the free fluorophore from both of the free proteins and the protein complex. It also

requires the cross-linker and the fluorophore to react with different amino acids. Post-column labeling could also be employed. Naphthalene-2-3-dicarbaldehyde (NDA) has low fluorescence until it conjugates with proteins and has been demonstrated to give low nanomolar LODs for CGE of proteins, however this requires modification of the background electrolyte[202]. Alternatively, a non-covalent approach using SYPRO Orange dye may be easier to implement. SYPRO Orange dye fluoresces when it associates with the hydrophobic core of SDS-protein complexes.[169]

Reducing Protein Consumption

The large amount of protein required for HTS is a significant contributor to the cost of screening, particularly for highly sensitive or difficult to produce proteins.[203,204]. While capillary and microchip electrophoresis require only nanoliter to picoliter injection volumes current instrumentation requires microliters of sample for injection. For example, an ideal injection volume (about 1% of capillary volume) on a 10 cm long, 25 μm internal diameter capillary, as used in Chapter 3, would be approximately 440 pL. However, sample preparation is typically performed on the microliter scale resulting in much wasted protein. Performing the sample preparation online has the potential to decrease the protein consumption by >100,000-fold in this case.

One strategy for decreasing protein consumption is to perform the assay within the capillary. Many strategies exist for mixing reagent plugs within the capillary for performing screening assays online. Mixing strategies include electrophoretically mediated microanalysis (EMMA)[74,77,79], transverse diffusion of laminar flow profiles (TDLFP)[80,81] and immobilized enzyme reactors (IMERs)[82–87]. IMERs is inherently incompatible with the PXCE method and while EMMA has been extensively

demonstrated on small numbers of compounds, it requires knowledge of electrophoretic mobility of each plug. TDLFP is therefore better suited for screening of diverse compound libraries. TDLFP exploits the mixing that occurs by parabolic plug flow induced by a pressure injection and is therefore mixing is independent of electrophoretic mobility. TDLFP has been extensively theoretically and experimentally investigated and exhibits good results for mixing of even slowly diffusing molecules such as proteins.[88,89] One study reported sufficient zone overlap of enzyme plug achieved in less than 1 min.[89] The TDLFP strategy has been demonstrated for screening of a limited number of compounds for enzyme targets alone[80,81,89] but has potential to scale up and apply to PPI targets using PXCE with minor modification. This strategy would involve sequentially injecting plugs of each protein binding partner and test compound, allowing interactions to equilibrate, injecting a plug of cross-linker, and electrophoresing (**Figure 5-5**). In this assay, protein consumption would be reduced to just 300 ng for assaying 10,000 test compounds.

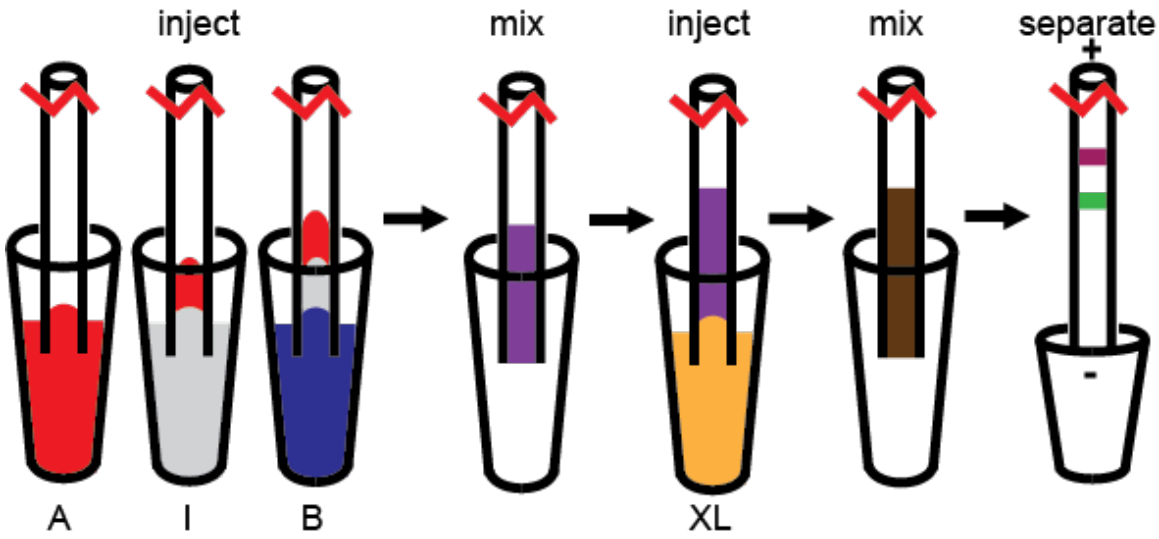

Figure 5-5. Schematic of online CE assay for PPI screening with mixing by TDLFP for PPI screening. Each protein (A and B) and test compound (I) is injected by pressure onto capillary inducing parabolic flow and transverse diffusion. Cross-linker (XL) is then added by hydrodynamic injection allowing for online protein cross-linking to occur prior to electrophoretic separation.

While in-capillary reaction strategies greatly reduce protein consumption to just picoliters per sample, the throughput is limited by the kinetics of the reactions performed online. For example, an on-chip assay of SIRT1 inhibition by three known inhibitors was demonstrated with 10 min of on-chip reaction time.[205] With this limitation, the in-capillary reaction strategy is most well suited for enzyme targets with rapid turnover or PPIs where binding occurs rapidly. To assay targets with slower kinetics using this strategy capillary array instrumentation is potentially useful. Further, test compound sample pooling is also potentially useful to increase throughput. Up to 10 test compounds per sample have been analyzed by CE.[28] This degree of test compound sample pooling would also further reduce protein consumption 10-fold. Test compound sample pooling is well suited for PPI screening where low hit rates have been reported. For example, a hit rate of just 0.03% was reported for one Hsp90-HOP screen.[206]

Alternatively, the entire assay could be performed in droplets prior to electrophoresis. While, the platform described in Chapter 4 introduces only nanoliter volumes of sample into the chip the system does not reduce sample requirements as the samples are originally prepared and formatted in microliter volumes in a multiwell plate. To reduce overall assay volume compound libraries could be reformatted into droplets to which protein could be added. There are many reported methods for addition of reagent to a sample droplet.[46,48,49,63,207,208] With addition of proteins to test compound containing droplet, the entire reaction could be performed in the droplet. This strategy has been demonstrated with fluorescence[70] and MS[46] detection. The droplet assay with fluorescence detection reported a 25,000-fold reduction in sample compared to bulk methods.[70]

One challenge with performing the entire assay in droplets is potential for protein activity to be impacted by the carrier phase interface The identity of the carrier phase has been demonstrated to have an effect on the activity of proteins, in some cases.[209] The carrier phase used in Chapter 4, silicone oil, is unlikely to be compatible with PPI assays due to potential for hydrophobic regions of the protein to adsorb to the oil-droplet interface. It is expected that a highly fluorinated carrier phase may be more inert and therefore suitable to assaying PPIs within droplets. Use of a heavily fluorinated carrier phase would require modification of the density-based oil drain described in Chapter 4 as the density of the carrier phase would be greater than the density of most background electrolytes. A simple modification to the current design would be to drill a hole through the device at the outlet of the fused silica droplet transfer capillary and attach a closed reservoir filled with background electrolyte above and below the device. The dense

immiscible fluorinated carrier phase would then drain to the bottom of this reservoir displacing only about 1 μL of background electrolyte per 100 samples.

Conclusion

Challenging method development has hindered analysis of protein-protein interactions by capillary electrophoresis. The use of protein cross-linking prior to electrophoresis simplifies method development by eliminating the need to maintain the native interaction during the separation. Inherent limitations of this strategy include the size and affinities of the complexes that can be analyzed in this manner. Nevertheless, this strategy has been demonstrated for analysis of eight different protein-protein interactions with micromolar to nanomolar K_d values. Separations are readily achieved using capillary or microchip electrophoresis and improvements to throughput have allowed separations in 1 min by commercial capillary electrophoresis and 2.5 s by microchip electrophoresis. A droplet microfluidic method for automated sample introduction for microchip electrophoresis achieved sample introduction throughput of 10 s/sample. Potential future work could further improve the throughput of sample introduction to microchip electrophoresis, modify the method for use with unlabeled protein, and take advantage of the low sample volume requirements of capillary electrophoresis.

REFERENCES

(1) Deeb, S. El; Wätzig, H.; El-Hady, D. A. *TrAC - Trends Anal. Chem.* **2013**, *48*, 112.

(2) Perrin, D.; Frémaux, C.; Shutes, A. *Expert Opin. Drug Discov.* **2009**, *15*, 51.

(3) Shanmuganathan, M.; Britz-McKibbin, P. *Anal. Chim. Acta* **2013**, *773*, 24.

(4) Perrin, D.; Martin, T.; Cambet, Y.; Frémaux, C.; Scheer, A. *Assay Drug Dev. Technol.* **2006**, *4* (2), 185.

(5) Rauch, J. N.; Nie, J.; Buchholz, T. J.; Gestwicki, J. E.; Kennedy, R. T. *Anal Chem* **2013**.

(6) Rauch, J. N.; Nie, J.; Buchholz, T. J.; Gestwicki, J. E.; Kennedy, R. T. *Anal. Chem.* **2013**, *85*, 9824.

(7) Perrin, D.; Frémaux, C.; Scheer, A. *J. Biomol. Screen.* **2006**, *11* (4), 359.

(8) Pommereau, A.; Pap, E.; Kannt, A. *J. Biomol. Screen.* **2004**, *9* (5), 409.

(9) Dunne, J.; Reardon, H.; Trinh, V.; Li, E.; Farinas, J. *Assay Drug Dev. Technol.* **2004**, *2* (2), 121.

(10) Liu, Y.; Gerber, R.; Wu, J.; Tsuruda, T.; McCarter, J. D. *Anal. Biochem.* **2008**, *378* (1), 53.

(11) Perrin, D.; Fremaux, C.; Besson, D.; Sauer, W. H.; Scheer, A. *J. Biomol. Screen.* **2006**, *11* (8), 996.

(12) Fourtounis, J.; Falgueyret, J. P.; Sayegh, C. E. *Anal. Biochem.* **2011**, *411* (1), 161.

(13) Jorgenson, J. W.; Lukacs, K. D. *Anal. Chem.* **1981**, *53* (8), 1298.

(14) Hai, X.; Wang, X.; El-Attug, M.; Adams, E.; Hoogmartens, J.; Van Schepdael, A. *Anal. Chem.* **2011**, *83* (1), 425.

(15) Moore, A. W.; Jorgenson, J. W. *Anal. Chem.* **1993**, *65* (24), 3550.

(16) Tao, L.; Thompson, J. E.; Kennedy, R. T. *Anal. Chem.* **1998**, *70* (19), 4015.

(17) Guetschow, E. D.; Steyer, D. J.; Kennedy, R. T. *Anal. Chem.* **2014**, *86*, 10373.

(18) Guetschow, E. D.; Kumar, S.; Lombard, D. B.; Kennedy, R. T. *Anal. Bioanal. Chem.* **2016**, 1.

(19) Jacobson, S. C.; Hergenroder, R.; Koutny, L. B.; Ramsey, J. M. *Anal Chem* **1994**, *66* (7), 1114.

(20) Lindenburg, P. W.; Haselberg, R.; Rozing, G.; Ramautar, R. *Chromatographia* **2015**, *78*, 367.

(21) Roche, M. E.; Oda, R. P.; Machacek, D.; Lawson, G. M.; Landers, J. P. *Anal. Chem.* **1997**, *69* (1), 99.

(22) Dishinger, J. F.; Kennedy, R. T. *Electrophoresis* **2008**, *29* (16), 3296.

(23) Huang, X. C.; Quesada, M. A.; Mathies, R. A. *Anal. Chem.* **1992**, *64* (8), 967.

(24) Ma, L.; Gong, X.; Yeung, E. S. *Anal. Chem.* **2000**, *72* (14), 3383.

(25) Emrich, C. A.; Tian, H.; Medintz, I. L.; Mathies, R. A. *Anal. Chem.* **2002**, *74* (19), 5076.

(26) Pei, J.; Dishinger, J. F.; Roman, D. L.; Rungwanitcha, C.; Neubig, R. R.; Kennedy, R. T. *Anal. Chem.* **2008**, *80* (13), 5225.

(27) Xu, H.; Ewing, A. G. *Electrophoresis* **2005**, *26* (24), 4711.

(28) Xu, M.; Liu, C.; Zhou, M.; Li, Q.; Wang, R.; Kang, J. *Anal. Chem.* **2016**, *88* (16),

8050.

(29) Xue, Q.; Wainright, A.; Gangakhedkar, S.; Gibbons, I. *Electrophoresis* **2001**, *22* (18), 4000.

(30) Yang, P. L.; Whelan, R. J.; Mao, Y. W.; Lee, A. W. M.; Carter-Su, C.; Kennedy, R. T. *Anal. Chem.* **2007**, *79* (4), 1690.

(31) Shackman, J. G.; Watson, C. J.; Kennedy, R. T. *J. Chromatogr. A* **2004**, *1040* (2), 273.

(32) Jacobson, S. C.; Hergenruder, R.; Moore, A. W.; Ramsey, J. M. *Anal. Chem.* **1994**, *66* (23), 4127.

(33) Monnig, C. A.; Jorgenson, J. W. *Anal. Chem.* **1991**, *63* (8), 802.

(34) Lemmo, A. V; Jorgenson, J. *Anal. Chem.* **1993**, *65* (7), 1576.

(35) Fang, X.; Fang, P.; Pan, J.; Fang, Q. *Electrophoresis* **2016**.

(36) Fishman, H. A.; Amudi, N. M.; Lee, T. T.; Scheller, R. H.; Zare, R. N. *Anal. Chem.* **1994**, *66* (14), 2318.

(37) Li, Q.; Zhu, Y.; Zhang, N.-Q.; Fang, Q. *Sci. Rep.* **2016**, *6*, 26654.

(38) Hassan, S. U.; Morgan, H.; Zhang, X.; Niu, X. *Anal. Chem.* **2015**, *87* (7), 3895.

(39) Du, W.; Li, L.; Nichols, K. P.; Ismagilov, R. F. *Lab Chip* **2009**, *9* (16), 2286.

(40) Ward, T.; Faivre, M.; Abkarian, M.; Stone, H. A. *Electrophoresis* **2005**, *26* (19), 3716.

(41) Song, H.; Tice, J. D.; Ismagilov, R. F. *Angew. Chemie - Int. Ed.* **2003**, *1*, 767.

(42) Garstecki, P.; Fuerstman, M. J.; Stone, H. a; Whitesides, G. M. *Lab Chip* **2006**, *6* (3), 437.

(43) Anna, S. L.; Bontoux, N.; Stone, H. A. *Appl. Phys. Lett.* **2003**, *82* (3), 364.

(44) Chabert, M.; Dorfman, K. D.; De Cremoux, P.; Roeraade, J.; Viovy, J. L. *Anal. Chem.* **2006**, *78* (22), 7722.

(45) Gielen, F.; Van Vliet, L.; Koprowski, B. T.; Devenish, S. R. A.; Fischlechner, M.; Edel, J. B.; Niu, X.; Demello, A. J.; Hollfelder, F. *Anal. Chem.* **2013**, *85* (9), 4761.

(46) Sun, S.; Slaney, T. R.; Kennedy, R. T. *Anal. Chem.* **2012**, *84* (13), 5794.

(47) Sun, S.; Kennedy, R. T. *Anal. Chem.* **2014**, *86* (18), 9309.

(48) Shestopalov, I.; Tice, J. D.; Ismagilov, R. F. *Lab Chip* **2004**, *4* (4), 316.

(49) Song, H.; Li, H. W.; Munson, M. S.; Ha, T. G. Van; Ismagilov, R. F. *Anal. Chem.* **2006**, *78* (14), 4839.

(50) Casadevall i Solvas, X.; Srisa-Art, M.; DeMello, A. J.; Edel, J. B. *Anal. Chem.* **2010**, *82* (9), 3950.

(51) Liau, A.; Kamik, R.; Majumdar, A.; Cate, J. H. D. *Anal. Chem.* **2005**, *77* (23), 7618.

(52) Song, H.; Bringer, M. R.; Tice, J. D.; Gerdts, C. J.; Ismagilov, R. F. *Appl. Phys. Lett.* **2003**, *83* (22), 4664.

(53) Niu, X.; Gulati, S.; Edel, J. B.; deMello, A. J. *Lab Chip* **2008**, *8* (11), 1837.

(54) Christopher, G. F.; Bergstein, J.; End, N. B.; Poon, M.; Nguyen, C.; Anna, S. L. *Lab Chip* **2009**, *9* (8), 1102.

(55) Fidalgo, L. M.; Abell, C.; Huck, W. T. S. *Lab Chip* **2007**, *7* (8), 984.

(56) Mazutis, L.; Baret, J.-C.; Griffiths, A. D. *Lab Chip* **2009**, *9* (18), 2665.

(57) Zagnoni, M.; Cooper, J. M. *Lab Chip* **2009**, *9* (18), 2652.

(58) Adamson, D. N.; Mustafi, D.; Zhang, J. X. J.; Zheng, B.; Ismagilov, R. F. *Lab Chip* **2006**, *6* (9), 1178.

(59) Link, D.; Anna, S.; Weitz, D.; Stone, H. *Phys. Rev. Lett.* **2004**, *92* (5), 54503.

(60) Nie, J.; Kennedy, R. T. *Anal. Chem.* **2010**, *82* (18), 7852.

(61) Choi, J.-H.; Lee, S.-K.; Lim, J.-M.; Yang, S.-M.; Yi, G.-R. *Lab Chip* **2010**, *10* (4), 456.

(62) Li, L.; Boedicker, J. Q.; Ismagilov, R. F. *Anal. Chem.* **2007**, *79* (7), 2756.

(63) Slaney, T. R.; Nie, J.; Hershey, N. D.; Thwar, P. K.; Linderman, J.; Burns, M. A.; Kennedy, R. T. **2011**, *83*, 5207.

(64) Roman, G. T.; Wang, M.; Shultz, K. N.; Jennings, C.; Kennedy, R. T. *Anal. Chem.* **2008**, *80* (21), 8231.

(65) Wang, M.; Roman, G. T.; Perry, M. L.; Kennedy, R. T. *Anal. Chem.* **2009**, *81* (21), 9072.

(66) Fidalgo, L. M.; Whyte, G.; Bratton, D.; Kaminski, C. F.; Abell, C.; Huck, W. T. S. *Angew. Chemie - Int. Ed.* **2008**, *47* (11), 2042.

(67) Angelescu, D. E.; Mercier, B.; Sless, D.; Schroetter, R. *Anal. Chem.* **2010**, *82* (6), 2412.

(68) Niu, X. Z.; Zhang, B.; Marszalek, R. T.; Ces, O.; Edel, J. B.; Klug, D. R.; deMello, A. J. *Chem. Commun. (Camb).* **2009**, No. 41, 6159.

(69) Pei, J.; Nie, J.; Kennedy, R. T. *Anal. Chem.* **2010**, *82* (22), 9261.

(70) Miller, O. J.; El, A.; Mangeat, T.; Baret, J.; Frenz, L.; El, B.; Mayot, E.; Samuels, M. L.; Rooney, E. K.; Dieu, P.; Galvan, M.; Link, D. R.; Griffiths, A. D. *Proc. Natl. Acad. Sci.* **2012**, *109* (2), 378.

(71) Edgar, J. S.; Pabbati, C. P.; Lorenz, R. M.; He, M.; Fiorini, G. S.; Chiu, D. T. *Anal. Chem.* **2006**, *78* (19), 6948.

(72) Delamarre, M. F.; Shippy, S. A. *Anal. Chem.* **2014**, *86*, 10193.

(73) Niu, X.; Pereira, F.; Edel, J. B.; Demello, A. J. *Anal. Chem.* **2013**, *85* (18), 8654.

(74) Jiang, T.-F.; Chong, L.; Yue, M.-E.; Wang, Y.-H.; Lv, Z.-H. *J. Anal. Chem.* **2016**, *71* (3), 283.

(75) Guo, L. P.; Jiang, T. F.; Lv, Z. H.; Wang, Y. H. *J. Pharm. Biomed. Anal.* **2010**, *53* (5), 1250.

(76) Zhang, W. H.; Lv, Z. H.; Jiang, T. F.; Wang, Y. H.; Guo, L. P. *J. Food Drug Anal.* **2012**, *20* (1), 159.

(77) Wang, H.; Xu, W.; Cao, J.; Wang, W. *Electrophoresis* **2015**, *36* (2), 319.

(78) Tang, Z.; Wang, Z. Y.; Kang, J. W. *Electrophoresis* **2007**, *28* (3), 360.

(79) Nehmé, H.; Nehmé, R.; Lafite, P.; Routier, S.; Morin, P. *J. Sep. Sci.* **2013**, *36* (13), 2151.

(80) Křížek, T.; Doubnerová, V.; Ryšlavá, H.; Coufal, P.; Bosáková, Z. *Anal. Bioanal. Chem.* **2013**, *405* (8), 2425.

(81) Nehmé, H.; Nehmé, R.; Lafite, P.; Routier, S.; Morin, P. *J. Chromatogr. A* **2013**, *1314*, 298.

(82) Lin, P.; Zhao, S.; Lu, X.; Ye, F.; Wang, H. *J. Sep. Sci.* **2013**, *36* (15), 2538.

(83) Zhao, S.; Ji, X.; Lin, P.; Liu, Y. M. *Anal. Biochem.* **2011**, *411* (1), 88.

(84) Camara, M. A.; Tian, M.; Guo, L.; Yang, L. *J. Chromatogr. B Anal. Technol. Biomed. Life Sci.* **2015**, *990*, 174.

(85) Iqbal, J. *Anal. Biochem.* **2011**, *414* (2), 226.

(86) Tang, Z.; Wang, T.; Kang, J. *Electrophoresis* **2007**, *28* (17), 2981.

(87) Tang, Z.; Kang, J. *Anal. Chem.* **2006**, *78*, 2514.

(88) Okhonin, V.; Liu, X.; Krylov, S. N. *Anal. Chem.* **2005**, *77* (18), 5925.

(89) Wong, E.; Okhonin, V.; Berezovski, M. V; Nozaki, T.; Waldmann, H.; Alexandrov, K.; Krylov, S. N. *J Am Chem Soc* **2008**, *130*, 11862.

(90) Zhao, H.; Chen, Z. *J. Chromatogr. A* **2014**, *1340* (2014), 139.

(91) Wang, S.; Su, P.; Yang, Y. *Anal. Biochem.* **2012**, *427* (2), 139.

(92) Ji, X.; Ye, F.; Lin, P.; Zhao, S. *Talanta* **2010**, *82*, 1170.

(93) Heegaard, N. H. H. *Electrophoresis* **2009**, *30*, 229.

(94) Galievsky, V. A.; Stasheuski, A. S.; Krylov, S. N. *Anal. Chem.* **2015**, *87*, 157.

(95) Zou, D.; Zhang, D.; Liu, S.; Zhao, B.; Wang, H. *Anal. Chem.* **2014**, *86* (3), 1775.

(96) Yang, P. L.; Mao, Y.; Lee, A. W. M.; Kennedy, R. T. *Electrophoresis* **2009**, *30* (3), 457.

(97) Pedersen, J. T.; Østergaard, J.; Houen, G.; Heegaard, N. H. H. *Electrophoresis* **2008**, *29* (8), 1723.

(98) Shimura, K.; Waki, T.; Okada, M.; Toda, T.; Kimoto, I.; Kasai, K. I. *Electrophoresis* **2006**, *27* (10), 1886.

(99) Chen, X.; Flynn, G. C. *J. Chromatogr. B* **2009**, *877* (27), 3012.

(100) Ouameur, A. A.; Tajmir-Riahi, H. A. *J. Biol. Chem.* **2004**, *279* (40), 42041.

(101) Ouameur, A. A.; Bourassa, P.; Tajmir-Riahi, H.-A. *RNA* **2010**, *16* (10), 1968.

(102) Quaglia, M.; Carazzone, C.; Sabella, S.; Colombo, R.; Giorgetti, S.; Bellotti, V.; De Lorenzi, E. *Electrophoresis* **2005**, *26* (21), 4055.

(103) Mcdonnell, P. A.; Caldwell, G. W.; Masucci, J. A. *Electrophoresis* **1998**, *19*, 448.

(104) Liu, L.; Xu, X.; Liu, Y.; Zhang, X.; Li, L.; Jia, Z. *J. Pharm. Biomed. Anal.* **2016**, *120*, 153.

(105) Hughes, D. Affinity Capillary Electrophoresis Method for Assessing a Biological Interaction of a Ligand/Receptor Pair Such as G Protein Coupled Receptor and its Targets as well as for Drug Screening. US 2012/0175255 A1, 2012.

(106) Shimura, K.; Karger, B. L. *Anal. Chem.* **1994**, *66* (1), 9.

(107) Farcas, E.; Bouckaert, C.; Servais, A.; Hanson, J.; Pochet, L.; Fillet, M. *Anal. Chim. Acta* **2017**, *984*, 211.

(108) Austin, C.; Pettit, S. N.; Magnolo, S. K.; Sanvoisin, J.; Chen, W.; Wood, S. P.; Freeman, L. D.; Pengelly, R. J.; Hughes, D. E. *J. Biomol. Screen.* **2012**, *17* (7), 868.

(109) Wells, J. A.; McClendon, C. L. *Nature* **2007**, *450* (7172), 1001.

(110) Arkin, M. R.; Tang, Y.; Wells, J. A. *Chem. Biol.* **2014**, *21* (9), 1102.

(111) Pryor, N. E.; Moss, M. A.; Hestekin, C. N. *Electrophoresis* **2014**, *35*, 1814.

(112) Picou, R. A.; Kheterpal, I.; Wellman, A. D.; Minnamreddy, M.; Ku, G.; Gilman, S. D. *J. Chromatogr. B Anal. Technol. Biomed. Life Sci.* **2011**, *879* (9–10), 627.

(113) Picou, R. A.; Schrum, D. P.; Ku, G.; Cerqua, R. A.; Kheterpal, I.; Gilman, S. D. *Anal. Biochem.* **2012**, *425* (2), 104.

(114) Liyanage, R.; Krylova, S. M.; Krylov, S. N. *J. Chromatogr. A* **2013**, *1322*, 90.

(115) de Jong, S.; Epelbaum, N.; Liyanage, R.; Krylov, S. N. *Electrophoresis* **2012**, *33* (16), 2584.

(116) Tan, L.; Zheng, X.; Chen, L.; Wang, Y. *J. Sep. Sci.* **2014**, *37* (20), 2974.

(117) You, J.; Zhao, L.; Wang, G.; Zhou, H.; Zhou, J.; Zhang, L. *J. Chromatogr. A* **2014**, *1343*, 160.

(118) Witos, J.; Karesoja, M.; Karjalainen, E.; Tenhu, H.; Riekkola, M. L. *J. Sep. Sci.*

2013, *36* (6), 1070.

(119) Saibil, H. *Nat. Publ. Gr.* **2013**, *14* (10), 630.

(120) Ciocca, D. R.; Calderwood, S. K. **2005**, *10*, 86.

(121) Blair, L. J.; Sabbagh, J. J.; Dickey, C. A. *Expert Opin. Ther. Targets* **2014**, *18* (10), 1219.

(122) Kundrat, L.; Regan, L. *Biochemistry* **2010**, *49*, 7428.

(123) Colvin, T. a.; Gabai, V. L.; Gong, J.; Calderwood, S. K.; Li, H.; Gummuluru, S.; Matchuk, O. N.; Smirnova, S. G.; Orlova, N. V.; Zamulaeva, I. a.; Garcia-Marcos, M.; Li, X.; Young, Z. T.; Rauch, J. N.; Gestwicki, J. E.; Takayama, S.; Sherman, M. Y. *Cancer Res.* **2014**, *74* (23), 4731.

(124) Shao, H.; Li, X.; Moses, M. A.; Gilbert, L. A.; Kalyanaraman, C.; Young, Z. T.; Chernova, M.; Journey, S. N.; Weissman, J. S.; Hann, B.; Jacobson, M. P.; Neckers, L.; Gestwicki, J. E. **2018**, *70*.

(125) Young, Z. T.; Rauch, J. N.; Assimon, V. A.; Zuiderweg, E. R. P.; Dickey, C. A.; Gestwicki, J. E.; Young, Z. T.; Rauch, J. N.; Assimon, V. A.; Jinwal, U. K.; Ahn, M.; Li, X. *Cell Chem. Biol.* **2016**, *23* (8), 992.

(126) Schopf, F. H.; Biebl, M. M.; Buchner, J. *Nat. Publ. Gr.* **2017**, *18* (6), 345.

(127) Thakur, J. K.; Arthanari, H.; Yang, F.; Pan, S.; Fan, X.; Breger, J.; Frueh, D. P.; Gulshan, K.; Li, D. K.; Mylonakis, E.; Struhl, K.; Moye-rowley, W. S.; Cormack, B. P.; Wagner, G.; Na, A. M. **2008**, *452* (April).

(128) Pomerantz, W. C.; Wang, N.; Lipinski, A. K.; Wang, R.; Cierpicki, T.; Mapp, A. K. *ACS Chem. Biol.* **2012**, *7* (8), 1345.

(129) Sakamoto, K. M.; Frank, D. A. **2009**, *15* (8), 2583.

(130) Hallam, T. M.; Bourtchouladze, R. **2006**, *63*, 1725.

(131) Koehler, A. N. *Curr. Opin. Chem. Biol.* **2010**, *14* (3), 331.

(132) Hafner, F. T.; Kautz, R. A.; Iverson, B. L.; Tim, R. C.; Karger, B. L. *Anal. Chem.* **2000**, *72* (23), 5779.

(133) Schultz, N. M.; Kennedy, R. T. *Anal. Chem.* **1993**, *65* (9), 3161.

(134) Lassen, K. S.; Bradbury, A. R. M.; Rehfeld, J. F.; Heegaard, N. H. H. *Electrophoresis* **2008**, *29* (12), 2557.

(135) Wan, Q. H.; Le, X. C. *Anal. Chem.* **1999**, *71* (19), 4183.

(136) Mohamadi, M. R.; Kaji, N.; Tokeshi, M.; Baba, Y. *Anal. Chem.* **2007**, *79* (10), 3667.

(137) Shi, M.; Zhao, S.; Huang, Y.; Liu, Y. M.; Ye, F. *J. Chromatogr. B Anal. Technol. Biomed. Life Sci.* **2011**, *879* (26), 2840.

(138) Babu, C. V. S.; Chung, B. C.; Lho, D. S.; Yoo, Y. S. *J. Chromatogr. A* **2006**, *1111* (2), 133.

(139) Berezovski, M.; Krylov, S. N. *J Am Chem Soc* **2002**, *124* (46), 13674.

(140) Thuy Tran, N.; Taverna, M.; Miccoli, L.; Angulo, J. F. *Electrophoresis* **2005**, *26* (16), 3105.

(141) Wang, H.; Xing, J.; Tan, W.; Lam, M.; Carnelley, T.; Weinfeld, M.; Le, X. C. *Anal. Chem.* **2002**, *74* (15), 3714.

(142) German, I.; Buchanan, D. D.; Kennedy, R. T. *Anal. Chem.* **1998**, *70* (21), 4540.

(143) Zhang, H.; Wang, Z.; Li, X. F.; Le, X. C. *Angew. Chemie - Int. Ed.* **2006**, *45* (10), 1576.

(144) Lauer, H. H.; McManigill, D. *Anal. Chem.* **1986**, *58*, 166.

(145) Mccormick, R. M. *Anal. Chem.* **1988**, *60* (21), 2322.

(146) Verzola, B.; Gelfi, C.; Righetti, P. G. *J. Chromatogr. A* **2000**, *874* (2), 293.

(147) Bushey, M. M.; Jorgenson, J. W. *J. Chromatogr.* **1989**, *480*, 301.

(148) Green, J. S.; Jorgenson, J. W. *J. Chromatogr.* **1989**, *478*, 63.

(149) Muskotál, A.; Kokol, V. *Electrophoresis* **2010**, *31* (6), 1097.

(150) Sutherland, B. W.; Toews, J.; Kast, J. *J. Mass Spectrom.* **2008**, *43* (7), 699.

(151) Assimon, V. A.; Gillies, A. T.; Rauch, J. N.; Gestwicki, J. E. *Curr. Pharm. Des.* **2013**, *19* (3), 404.

(152) Chang, L.; Thompson, A. D.; Ung, P.; Carlson, H. A.; Gestwicki, J. E. *J. Biol. Chem.* **2010**, *285* (28), 21282.

(153) Miyata, Y.; Chang, L.; Bainor, A.; Mcquade, T. J.; Walczak, C. P.; Zhang, Y.; Larsen, M. J.; Kirchhoff, P.; Gestwicki, J. E. *J. Biomol. Screen.* **2010**, *15* (10), 1211.

(154) Shemetov, A. A.; Gusev, N. B. *Arch. Biochem. Biophys.* **2011**, *513* (1), 1.

(155) Uversky, V. N. *Expert Opin. Drug Discov.* **2012**, *7* (6), 475.

(156) Ganzler, K.; Greve, K. S.; Cohen, A. S.; Karger, B. L.; Guttman, A.; Cooke, N. C. *Anal. Chem.* **1992**, *64* (22), 2665.

(157) Vasilescu, J.; Guo, X.; Kast, J. *Proteomics* **2004**, *4* (12), 3845.

(158) Klockenbusch, C.; O'Hara, J. E.; Kast, J. *Anal. Bioanal. Chem.* **2012**, *404* (4), 1057.

(159) Solomon, M. J.; Larsen, P. L.; Varshavsky, A. *Cell* **1988**, *53* (6), 937.

(160) Mattson, G.; Conklin, E.; Desai, S.; Nielander, G.; Savage, M. D.; Morgensen, S. *Mol. Biol. Rep.* **1993**, *17* (3), 167.

(161) Richter, K.; Muschler, P.; Hainzl, O.; Buchner, J. *J. Biol. Chem.* **2001**, *276* (36), 33689.

(162) Bopp, B.; Ciglia, E.; Ouald-chaib, A.; Groth, G.; Gohlke, H.; Jose, J. *Biochim. Biophys. Acta* **2016**, *1860* (6), 1043.

(163) Briknarová, K.; Takayama, S.; Brive, L.; Havert, M. L.; Knee, D. A.; Velasco, J.; Homma, S.; Cabezas, E.; Stuart, J.; Hoyt, D. W.; Satterthwait, A. C.; Llinás, M.; Reed, J. C.; Ely, K. R. *Nat. Struct. Biol.* **2001**, *8* (4), 349.

(164) Li, X.; Srinivasan, S. R.; Connarn, J.; Ahmad, A.; Young, Z. T.; Kabza, A. M.; Zuiderweg, E. R. P.; Sun, D.; Gestwicki, J. E. *ACS Med. Chem. Lett.* **2013**, *4* (11), 1042.

(165) Li, X.; Colvin, T.; Rauch, J. N.; Acosta-Alvear, D.; Kampmann, M.; Dunyak, B.; Hann, B.; Aftab, B. T.; Murnane, M.; Cho, M.; Walter, P.; Weissman, J. S.; Sherman, M. Y.; Gestwicki, J. E. *Mol. Cancer Ther.* **2015**, *14* (3), 642.

(166) Koya, K.; Li, Y.; Wang, H.; Ukai, T.; Tatsuta, N.; Kawakami, M.; Shishido, T.; Chen, L. B. *Cancer Res.* **1996**, *56* (3), 538.

(167) Mädler, S.; Seitz, M.; Robinson, J.; Zenobi, R. *J. Am. Soc. Mass Spectrom.* **2010**, *21* (10), 1775.

(168) Schmiedeberg, L.; Skene, P.; Deaton, A.; Bird, A. *PLoS One* **2009**, *4* (2), e4636.

(169) Bousse, L.; Mouradian, S.; Minalla, a.; Yee, H.; Williams, K.; Dubrow, R. *Anal. Chem.* **2001**, *73* (6), 1207.

(170) Ouimet, C. M.; Dawod, M.; Grinias, J.; Assimon, V. A.; Lodge, J.; Mapp, A. K.; Gestwicki, E.; Kennedy, R. T. *Analyst* **2018**, *143*, 1805.

(171) Ouimet, C. M.; Shao, H.; Rauch, J. N.; Dawod, M.; Nordhues, B. A.; Dickey, C.

A.; Gestwicki, J. E.; Kennedy, R. T. *Anal. Chem.* **2016**, *88* (16), 8272.

(172) Hopwood, D.; Allen, C. R.; McCabe, M. *Histochem. J.* **1970**, *2* (2), 137.

(173) Subbotin, R. I.; Chait, B. T. *Mol. Cell. Proteomics* **2014**, No. 2, 2824.

(174) Assimon, V. A.; Southworth, D. R.; Gestwicki, J. E. *Biochemistry* **2015**, *54* (48), 7120.

(175) Hopwood, D. *Histochemie* **1969**, *161*, 151.

(176) Chen, S.; Prapapanich, V.; Rimerman, R. A.; Honoré, B.; Smith, D. F. *Mol. Endocrinol.* **1996**, *10* (6), 682.

(177) Brinker, A.; Scheufler, C.; Von Der Mulbe, F.; Fleckenstein, B.; Herrmann, C.; Jung, G.; Moarefi, I.; Ulrich Hartl, F. *J. Biol. Chem.* **2002**, *277* (22), 19265.

(178) Yi, F.; Doudevski, I.; Regan, L. *Protein Sci.* **2010**, *19*, 19.

(179) Rozbesky, D.; Rosulek, M.; Kukacka, Z.; Chmelik, J.; Man, P.; Novák, P.; Rozbeský, D.; Rosůlek, M.; Kukačka, Z.; Chmelík, J.; Man, P. *Anal. Chem.* **2017**.

(180) Wine, Y.; Cohen-hadar, N.; Freeman, A.; Frolow, F. *Biotechnol. Bioeng.* **2007**, *98*, 711.

(181) Benaroudj, N.; Fang, B.; Triniolles, F.; Ghelis, C.; Ladjimi, M. M. *Biochemistry* **1995**, *128*, 121.

(182) Thompson, A. D.; Bernard, S. M.; Skiniotis, G.; Gestwicki, J. E. *Cell Stress Chaperones* **2012**, *17* (3), 313.

(183) Benaroudj, N.; Fang, B.; Triniolles, F.; Ghelis, C.; Ladjimi, M. M. *Eur. J. Biochem.* **1994**, *128*, 121.

(184) Ye, X.; Mori, S.; Yamada, M.; Inoue, J.; Xu, Z.; Hirokawa, T. *Electrophoresis* **2013**, *34* (4), 583.

(185) Han, F.; Huynh, B. H.; Ma, Y.; Lin, B. *Anal. Chem.* **1999**, *71* (13), 2385.

(186) Kovács, Z.; Szarka, M.; Szigeti, M.; Guttman, A. *J. Pharm. Biomed. Anal.* **2016**, *128*, 367.

(187) Smith, M. C.; Scaglione, K. M.; Assimon, V. A.; Patury, S.; Thompson, A. D.; Dickey, C. A.; Southworth, D. R.; Paulson, H. L.; Gestwicki, J. E.; Zuiderweg, E. R. P. *Biochemistry* **2013**, *52* (32), 5354.

(188) Kubo, T.; Nishimura, N.; Furuta, H.; Kubota, K.; Naito, T.; Otsuka, K. *J. Chromatogr. A* **2017**, *1523*, 107.

(189) Ouimet, C. M.; D'Amico, C. I.; Kennedy, R. T. *Expert Opin. Drug Discov.* **2017**, *12* (2), 213.

(190) Lo, C. T.; Throckmorton, D. J.; Singh, A. K.; Herr, A. E. *Lab Chip* **2008**, *8* (8), 1273.

(191) Nagata, H.; Tabuchi, M.; Hirano, K.; Baba, Y. *Electrophoresis* **2005**, *26*, 2687.

(192) Harrison, D. J.; Fluri, K.; Seiler, K.; Fan, Z.; Effenhauser, C. S.; Manz, A. *Science (80).* **1993**, *261* (5123), 895.

(193) Roper, M. G.; Shackman, J. G.; Dahlgren, G. M.; Kennedy, R. T. *Anal Chem* **2003**, *75* (18), 4711.

(194) Simpson, P. C.; Woolley, A. T.; Mathies, R. a. *Biomed. Microdevices* **1998**, *1* (12), 7.

(195) Jacobson, S. C.; Koutny, L. B.; Hergenroder, R.; Moore, A. W.; Ramsey, J. M. *Anal. Chem.* **1994**, *66* (20), 3472.

(196) Du, J.; Zhou, Y.; Su, X.; Yu, J. J.; Khan, S.; Jiang, H.; Kim, J. H.; Woo, J.; Kim, J. H.; Choi, B. H.; He, B.; Chen, W.; Zhang, S.; Cerione, R. a.; Auwerx, J.; Hao, Q.;

Lin, H. *Science (80)*. **2011**, *334* (6057), 806.

(197) Park, J.; Chen, Y.; Tishkoff, D. X.; Peng, C.; Tan, M.; Dai, L.; Xie, Z.; Zhang, Y.; Zwaans, B. M. M.; Skinner, M. E.; Lombard, D. B.; Zhao, Y. *Mol. Cell* **2013**, *50* (6), 919.

(198) Lu, W.; Zuo, Y.; Feng, Y.; Zhang, M. *Tumor Biol.* **2014**, 10699.

(199) Rundlett, K. L.; Armstrong, D. W. *Anal Chem* **1996**, *68* (19), 3493.

(200) Galloway, M.; Stryjewski, W.; Henry, A.; Ford, S. M.; Llopis, S.; Mccarley, R. L.; Soper, S. A. *Anal Chem* **2002**, *74* (10), 2407.

(201) Breadmore, M. C.; Tubaon, R. M.; Shallan, A. I.; Phung, S. C.; Abdul Keyon, A. S.; Gstoettenmayr, D.; Prapatpong, P.; Alhusban, A. A.; Ranjbar, L.; See, H. H.; Dawod, M.; Quirino, J. P. *Electrophoresis* **2016**, *36* (1), 36.

(202) Kaneta, T.; Yamamoto, D.; Imaskaka, T. *Electrophoresis* **2009**, *30*, 3780.

(203) Lea, W. A.; Simeonov, A. *Expert Opin. Drug Discov.* **2012**, *6* (1), 17.

(204) Mayr, L. M.; Fuerst, P. *J. Biomol. Screen.* **2008**, *13* (6), 443.

(205) Ohla, S.; Beyreiss, R.; Scriba, G. K. E.; Fan, Y.; Belder, D. *Electrophoresis* **2010**, *31* (19), 3263.

(206) Yi, F.; Zhu, P.; Southall, N.; Inglese, J.; Austin, C. P.; Zheng, W.; Regan, L. *J. Biomol. Screen.* **2009**, *14* (3), 273.

(207) Doonan, S. R.; Bailey, R. C. *Anal Chem* **2017**, *89*, 4091.

(208) Abate, A. R.; Hung, T.; Mary, P.; Agresti, J. J.; Weitz, D. a. *Proc. Natl. Acad. Sci.* **2010**, *107* (45), 19163.

(209) Roach, L. S.; Song, H.; Ismagilov, R. F. *Anal Chem* **2005**, *77* (3), 785.